The Organization of Synapses on Visual Thalamus Dendrites in the Mouse: A 3D-Connectomics Approach

Erin Elizabeth Maher
Dayton, Ohio

B.S., Elon University, 2014
M.A., University of Virginia 2017

A Dissertation presented to the Graduate Faculty of the
University of Virginia in Candidacy for the Degree of Doctor of Philosophy

Department of Psychology

University of Virginia
May 2020

Committee Members

Alev Erisir, Chair | Jianhua Cang | Hudson Golino | Adema Ribic

ABSTRACT

The lateral geniculate nucleus (LGN) of the thalamus modulates and relays visual information from the retina to the visual cortex. Synapses onto LGN neurons include input from the retina, the brainstem, the cortex, the thalamic reticular nucleus (TRN), and local inhibitory interneurons and these inputs shape the signal that is sent out of the LGN by relay cells. Previous studies of the LGN have described the organization of these inputs onto geniculate dendrites. However, key information is missing describing how inputs from different origins organize onto different LGN neuron dendrites subtypes and neuronal dendrite segments. The experiments in this dissertation sought to use a connectomics approach to characterize inputs onto LGN relay cell dendrites and interneuron dendrites with the goal of describing their organization in order to further explore how the setup of inputs into the LGN modulate visual information. Chapter II describes a method for determining putative terminal origin in the LGN through normal distribution based modeling of terminal volumes. This method was then used to study the organization of terminals onto different segments of LGN relay cell dendrites. Terminals from different origins show selectivity for different segments of relay cell dendrites based on both dendrite size and branch order. These terminals also show a selectivity for interactions with other distinct terminals on dendrite segments. Chapter III describes input selectivity onto LGN interneuron dendrites inside and outside of glomerular arrangements. Triadic motifs described in this chapter provide anatomical data that demonstrates how inputs onto interneurons affect inhibition of relay cells and therefore, the information that is sent by relay cells to the cortex. The results of these experiments detail the organization of terminals onto dendrites in a volume of LGN tissue and allows for more accurate speculation as to how this organization serves to modify visual information before it reaches the cortex.

ACKNOWLEDGEMENTS

This dissertation project would not have been possible without the encouragement and support of numerous people that surround me in my life. While I am sure I will accidently omit some names, I would like to acknowledge a few significant contributors.

- My parents, Stan and Louise Maher, who have always given me their unwavering support in all that I do. Thank you both so much for shaping me into the person I am today and for always being there for me no matter what. I could have never done this without you
- To my sisters Sarah Hatfield and Nicole Maher for always showing interest in my work (whether real or sarcastic) and for your patience and support through not only this process, but throughout life. I am incredibly lucky to have had you as sisters and friends.
- To my other family and friends, especially: my Aunt Barbara, who helped guide and assure me though graduate school; Kellen Chen for all of the love and support he has provided and for the light and ever positive he has brought into my life; Fellow corhort members, especially Victoria Mauer and Sierra Eisen for helping motivate me over the finish line.
- The members of my committee, Alev Erisir, JC Cang, Hudson Golino and Adema Ribic, for their valuable input on the design and interpretation of the experiments in this dissertation and for their support.

- All of the members of the Erisir Lab. I would like to especially acknowledge Alex Briegel and Shahrozia Imtiaz, for their extensive help in the data collection and interpretation in these experiments.
- To my advisor and friend, Alev Erisir, for providing guidance and training through every phase of my graduate career. In the past 6 years at the University of Virginia, I have grown immensely as a scientist, as a thinker, and as a person thanks to your mentorship. Thank you for affording me this opportunity and I hope that the achievement here has made you proud and that I will continue to do so throughout my scientific career.

TABLE OF CONTENTS

CHAPTER I

General Introduction

Of the five human senses, vision shows its importance as the navigator of everyday life. Our visual system must gather and combine features from the environment such as color, shapes, luminance, orientation, and movement to create a meaningful representation of the world. Each stop in the visual pathway performs a function that transforms more basic visual features into complex higher-order representations. Of particular interest to visual scientists, the lateral geniculate nucleus stands out because of its role as the principle relay of visual information from the retina to the cortex. This dissertation work aims to understand the anatomical and organizational principles that modify and modulate the response properties of the geniculate relay cells and interneurons. It also aims to reveal distinct synaptic circuitry properties for the pathways that encode different features for the visual signal processing. This introduction will provide a brief review of the extensive literature over the past six decades that has identified and characterized the anatomical and physiological properties of neuronal circuitries in the first two stops of the visual pathway, the retinal ganglion cells (RGCs) of the retina and the lateral geniculate nucleus (LGN).

The Origin of the Visual Pathway: Retinal Ganglion Cells

Retinal ganglion cells (RGCs) are the sole source of visual information that reaches the thalamus. Over 20 different classes of RGCs have been identified (for review, see Sanes & Masland, 2015). Different RGCs are tuned to distinct features of the visual environment, including luminance, orientation and direction (Kuffler, 1953; Levick, 1967). The RGCs are categorized into groups based on morphological, physiological and gene expression properties (Madisen et al., 2012; Polyak, 1957; Siegert et al., 2009). Although specific RGC cell types vary

among different species, many share similar properties and are considered homologous to each other. A description follows of four relatively well studied classes of RGCs appearing in studies that took advantage of the advances in transgenic and viral tracer techniques in the mouse.

Alpha RGCs are one of the most extensively studied RGC types. Their homologues have been identified in mice, rabbits, cats, and primates (more commonly referred to as Y-type RGCs in cats and tree shrews, brisk-transient cells in rabbits, and parasol cells or M-cells in primates). This class of RGCs has large cell bodies, large and monostratified dendritic fields in the retina, and thick, myelinated axons that innervate magnocellular cells in the LGN (Boycott & Wässle, 1974; Peichl, Ott, & Boycott, 1987). The studies by Cleland, Wassle and Peichl classified alpha RGCs into four physiological subtypes: 1) sustained ON 2) sustained OFF 3) transient OFF 4) sustained OFF (Cleland, Levick, & Wässle, 1975; Peichl, 1991; Van Wyk, Wässle, & Taylor, 2009; Wässle, Peichl, & Boycott, 1981). In mice, alpha RGCs have extensive projections to most visual nuclei of the hypothalamus (supraoptic nucleus), midbrain (superior colliculus), and the LGN (Huberman, Feller, & Chapman, 2008; Martersteck et al., 2017). In primates, studies that used single RGC axon physiology/anatomy approaches showed that parasol RGCs projected to the magnocellular layers of the LGN (Leventhal, Rodieck, & Dreher, 1981; Perry, Oehler, & Cowey, 1984).

Beta RGCs are described extensively in the rabbit, the cat, and the primate, and these are referred to as X-cells in the cat and the tree shrew, and midget or P- cells in the primate (Silveira & Perry, 1991; Wong & Oakley, 1996). The beta RGCs have small cell bodies, a narrow dendritic spread, and thinner axons that innervate parvocellular cells in the LGN (Dacey, 1993; Dacey & Petersen, 1992; Leventhal et al., 1981; Perry et al., 1984; Watanabe & Rodieck, 1989).

They are tuned to high spatial frequencies and thus detect details in the visual environment with high acuity. These RGCs have simple receptive fields with either an ON or OFF center, antagonist surround, and a sustained response to light (Stone & Fukuda, 1974). Compared to alpha RGCs, beta RGCs are more numerous, but they have smaller receptive fields (Hochstein & Shapley, 1976). Although beta RGCs have not been identified as a morphologically cohesive group in the mouse retina, mice do have RGCs with homologous receptive field size and response to light, suggesting these may function similarly to beta RGCs (Stone & Fukuda, 1974).

Small bistratified RGCs are a diverse class of RGCs that relay chromatic information from across the visual field. Small bistratified RGCs are analogous to W-type RGCs in cats and primates and project to koniocellular relay cells in the LGN (Heine & Passaglia, 2011). These RGCs have large receptive fields with a center-surround organization and low visual response (Field et al., 2007; Stone & Fukuda, 1974; P. D. Wilson, Rowe, & Stone, 1976). In primates specifically, small bistratified RGCs have a blue-ON center organization (Dacey & Lee, 1994). Small bistratified RGCs are smaller than both alpha and beta RGCs with a variable dendritic field diameter depending on if the soma is in the center or periphery of the retina (Dacey, 1993).

Another type of retinal ganglion cell present in the mammalian retina is intrinsically photosensitive retinal ganglion cells (ipRGCs). As their name suggests, ipRGCs are photosensitive and contain the photopigment melanopsin. These RGCs have large dendritic arbors and a primary projection to the suprachiasmatic nucleus, where the RGCs function to synchronize circadian rhythm (Do & Yau, 2010; Hattar, Liao, Takao, Berson, & Yau, 2002; Hattar et al., 2003; Panda et al., 2002; Provencio et al., 2000; Qiu et al., 2005). Recent studies

have shown that some ipRGCs project to the LGN, however this projection is not well characterized and will not be considered further for this dissertation (Kim et al., 2019).

Retinal inputs into the LGN are organized into parallel pathways that segregate different streams of visual information before they reach the cortex. RGCs located in the nasal retina of each eye cross the midline at the optic chiasm and provide contralateral innervation onto geniculate dendrites which are generally segregated from dendrites that receive ipsilateral eye input (Guillery, 1970; Martersteck et al., 2017). The projections from morphologically and physiologically distinct RGCs (i.e., Y vs. X; ON vs. OFF) also remain together in the LGN to form parallel-pathway-specific laminae (Bishop, 1933; Callaway, 2005; Hendry & Reid, 2000; Livingstone & Hubel, 1988). The geniculate relay cells located in pathway-specific laminae in the LGN are morphologically distinct and display response properties reflecting the input RGC (Callaway, 2005; Connolly & Van Essen, 1984; Derrington & Lennie, 1984; Durand et al., 2016; Schiller, 2010; Usrey, Reppas, & Reid, 1999; Xu et al., 2001). Thus the projections that originate from distinct RGCs may start a functionally distinct parallel pathway that remains segregated at least until the pathway reaches the cortex.

LGN Cell Types

The LGN contains two main cell types: thalamocortical relay cells that project to the primary visual cortex; and interneurons, whose axons remain within the nucleus and provide local inhibitory synapses (reviewed in Bickford, 2019; Casagrande, Royal, & Sáry, 2006). Primates have been shown to have three relay cell populations (Dacey, Peterson, Robinson, & Gamlin, 2003): Magnocellular (M) cells, Parvocellular (P) cells, and the more recently

discovered Koniocellular (K) cells. Respectively, these geniculate cells receive synapses exclusively from the parasol, the midget, and bistratified cells (Szmajda, Grünert, & Martin, 2008; Watanabe & Rodieck, 1989). Thalamocortical cells analogous to primate M, P, and K cells have been morphologically identified in mice (Parnavelas, Sullivan, Lieberman, & Webster, 1977; Rafols & Valverde, 1973), and these occupy overlapping regions in mouse LGN (Howarth, Walmsley, & Brown, 2014; Krahe, El-Danaf, Dilger, Henderson, & Guido, 2011). Because of the extensive overlap of retinal inputs in the mouse LGN, parallel pathways through the mouse LGN are not as clear as seen in other species with anatomically defined LGN layers.

The morphology of different relay cell types is described in the cat (Guillery, 1966), monkey (Saini & Garey, 1981), and mouse (Krahe et al., 2011). In the cat LGN, the X (P) cells have a small body, with short, thin, and twisting dendrites that have several "grape-like" appendages (Friedlander, Lin, Stanford, & Sherman, 1981; Guillery, 1966). The Y (M) cells have morphological features that include a large cell body and large dendrites that are fairly straight, with few appendages (Friedlander et al., 1981; Guillery, 1966). In the mouse, X- and Y-like relay cells were described based on their morphological similarities to the cat relay cells, although mouse relay cells did not show any additional distinguishing characteristics (Krahe et al., 2011).

Electrophysiologically, the cat X, Y and W relay cells also have distinct properties that parallel those of the corresponding RGCs (reviewed in Kaplan, 2014, Schiller 2010). In primates, it has been shown that P cells have a higher spatial resolution but a lower temporal resolution (Derrington & Lennie, 1984; O'Keefe, Levitt, Kiper, Shapley, & Movshon, 1998; So & Shapley, 1979). Conversely, M cells have a shorter latency of response, a lower spatial resolution, and a

higher temporal resolution than P cells (Cheong & Johannes Pietersen, 2014; Derrington & Lennie, 1984; O'Keefe et al., 1998; Shapley, Kaplan, & Soodak, 1981; Usrey & Reid, 2000). These response properties (conductance and spatial versus temporal resolution) indicate that M cells may be important in motion perception, while P cells are important for the perception of fine spatial details (DeYoe & Van Essen, 1988; Livingstone & Hubel, 1988). K type relay cells are harder to generalize than their M and P counterparts, although most display poor spatial resolution and have large receptive fields (Hendry & Reid, 2000; White, Solomon, & Martin, 2001; Xu et al., 2001). K (W) cells are also the only thalamocortical cells to receive input from the superior colliculus and to project to superficial layers of V1 (Hendry & Reid, 2000; White et al., 2001; Xu et al., 2001).

The cat LGN has two identified types of interneurons that can be distinguished by morphology and synaptic connections (Bickford, Carden, & Patel, 1999). One type of interneuron stains positive for brain nitric oxide synthase (BNOS), has a slightly larger soma size, and has dendritic arbors that are composed of thin, widespread, but sparse dendrites. These interneurons were observed to create extraglomerular dendro-dendritic synapses. The second type of interneuron is negative for BNOS, has a small soma, and has compact dendritic trees. These interneurons participate in triadic arrangements in glomeruli (these structures are discussed in more detail in the next section) (Bickford et al., 1999; Famiglietti & Peters, 1972; Hamos, Van Horn, Raczkowski, Uhlrich, & Sherman, 1985; Montero, 1986). Similar to the relay cells, the geniculate interneurons have receptive fields with center-surround organization and are either classified as ON-center or OFF-center (X. Wang, Vaingankar, Sanchez, Sommer, & Hirsch, 2011). Although these differences in interneuron morphology and physiology have been

identified, it still remains to be determined if there are differential inputs onto different types of interneurons.

LGN synaptic circuitry

Since the 1960s, the anatomical organization of the synaptic circuitry in the LGN has been studied and characterized using track tracing, degeneration, and immunohistochemical techniques in combination with both light and electron microscope imaging (Balaram, Isaamullah, Petry, Bickford, & Kaas, 2015; Bickford, 2019; Bickford et al., 2000; Bickford, Zhou, Krahe, Govindaiah, & Guido, 2015; Briggs & Usrey, 2011; Campbell, Jane, & Yashon, 1967; Connolly & Van Essen, 1984; Erişir, Van Horn, Bickford, & Sherman, 1997; Erişir, Van Horn, & Sherman, 1998, 1997; Guillery, 1966, 1970; Kaas, Guillery, & Allman, 1972; Kaas, Huerta, Weber, & Harting, 1978; Kaas, Ling, & Casagrande, 1976). These studies revealed that the distinct inputs making up the geniculate circuitry have distinct morphological features (Balaram et al., 2015; Cucchiaro, Bickford, & Sherman, 1991; Erişir, Van Horn, Bickford, et al., 1997; Erişir et al., 1998; Erişir, Van Horn, & Sherman, 1997; Guillery, 1969b; Sherman & Guillery, 1996, 2001). Furthermore, the studies provided evidence that specific input-target relationships may be primary in determining the output of LGN relay cells and network properties of the visual pathways (Bickford et al., 2010; Çavdar, Hacioğlu, Şirvanci, Keskinöz, & Onat, 2011; Coomes, Bickford, & Schofield, 2002; Erişir, Van Horn, Bickford, et al., 1997; Erişir et al., 1998; Erişir, Van Horn, & Sherman, 1997; Govindaiah & Cox, 2006; Guillery & Sherman, 2002; Jones, 2002; Liu, Honda, & Jones, 1995; McCormick, 1992; Rovó, Ulbert, & Acsády, 2012; Sherman, 2007, 2016; Sherman & Guillery, 1996, 2002; Van Horn, Erişir, &

Sherman, 2000; S. Wang, Eisenback, Datskovskaia, Boyce, & Bickford, 2002). For example, large inputs onto proximal dendrites exert a strong post-synaptic influence, whereas small distal terminals have a much weaker influence on post-synaptic firing. Therefore, understanding the patterns of synaptic inputs from distinct origins onto geniculate dendrites may impact future studies of network modeling.

The primary excitatory synapses to LGN cells come from RGC axons. The retinal axons synapse onto geniculate relay cell dendrites via very large-size glutamatergic axon terminals (Erişir et al., 1998; Hamos, Van Horn, Raczkowski, & Sherman, 1987; Sherman & Guillery, 2001; Van Horn et al., 2000). Although retinal terminals are the largest in size, they comprise only about 3-5% of the total terminals in the LGN (Erişir et al., 1998; Guillery, 1969a; Sherman & Guillery, 2001), they synapse on larger-caliber dendrites, and they engage in triads within glomeruli (more on that below). While selectivity of RGC inputs into the thalamus and differences in function suggest there may be different axon bouton structure, it is currently unknown if different RGC terminal boutons can be morphologically identified.

In most species (excluding mice), only a single RGC provides the dominant input that drives relay cell firing, while several other RGC axons converge on that neuron in a smaller capacity (Sincich, Adams, Economides, & Horton, 2007; Usrey et al., 1999; Weyand, 2007). This primary input provides a strong enough EPSP that can result in an action potential in the relay cell (Balaram et al., 2015; Bickford, 2015). It is not known whether the dominant axons accomplish this with a few synapses or many synapses. Recent studies in mouse LGN and older studies in cat LGN have revealed that each RGC can target several relay cells at the same time,

although the divergence of RGC axons has not been studied in primates (Hamos et al., 1987; Morgan, Berger, Wetzel, & Lichtman, 2016).

The LGN also receives four major modulatory inputs: 1) Glutamatergic feedback from layer 6 of the cortex (corticothalamic input) (Bartlett, Stark, Guillery, & Smith, 2000; Colonnier & Guillery, 1964; Erişir, Van Horn, Bickford, et al., 1997; Erişir, Van Horn, & Sherman, 1997; Smith, O'Leary, Harris, & Gay, 1964); 2) Cholinergic brainstem inputs (Bickford, 2019; Casagrande et al., 2006); 3) GABAergic input from the thalamic reticular nucleus (Guillery, 1966); and 4) GABAergic input from local interneurons (Coomes et al., 2002; Ohara, Chazal, & Ralston, 1989; Van Horn et al., 2000; S. Wang et al., 2002). These inputs gate or modulate the action potentials generated in relay cells, and thus play a role in shaping the visual information that is relayed to the cortex. A brief review of these modulatory inputs follows.

Corticothalamic (CT) axons provide feedback excitation to the thalamus. The terminal boutons of thalamocortical axons are very small (Erişir, Van Horn, Bickford, et al., 1997; Erişir, Van Horn, & Sherman, 1997), and they emerge from axons as single boutons with very thin stalks. These boutons rarely contain mitochondria. Erisir et al demonstrated that CT terminals synapse on small caliber dendrites, determining from this result that CT terminals are located on distal dendrite segments (Erişir, Van Horn, Bickford, et al., 1997; Erişir, Van Horn, & Sherman, 1997). The function of corticothalamic input is thought to be to change the gain of thalamocortical cells (Cano, Bezdudnaya, Swadlow, & Alonso, 2006; Przybyszewski, Gaska, Foote, & Pollen, 2000). Studies in the cat and in the owl monkey show that feedback from the cortex to the LGN is organized retinotopically to match zones from which it receives LGN input (Grieve & Sillito, 1995; Ichida & Casagrande, 2002). Although the function of feedback from

the cortex remains a relative mystery, the prevailing idea is that corticothalamic feedback may function to enhance LGN relay firing related to a salient stimulus or focal attention (Sillito, Jones, Gerstein, & West, 1994).

Cholinergic inputs to the LGN originate in the cholinergic cells located in the brachium region of the brainstem (PBN). Similar to the corticothalamic terminals, brainstem inputs are small, although larger than CT terminals (Erişir, Van Horn, Bickford, et al., 1997); they have dark mitochondria; and they synapse on small- to medium-caliber dendrites. Cholinergic terminals are also observed at the edges of the glomerular arrangements (Erişir, Van Horn, Bickford, et al., 1997; Erişir, Van Horn, & Sherman, 1997). The release of acetylcholine depolarizes thalamocortical relay cells and makes retinal stimulus more effective (McCormick, 1992). Cholinergic inputs also suppress inhibitory cells, which may have an indirect effect on relay cell excitability (McCormick & Prince, 1987). Cholinergic inputs are diffuse, that is, they do not obey retinotopy, and thus they have the capacity to modulate all geniculate input at once—a function that may switch the saliency of visual information at the expense of the other senses (Kobayashi & Isa, 2002). The cellular response properties of geniculate cells in response to acetylcholine provide evidence for the impact of brainstem cholinergic input in modulating the output of the LGN: the cholinergic terminals are associated with switching relay cell dynamics from burst firing to tonic firing modes (Jahnsen & Llinas, 1984a, 1984b; McCormick, 1992); burst firing mode follows activation of voltage- and time-dependent calcium currents, while tonic firing occurs with inactivation of voltage- and time-dependent calcium currents and is associated with a linear transmission of visual information (McCormick, 1992). Like TC terminals, brainstem inputs synapse on small-caliber dendrites and thus are assumed to be

located on distal dendrite segments, although some were observed close to glomeruli (Erişir, Van Horn, Bickford, et al., 1997; Erişir, Van Horn, & Sherman, 1997). There also exist small inputs from the dorsal raphe nucleus that release serotonin and from the tuberomammillary nucleus of the hypothalamus that release histamine (Bickford et al., 2000; Uhlrich, Manning, & Pienkowski, 1993).

The axons from the *thalamic reticular nucleus* receive excitatory inputs from the collaterals of geniculocortical and corticogeniculate axons, and then provide GABAergic synapses onto geniculate relay cells and interneurons. These terminals are classified as F type because of the flat vesicles they contain (Sherman & Guillery, 2001). Because of the TRN's reciprocal and topographic connections with the LGN, it was hypothesized that TRN inputs were involved in spatial and focal attention (Cucchiaro, Uhlrich, & Sherman, 1991; Ide, 1982). Experiments by McAlonan further demonstrated that the mechanism for this may be one of disinhibition of relay cells because attention reduces TRN activity (McAlonan, Cavanaugh, & Wurtz, 2008) (McAlonan, Cavanaugh, & Wurtz, 2008). TRN neurons have been shown to have a topographical input into the LGN and are selective for complex and localized visual features (Y. W. Lam & Sherman, 2011; Uhlrich & Cucchiaro, 1992; Vaingankar, Sanchez, Wang, Sommer, & Hirsch, 2012). TRN axons primarily target medium-sized geniculate dendrites (Van Horn et al., 2000).

Finally, the axons and dendrites of *local interneurons* provide feedforward inhibition on the relay cells (Colonnier & Guillery, 1964; McCormick & Bal, 1994; Montero, 1986; Smith et al., 1964). Interneurons can provide inhibitory inputs by releasing GABA either from their axon or presynaptic dendrites (Coomes et al., 2002; Uhlrich & Cucchiaro, 1992). Interneuron axon

boutons are termed F1 type terminals and create symmetrical synapses on relay cell dendrites (Friedlander et al., 1981; Sherman, 2007; Sherman & Guillery, 2001). Pre-synaptic interneuron dendrite boutons are termed F2 type terminals and can both receive input from RGCs and synapse onto relay cells (Montero, 1986; Sherman & Guillery, 2001; Uhlrich & Cucchiaro, 1992). Interneuron dendrites get synaptic input as well as send it, and are known to receive input from the retina, other interneuron dendrites, the TRN, the PBN and perhaps even the cortex (Cox, Zhou, & Sherman, 1998; Hamos et al., 1985; Jones & Powell, 1969; McCormick & Pape, 1988; Weber, Kalil, & Behan, 1989). Depending on the local network circuit and the receptor utilized by the interneuron, F2 terminals can either provide an increase in spontaneous inhibitory postsynaptic current (sIPSC) or a suppression of sIPSCs, affecting the strength of inhibition on postsynaptic relay cells (Cox & Sherman, 2000).

Triads and Glomeruli: Geniculate inputs can interact with each other on relay cell dendrites and interneuron dendrites to create complex synaptic arrangements called *triadic arrangements* (Famiglietti & Peters, 1972; Lieberman & Webster, 1974). Triadic arrangements consist of a retinal terminal that synapses onto a relay cell dendrite and an interneuron dendrite. That same interneuron dendrite, in turn, synapses onto the relay cell dendrite that is contacted by the same retinal input (Famiglietti & Peters, 1972; Hamos et al., 1987, 1985; Y. Lam, Cox, Varela, & Sherman, 2005). These synaptic organizations are encapsulated in a glial sheath, leading to a structure called a *glomerulus*. The glial encapsulation is thought to generate an electrically shielded environment in which nonspecific effects of neurotransmitter diffusion are prevented (Sherman & Guillery, 2001). In the triadic arrangement, the interneurons are situated to create feedforward inhibition on relay cells, thus increasing the timed precision of retinothalamic responses (Famiglietti & Peters, 1972; Lieberman & Webster, 1974; Liu et al.,

1995; Montero, 1986). Although not directly involved in the triadic arrangements, afferent inputs from the PBN also synapse onto interneuron dendrites in glomeruli however, feedback inputs from the cortex very rarely participate in the glomerular complex (Erişir, Van Horn, & Sherman, 1997). Interestingly, studies in the cat have shown that only X-type relay cells (comparable to P cells in primates) have glomeruli associated with them, and these arrangements are absent on Y-type relay cells (comparable to M cells in primates) (Hamos et al., 1987, 1985; J. R. Wilson, Friedlander, & Sherman, 1984).

The terminal cross-section areas and the relative contribution of input synapses to geniculate circuitry was studied in transmission electron microscopy (TEM) studies in the cat (Erişir, Van Horn, Bickford, et al., 1997; Erişir et al., 1998; Erişir, Van Horn, & Sherman, 1997): Corticothalamic axons have terminals that are the smallest in size, while cholinergic inputs are only slightly larger. Together, these two terminal populations make up about 60% of all LGN terminals (Erişir, Van Horn, Bickford, et al., 1997; Erişir, Van Horn, & Sherman, 1997; Sherman & Guillery, 2001). GABAergic terminals, including interneuron and TRN terminals, are medium in size while making up about 33% of LGN inputs (Guillery, 1969a; Sherman & Guillery, 2001; Van Horn et al., 2000). The retinal axons provide 6% of synapses in the LGN, and these are the largest terminal boutons found in the LGN (Erişir, Van Horn, & Sherman, 1997; Guillery, 1969a; Sherman & Guillery, 2001; Van Horn et al., 2000). In summary, a vast literature on anatomical and functional organization of LGN now tells us how several distinct inputs organize in the LGN. Furthermore, the response properties of the geniculate neurons receiving these inputs are driven by distinct streams of retinal inputs, are refined by a rich

network of interneuron inputs and a pervasive cortical feedback, and are modulated by primarily cholinergic and other GABAergic inputs.

Summary

While vast knowledge on synaptic circuitry of the LGN has been accumulated, this also exposed many other questions about synaptic circuitry in the LGN: How are axon terminals from different origins organized down a length of relay cell dendrite? Do terminals from different origins synapse on the same dendrite segment as other inputs preferentially? How do terminals in the same glomeruli organize together? Determining input patterns onto different neurons is key to understanding whether there is a signature pattern for synaptic networks that impinge on functionally distinct geniculate cells. Further characterization of inputs into the mouse LGN may clarify if the functional differences in parallel pathways of vision are determined more via the retinal ganglion cells, or via organizations of retinal and modulatory inputs onto LGN dendrites. The detailed descriptions of unique synaptic networks onto geniculate neurons may inform future studies that utilize network modeling and electrophysiology approaches.

In summary, the aim of this dissertation is to qualitatively and quantitatively describe the synaptic circuitry onto relay cell and interneuron dendrites in the LGN of the mouse with the goal of answering the questions posed above. In the coming chapters, I probe these questions with a series of experiments that take advantage of connectomics applied for SBEM image stacks, and I describe the synaptic circuitry in the mouse LGN in more detail that is allowed by 2D EM techniques. Therefore my overarching **hypothesis has been that inputs onto LGN neurons show selectivity in their locations both in terms of dendrite properties and**

proximity to other terminals. The results I report in following chapters of this study will reveal and outline several novel observations and analyses about how terminals in the LGN are organized on relay and interneuron dendrite segments, and describe novel synaptic motifs that may provide a substrate for modification and modulation of of visual information that is relayed to cortex.

LITERATURE CITED

Balaram, P., Isaamullah, M., Petry, H. M., Bickford, M. E., & Kaas, J. H. (2015). Distributions of vesicular glutamate transporters 1 and 2 in the visual system of tree shrews (Tupaia belangeri). *Journal of Comparative Neurology*, *523*(12), 1792–1808. https://doi.org/10.1002/cne.23727

Bartlett, E. L., Stark, J. M., Guillery, R. W., & Smith, P. H. (2000). Comparison of the fine structure of cortical and collicular terminals in the rat medial geniculate body. *Neuroscience*, *100*(4), 811–828. https://doi.org/10.1016/S0306-4522(00)00340-7

Bickford, M. E. (2015). Thalamic circuit diversity: Modulation of the driver/modulator framework. *Frontiers in Neural Circuits*, *9*(JAN2016), 1–8. https://doi.org/10.3389/fncir.2015.00086

Bickford, M. E. (2019). Synaptic organization of the dorsal lateral geniculate nucleus. *European Journal of Neuroscience*, *49*(7), 938–947. https://doi.org/10.1111/ejn.13917

Bickford, M. E., Carden, W. B., & Patel, N. C. (1999). Two types of interneurons in the cat visual thalamus are distinguished by morphology, synaptic connections, and nitric oxide synthase content. *Journal of Comparative Neurology*, *413*(1), 83–100. https://doi.org/10.1002/(SICI)1096-9861(19991011)413:1<83::AID-CNE6>3.0.CO;2-E

Bickford, M. E., Ramcharan, E., Godwin, D. W., Erişir, A., Gnadt, J., & Sherman, S. M. (2000). Neurotransmitters contained in the subcortical extraretinal inputs to the monkey lateral geniculate nucleus. *Journal of Comparative Neurology*, *424*(4), 701–717. https://doi.org/10.1002/1096-9861(20000904)424:4<701::AID-CNE11>3.0.CO;2-B

Bickford, M. E., Slusarczyk, A. S., Dilger, E. K., Krahe, T. E., Kucuk, C., & Guido, W. (2010). Synaptic development of the mouse dorsal lateral geniculate nucleus. *Journal of*

Comparative Neurology, *518*(5), 622–635. https://doi.org/10.1002/cne.22223

Bickford, M. E., Zhou, N., Krahe, T. E., Govindaiah, G., & Guido, W. (2015). Retinal and tectal "Driver-Like" inputs converge in the shell of the mouse dorsal lateral geniculate nucleus. *Journal of Neuroscience*, *35*(29), 10523–10534. https://doi.org/10.1523/JNEUROSCI.3375-14.2015

Bishop, G. H. (1933). Fiber Groups in the Optic Nerve. *American Journal of Physiology-Legacy Content*, *106*(2), 460–474. https://doi.org/10.1111/j.1755-3768.1965.tb05477.x

Boycott, B. B., & Wässle, H. (1974). The morphological types of ganglion cells of the domestic cat's retina. *The Journal of Physiology*, *240*(2), 397–419. https://doi.org/10.1113/jphysiol.1974.sp010616

Briggs, F., & Usrey, W. M. (2011). Corticogeniculate feedback and visual processing in the primate. *Journal of Physiology*, *589*(1), 33–40. https://doi.org/10.1113/jphysiol.2010.193599

Callaway, E. M. (2005). Structure and function of parallel pathways in the primate early visual system. *Journal of Physiology*, *566*(1), 13–19. https://doi.org/10.1113/jphysiol.2005.088047

Campbell, C. B. G., Jane, J. A., & Yashon, D. (1967). The retinal projections of the tree shrew and hedgehog. *Brain Research*, *5*, 406–418. https://doi.org/10.1136/bmj.3.5565.607

Cano, M., Bezdudnaya, T., Swadlow, H. A., & Alonso, J. M. (2006). Brain state and contrast sensitivity in the awake visual thalamus. *Nature Neuroscience*, *9*(10), 1240–1242. https://doi.org/10.1038/nn1760

Casagrande, V. A., Royal, D. W., & Sáry, G. (2006). Extraretinal Inputs and Feedback Mechanisms to the Lateral Geniculate Nucleus (LGN). *The Primate Visual System: A Comparative Approach*. https://doi.org/10.1002/0470868112.ch7

Çavdar, S., Hacioğlu, H., Şirvanci, S., Keskinöz, E., & Onat, F. (2011). Synaptic organization of the rat thalamus: A quantitative study. *Neurological Sciences*, *32*(6), 1047–1056. https://doi.org/10.1007/s10072-011-0606-4

Cheong, S. K., & Johannes Pietersen, A. N. (2014). Antidromic latency of magnocellular, parvocellular, and koniocellular (Blue-ON) geniculocortical relay cells in marmosets. *Visual Neuroscience*, *31*(3), 263–273. https://doi.org/10.1017/S0952523814000066

Cleland, B. Y. B. G., Levick, W. R., & Wässle, H. (1975). Australia, 2601 (Received 17, 151–171.

Colonnier, M., & Guillery, R. W. (1964). Synaptic organization in the lateral geniculate nucleus of the monkey. *Zeitschrift Für Zellforschung Und Mikroskopische Anatomie*, *62*(3), 333–355.

Connolly, M., & Van Essen, D. (1984). The representation of the visual field in parvicellular and magnocellular layers of the lateral geniculate nucleus in the macaque monkey. *Journal of Comparative Neurology*, *226*(4), 544–564. https://doi.org/10.1002/cne.902260408

Coomes, D. L., Bickford, M. E., & Schofield, B. R. (2002). GABAergic circuitry in the dorsal division of the cat medial geniculate nucleus. *Journal of Comparative Neurology*, *453*(1), 45–56. https://doi.org/10.1002/cne.10387

Cox, C. L., & Sherman, S. M. (2000). Control of dendritic outputs of inhibitory interneurons in the lateral geniculate nucleus. *Neuron*, *27*(3), 597–610. https://doi.org/10.1016/S0896-6273(00)00069-6

Cox, C. L., Zhou, Q., & Sherman, S. M. (1998). Glutamate locally activates dendritic outputs of thalamic internuerons. *Nature*, *394*, 478–481. https://doi.org/10.1038/246170a0

Cucchiaro, J. B., Bickford, M. E., & Sherman, S. M. (1991). A GABAergic projection from the

pretectum to the dorsal lateral geniculate nucleus in the cat. *Neuroscience*, *41*(1), 213–226. https://doi.org/10.1016/0306-4522(91)90211-6

Cucchiaro, J. B., Uhlrich, D. J., & Sherman, S. M. (1991). Electron-microscopic analysis of synaptic input from the perigeniculate nucleus to the A-laminae of the lateral geniculate nucleus in cats. *Journal of Comparative Neurology*, *310*(3), 316–336. https://doi.org/10.1002/cne.903100304

Dacey, D. M. (1993). Morphology of a small-field bistratified ganglion cell type in the macaque and human retina. *Visual Neuroscience*, *10*(6), 1081–1098.

Dacey, D. M., & Lee, B. B. (1994). The "blue-on" opponent pathway in primate retina originates from a distinct bistratified ganglion cell type. *Nature*, *367*(6465), 731–735. https://doi.org/10.1038/367731a0

Dacey, D. M., & Petersen, M. R. (1992). Dendritic field size and morphology of midget and parasol ganglion cells of the human retina. *Proceedings of the National Academy of Sciences of the United States of America*, *89*(20), 9666–9670. https://doi.org/10.1073/pnas.89.20.9666

Dacey, D. M., Peterson, B. B., Robinson, F. R., & Gamlin, P. D. (2003). Fireworks in the primate retina: In vitro photodynamics reveals diverse LGN-projecting ganglion cell types. *Neuron*, *37*(1), 15–27. https://doi.org/10.1016/S0896-6273(02)01143-1

Derrington, A. M., & Lennie, P. (1984). Spatial and temporal contrast sensitivities of neurones in lateral geniculate nucleus of macaque. *The Journal of Physiology*, *357*(1), 219–240. https://doi.org/10.1113/jphysiol.1984.sp015498

DeYoe, E. A., & Van Essen, D. (1988). Concurrent processing streams in monkey visual cortex. *Trends in Neurosciences*, *11*(5), 219–226. https://doi.org/10.1016/0166-2236(88)90130-0

Do, M. T. H., & Yau, K. W. (2010). Intrinsically photosensitive retinal ganglion cells. *Physiological Reviews*, *90*(4), 1547–1581. https://doi.org/10.1152/physrev.00013.2010

Durand, S., Iyer, R., Mizuseki, K., De Vries, S., Mihalas, S., & Reid, R. C. (2016). A comparison of visual response properties in the lateral geniculate nucleus and primary visual cortex of awake and anesthetized mice. *Journal of Neuroscience*, *36*(48), 12144–12156. https://doi.org/10.1523/JNEUROSCI.1741-16.2016

Erişir, A., Van Horn, S. C., Bickford, M. E., & Sherman, S. M. (1997). Immunocytochemistry and distribution of parabrachial terminals in the lateral geniculate nucleus of the cat: A comparison with corticogeniculate terminals. *Journal of Comparative Neurology*, *377*(4), 535–549. https://doi.org/10.1002/(SICI)1096-9861(19970127)377:4<535::AID-CNE5>3.3.CO;2-Q

Erişir, A., Van Horn, S. C., & Sherman, S. M. (1997). Relative numbers of cortical and brainstem inputs to the lateral geniculate nucleus. *Proceedings of the National Academy of Sciences of the United States of America*, *94*(4), 1517–1520. https://doi.org/10.1073/pnas.94.4.1517

Erişir, A., Van Horn, S. C., & Sherman, S. M. (1998). Distribution of synapses in the lateral geniculate nucleus of the cat: Differences between laminae A and A1 and between relay cells and interneurons. *Journal of Comparative Neurology*, *390*(2), 247–255. https://doi.org/10.1002/(SICI)1096-9861(19980112)390:2<247::AID-CNE7>3.0.CO;2-1

Famiglietti, E. V., & Peters, A. (1972). The synaptic glomerulus and the intrinsic neuron in the dorsal lateral geniculate nucleus of the cat. *Journal of Comparative Neurology*, *144*(3), 285–333. https://doi.org/10.1002/cne.901440304

Field, G. D., Sher, A., Gauthier, J. L., Greschner, M., Shlens, J., Litke, A. M., & Chichilnisky, E.

J. (2007). Spatial properties and functional organization of small bistratified ganglion cells in primate retina. *Journal of Neuroscience*, *27*(48), 13261–13272. https://doi.org/10.1523/JNEUROSCI.3437-07.2007

Friedlander, M. J., Lin, C. S., Stanford, L. R., & Sherman, S. M. (1981). Morphology of functionally identified neurons in lateral geniculate nucleus of the cat. *Journal of Neurophysiology*, *46*(1), 80–129. https://doi.org/10.1152/jn.1981.46.1.80

Govindaiah, G., & Cox, C. L. (2006). Excitatory actions of synaptically released catecholamines in the rat lateral geniculate nucleus. *Neuroscience*, *137*(2), 671–683. https://doi.org/10.1016/j.neuroscience.2005.09.021

Grieve, K. L., & Sillito, A. M. (1995). Differential properties of cells in the feline primary visual cortex providing the corticofugal feedback to the lateral geniculate nucleus and visual claustrum. *Journal of Neuroscience*, *15*(7 I), 4868–4874. https://doi.org/10.1523/jneurosci.15-07-04868.1995

Guillery, R. W. (1966). A study of Golgi preparations from the dorsal lateral geniculate nucleus of the adult cat. *Journal of Comparative Neurology*, *128*(1), 21–49. https://doi.org/10.1002/cne.901280104

Guillery, R. W. (1969a). A quantitative study of synaptic interconnections in the dorsal lateral geniculate nucleus of the cat. *Zeitschrift Für Zellforschung Und Mikroskopische Anatomie*, *96*(1), 39–48.

Guillery, R. W. (1969b). The organization of synaptic interconnections in the laminae of the dorsal lateral geniculate nucleus of the cat. *Zeitschrift Für Zellforschung Und Mikroskopische Anatomie*, *96*(1), 1–38.

Guillery, R. W. (1970). The laminar distribution of retinal fibers in the dorsal lateral geniculate

nucleus of the cat: A new interpretation. *Journal of Comparative Neurology*, *138*(3), 339–367. https://doi.org/10.1002/cne.901380307

Guillery, R. W., & Sherman, S. M. (2002). Thalamic relay functions and their role in corticocortical communication: Generalizations from the visual system. *Neuron*, *33*(2), 163–175. https://doi.org/10.1016/S0896-6273(01)00582-7

Hamos, J. E., Van Horn, S. C., Raczkowski, D., & Sherman, S. M. (1987). Synaptic circuits involving an individual retinogeniculate axon in the cat. *Journal of Comparative Neurology*, *259*(2), 165–192. https://doi.org/10.1002/cne.902590202

Hamos, J. E., Van Horn, S. C., Raczkowski, D., Uhlrich, D. J., & Sherman, S. M. (1985). Synaptic connectivity of a local circuit neurone in lateral geniculate nucleus of the cat. *Nature*, *317*(6038), 618–621. https://doi.org/10.1038/317618a0

Hattar, S., Liao, H. W., Takao, M., Berson, D. M., & Yau, K. W. (2002). Melanopsin-containing retinal ganglion cells: Architecture, projections, and intrinsic photosensitivity. *Science*, *295*(5557), 1065–1070. https://doi.org/10.1126/science.1069609

Hattar, S., Lucas, R. J., Mrosovsky, N., Thompson, S., Douglas, R. H., Hankins, M. W., … Yau, K. W. (2003). Melanopsin and rod—cone photoreceptive systems account for all major accessory visual functions in mice. *Nature*, *424*(6944), 76–81. https://doi.org/10.1038/nature01761

Heine, W. F., & Passaglia, C. L. (2011). Spatial receptive field properties of rat retinal ganglion cells. *Visual Neuroscience*, *28*(5), 403–417. https://doi.org/10.1017/S0952523811000307

Hendry, S. H. C., & Reid, R. C. (2000). The koniocellular pathway in primate vision. *Annual Review of Neuroscience*, *23*, 127–153. https://doi.org/10.1146/annurev.arplant.53.100301.135248

Hochstein, S., & Shapley, R. M. (1976). Quantitative analysis of retinal ganglion cell classifications. *The Journal of Physiology*, *262*(2), 237–264. https://doi.org/10.1113/jphysiol.1976.sp011594

Howarth, M., Walmsley, L., & Brown, T. M. (2014). Binocular integration in the mouse lateral geniculate nuclei. *Current Biology*, *24*(11), 1241–1247. https://doi.org/10.1016/j.cub.2014.04.014

Huberman, A. D., Feller, M. B., & Chapman, B. (2008). Mechanisms Underlying Development of Visual Maps and Receptive Fields. *Annual Review of Neuroscience*, *31*(1), 479–509. https://doi.org/10.1146/annurev.neuro.31.060407.125533

Ichida, J. M., & Casagrande, V. A. (2002). Organization of the feedback pathway from striate cortex (V1) to the lateral geniculate nucleus (LGN) in the owl monkey (aotus trivirgatus). *Journal of Comparative Neurology*, *454*(3), 272–283. https://doi.org/10.1002/cne.10441

Ide, L. S. (1982). The fine structure of the perigeniculate nucleus in the cat. *Journal of Comparative Neurology*, *210*(4), 317–334. https://doi.org/10.1002/cne.902100402

Jahnsen, H., & Llinas, R. (1984a). Electrophysiological properties of guinea-pig thalamic neurones:, 205–226.

Jahnsen, H., & Llinas, R. (1984b). Ionic basis for the electro-responsiveness and oscillatory properties of guinea-pig thalamic neurones in vitro. *The Journal of Physiology*, *349*(1), 227–247. https://doi.org/10.1113/jphysiol.1984.sp015154

Jones, E. G. (2002). Thalamic organization and function after Cajal. *Progress in Brain Research*, *136*, 333–357. https://doi.org/10.1016/S0079-6123(02)36029-1

Jones, E. G., & Powell, T. P. (1969). Electron microscopy of synaptic glomeruli in the thalamic relay nuclei of the cat. *Proceedings of the Royal Society of London. Series B. Biological*

Sciences, *172*(27), 153–171. https://doi.org/10.1098/rspb.1969.0017

Kaas, J. H., Guillery, R. W., & Allman, J. M. (1972). Some principles of organization in the dorsal lateral geniculate nucleus. *Brain, Behavior and Evolution*, *6*(1), 253–299. https://doi.org/10.1159/000123715

Kaas, J. H., Huerta, M. F., Weber, J. T., & Harting, J. K. (1978). Patterns of retinal terminations and laminar organization of the lateral geniculate nucleus of primates. *Journal of Comparative Neurology*, *182*(3), 517–553. https://doi.org/10.1002/cne.901820308

Kaas, J. H., Ling, C. S., & Casagrande, V. A. (1976). The relay of ipsilateral and contralateral retinal input from the lateral geniculate nucleus to striate cortex in the owl monkey: a transneuronal transport study. *Brain Research*, *106*(2), 371–378. https://doi.org/10.1016/0006-8993(76)91032-5

Kaplan, E. (2014). The M , P and K pathways of the Primate Visual System revisited The M , P and K pathways of the Primate Visual System revisited Ehud Kaplan Current address : The Neuroscience Department and the Friedman Brain Institute , The Mount, (May).

Kim, K.-Y., Rios, L. C., Le, H., Perez, A. J., Phan, S., Bushong, E. A., … Panda, S. (2019). Synaptic Specializations of Melanopsin-Retinal Ganglion Cells in Multiple Brain Regions Revealed by Genetic Label for Light and Electron Microscopy. *Cell Reports*, *29*(3), 628–644.

Kobayashi, Y., & Isa, T. (2002). Sensory-motor gating and cognitive control by the brainstem cholinergic system, *15*, 731–741.

Krahe, T. E., El-Danaf, R. N., Dilger, E. K., Henderson, S. C., & Guido, W. (2011). Morphologically distinct classes of relay cells exhibit regional preferences in the dorsal lateral geniculate nucleus of the mouse. *Journal of Neuroscience*, *31*(48), 17437–17448.

https://doi.org/10.1523/JNEUROSCI.4370-11.2011

Kuffler, S. W. (1953). Discharge patterns and functional organization of mammalian retina. *Journal of Neurophysiology*, *16*(1), 37–68. https://doi.org/10.1152/jn.1953.16.1.37

Lam, Y., Cox, C. L., Varela, C., & Sherman, S. M. (2005). Morphological correlates of triadic circuitry in the lateral geniculate nucleus of cats and rats. *Journal of Neurophysiology*, *93*(2), 748–757. https://doi.org/10.1152/jn.00256.2004

Lam, Y. W., & Sherman, S. M. (2011). Functional organization of the thalamic input to the thalamic reticular nucleus. *Journal of Neuroscience*, *31*(18), 6791–6799. https://doi.org/10.1523/JNEUROSCI.3073-10.2011

Leventhal, A. G., Rodieck, R. W., & Dreher, B. (1981). Retinal ganglion cell classes in the Old World monkey: morphology and central projections. *Science*, *213*(4512), 1139–1142.

Levick, W. R. (1967). Receptive fields and trigger features of ganglion cells in the visual streak of the rebbit's retina. *Journal of Physiology*, *188*, 285–307.

Lieberman, A. R., & Webster, K. E. (1974). Aspects of the synaptic organization of intrinsic neurons in the dorsal lateral geniculate nucleus. *Journal of Neurosytology*, *3*(6), 677–710.

Liu, X. -B, Honda, C. N., & Jones, E. G. (1995). Distribution of four types of synapse on physiologically identified relay neurons in the ventral posterior thalamic nucleus of the cat. *Journal of Comparative Neurology*, *352*(1), 69–91. https://doi.org/10.1002/cne.903520106

Livingstone, M., & Hubel, D. (1988). Segregation of form, color, movement, and depth: anatomy, physiology, and perception. *Science*, *240*(4853), 740–749.

Madisen, L., Mao, T., Koch, H., Zhuo, J. M., Berenyi, A., Fujisawa, S., … Zeng, H. (2012). A toolbox of Cre-dependent optogenetic transgenic mice for light-induced activation and silencing. *Nature Neuroscience*, *15*(5), 793–802. https://doi.org/10.1038/nn.3078

Martersteck, E. M., Hirokawa, K. E., Evarts, M., Bernard, A., Duan, X., Li, Y., … Harris, J. A. (2017). Diverse Central Projection Patterns of Retinal Ganglion Cells. *Cell Reports*, *18*(8), 2058–2072. https://doi.org/10.1016/j.celrep.2017.01.075

McAlonan, K., Cavanaugh, J., & Wurtz, R. H. (2008). Guarding the gateway to cortex with attention in visual thalamus. *Nature*, *456*(7220), 391–394. https://doi.org/10.1038/nature07382

McCormick, D. A. (1992). Neurotransmitter actions in the thalamus and cerebral cortex and their role in neuromodulation of thalamocortical activity. *Progress in Neurobiology*, *39*(4), 337–388. https://doi.org/10.1016/0301-0082(92)90012-4

McCormick, D. A., & Bal, T. (1994). Sensory gating mechanisms of the thalamus. *Current Opinion in Neurobiology*, *4*(4), 550–556. https://doi.org/10.1016/0959-4388(94)90056-6

McCormick, D. A., & Pape, H. C. (1988). Acetylcholine inhibits identified interneurons in the cat lateral geniculate nucleus. *Nature*, *334*(6179), 246–248. https://doi.org/10.1038/334246a0

McCormick, D. A., & Prince, D. A. (1987). Actions of acetylcholine in the guinea-pig and cat medial and lateral geniculate nuclei, in vitro. *The Journal of Physiology*, *392*(1), 147–165. https://doi.org/10.1113/jphysiol.1987.sp016774

Montero, V. M. (1986). Localization of γ-aminobutyric acid (GABA) in type 3 cells and demonstration of their source to f2 terminals in the cat lateral geniculate nucleus: A golgi-electron-microscopic GABA-immunocytochemical study. *Journal of Comparative Neurology*, *254*(2), 228–245. https://doi.org/10.1002/cne.902540207

Morgan, J. L., Berger, D. R., Wetzel, A. W., & Lichtman, J. W. (2016). The Fuzzy Logic of Network Connectivity in Mouse Visual Thalamus. *Cell*, *165*(1), 192–206.

https://doi.org/10.1016/j.cell.2016.02.033

O'Keefe, L. P., Levitt, J. B., Kiper, D. C., Shapley, R. M., & Movshon, J. A. (1998). Functional organization of owl monkey lateral geniculate nucleus and visual cortex. *Journal of Neurophysiology*, *80*(2), 594–609. https://doi.org/10.1152/jn.1998.80.2.594

Ohara, P. T., Chazal, G., & Ralston, H. J. (1989). Ultrastructural analysis of gaba-immunoreactive elements in the monkey thalamic ventrobasal complex. *Journal of Comparative Neurology*, *283*(4), 541–558. https://doi.org/10.1002/cne.902830408

Panda, S., Antoch, M. P., Miller, B. H., Su, A. I., Schook, A. B., Straume, M., … Hogenesch, J. B. (2002). Coordinated transcription of key pathways in the mouse by the circadian clock. *Cell*. https://doi.org/10.1016/S0092-8674(02)00722-5

Parnavelas, J. G., Sullivan, K., Lieberman, A. R., & Webster, K. E. (1977). Neurons and their synaptic organization in the visual cortex of the rat. *Cell and Tissue Research*, *183*(4), 499–517.

Peichl, L. (1991). Alpha ganglion cells in mammalian retinae: Common properties, species differences, and some comments on other ganglion cells. *Visual Neuroscience*, *7*(1–2), 155–169.

Peichl, L., Ott, H., & Boycott, B. B. (1987). Alpha ganglion cells in mammalian retinae. *Proceedings of the Royal Society of London - Biological Sciences*, *231*(1263), 169–197. https://doi.org/10.1098/rspb.1987.0040

Perry, V. H., Oehler, R., & Cowey, A. (1984). Retinal ganglion cells that project to the dorsal lateral geniculate nucleus in the macaque monkey. *Neuroscience*, *12*(4), 1101–1123. https://doi.org/10.1016/0306-4522(84)90006-X

Polyak, S. (1957). *Thevertebrate visual system* (Vol. 277). Chicago: University of Chicago Press.

Provencio, I., Rodriguez, I. R., Jiang, G., Hayes, W. P., Moreira, E. F., & Rollag, M. D. (2000). A novel human opsin in the inner retina. *Journal of Neuroscience*, *20*(2), 600–605. https://doi.org/10.1523/jneurosci.20-02-00600.2000

Przybyszewski, A. W., Gaska, J. P., Foote, W., & Pollen, D. A. (2000). Striate cortex increases contrast gain of macaque LGN neurons. *Visual Neuroscience*, *17*(4), 485–494. https://doi.org/10.1017/S0952523800174012

Qiu, X., Kumbalasiri, T., Carlson, S. M., Wong, K. Y., Krishna, V., Provencio, I., & Berson, D. M. (2005). Induction of photosensitivity by heterologous expression of melanopsin. *Nature*, *433*(7027), 745–749. https://doi.org/10.1038/nature03345

Rafols, J. A., & Valverde, F. (1973). The structure of the dorsal lateral geniculate nucleus in the mouse. A golgi and electron microscopic study. *Journal of Comparative Neurology*, *150*(3), 303–331. https://doi.org/10.1002/cne.901500305

Rovó, Z., Ulbert, I., & Acsády, L. (2012). Drivers of the primate thalamus. *Journal of Neuroscience*, *32*(49), 17894–17908. https://doi.org/10.1523/JNEUROSCI.2815-12.2012

Saini, K. D., & Garey, L. J. (1981). Morphology of neurons in the lateral geniculate nucleus of the monkey. *Experimental Brain Research*, *42*(3–4), 235–248.

Sanes, J. R., & Masland, R. H. (2015). The Types of Retinal Ganglion Cells: Current Status and Implications for Neuronal Classification. *Annual Review of Neuroscience*, *38*(1), 221–246. https://doi.org/10.1146/annurev-neuro-071714-034120

Schiller, P. H. (2010). Parallel information processing channels created in the retina. *Proceedings of the National Academy of Sciences of the United States of America*, *107*(40), 17087–17094. https://doi.org/10.1073/pnas.1011782107

Shapley, R. M., Kaplan, E., & Soodak, R. (1981). Spatial summation and contrast sensitivity of

X and Y cells in the lateral geniculate nucleus of the macaque. *Nature*. https://doi.org/10.1038/292543a0

Sherman, S. M. (2007). The thalamus is more than just a relay. *Current Opinion in Neurobiology*, *17*(4), 417–422. https://doi.org/10.1016/j.conb.2007.07.003

Sherman, S. M. (2016). Thalamus plays a central role in ongoing cortical functioning. *Nature Neuroscience*, *19*(4), 533–541. https://doi.org/10.1038/nn.4269

Sherman, S. M., & Guillery, R. W. (1996). Functional Organization of Thalamocortical Relays. *Journal of Neurophysiology*, *76*(3), 1367–1395. https://doi.org/10.1074/jbc.271.4.1849

Sherman, S. M., & Guillery, R. W. (2001). *Exploring the thalamus*. Elsevier.

Sherman, S. M., & Guillery, R. W. (2002). The role of the thalamus in the flow of information to the cortex. *Philosophical Transactions of the Royal Society B: Biological Sciences*, *357*(1428), 1695–1708. https://doi.org/10.1098/rstb.2002.1161

Siegert, S., Scherf, B. G., Del Punta, K., Didkovsky, N., Heintz, N., & Roska, B. (2009). Genetic address book for retinal cell types. *Nature Neuroscience*, *12*(9), 1197–1204. https://doi.org/10.1038/nn.2370

Sillito, A. M., Jones, H. E., Gerstein, G. L., & West, D. C. (1994). Feature-linked synchronization of thalamic relay cell firing induced by feedback from the visual cortex. *Nature*, *369*(6480), 479–482. https://doi.org/10.1007/978-3-319-39581-4_12

Silveira, L. C. L., & Perry, V. H. (1991). The topography of magnocellular projecting ganglion cells (M-ganglion cells) in the primate retina. *Neuroscience*, *40*(1), 217–237. https://doi.org/10.1016/0306-4522(91)90186-R

Sincich, L. C., Adams, D. L., Economides, J. R., & Horton, J. C. (2007). Transmission of spike trains at the retinogeniculate synapse. *Journal of Neuroscience*, *27*(10), 2683–2692.

https://doi.org/10.1523/JNEUROSCI.5077-06.2007

Smith, J. M., O'Leary, J. L., Harris, A. B., & Gay, A. J. (1964). Ultrastructural features of the lateral geniculate nucleus of the cat. *Journal of Comparative Neurology*, *123*(3), 357–377. https://doi.org/10.1002/cne.901230305

So, Y. T., & Shapley, R. M. (1979). Spatial properties of X and Y cells in the lateral geniculate nucleus of the cat and conduction velocities of their inputs. *Experimental Brain Research*, *36*(3), 533–550.

Stone, J., & Fukuda, Y. (1974). Properties of cat retinal ganglion cells: a comparison of W-cells with X- and Y-cells. *Journal of Physiology*, *34*(7), 722–748.

Szmajda, B. A., Grünert, U., & Martin, P. R. (2008). Retinal ganglion cell inputs to the koniocellular pathway. *Journal of Comparative Neurology*, *510*(3), 251–268. https://doi.org/10.1002/cne.21783

Uhlrich, D. J., & Cucchiaro, J. B. (1992). GABAergic circuits in the lateral geniculate nucleus of the cat. *Progress in Brain Research*, *90*, 171–192.

Uhlrich, D. J., Manning, K. A., & Pienkowski, T. P. (1993). The histaminergic innervation of the lateral geniculate complex in the cat. *Visual Neuroscience1*, *10*(2), 225–235.

Usrey, W. M., & Reid, R. C. (2000). Visual physiology of the lateral geniculate nucleus in two species of New World monkey: Saimiri sciureus and Aotus trivirgatis. *Journal of Physiology*, *523*(3), 755–769. https://doi.org/10.1111/j.1469-7793.2000.00755.x

Usrey, W. M., Reppas, J. B., & Reid, R. C. (1999). Specificity and strength of retinogeniculate connections. *Journal of Neurophysiology*, *82*(6), 3527–3540. https://doi.org/10.1152/jn.1999.82.6.3527

Vaingankar, V., Sanchez, C. S., Wang, X., Sommer, F. T., & Hirsch, J. A. (2012). Neurons in the

thalamic reticular nucleus are selective for diverse and complex visual features. *Frontiers in Integrative Neuroscience*, *6*(NOV), 1–17. https://doi.org/10.3389/fnint.2012.00118

Van Horn, S. C., Erişir, A., & Sherman, S. M. (2000). Relative distribution of synapses in the A-laminae of the lateral geniculate nucleus of the cat. *Journal of Comparative Neurology*, *416*(4), 509–520. https://doi.org/10.1002/(SICI)1096-9861(20000124)416:4<509::AID-CNE7>3.0.CO;2-H

Van Wyk, M., Wässle, H., & Taylor, W. R. (2009). Receptive field properties of ON- and OFF-ganglion cells in the mouse retina Michiel. *Visual Neuroscience*, *26*(3), 297–308. https://doi.org/10.1017/S0952523809990137.Receptive

Wang, S., Eisenback, M., Datskovskaia, A., Boyce, M., & Bickford, M. E. (2002). GABAergic pretectal terminals contact GABAergic interneurons in the cat dorsal lateral geniculate nucleus, *323*, 141–145.

Wang, X., Vaingankar, V., Sanchez, C. S., Sommer, F. T., & Hirsch, J. A. (2011). Thalamic interneurons and relay cells use complementary synaptic mechanisms for visual processing. *Nature Neuroscience*, *14*(2), 224–233. https://doi.org/10.1038/nn.2707

Wässle, H., Peichl, L., & Boycott, B. B. (1981). Dendritic territories of cat retinal ganglion cells. *Nature*, *292*(5821), 344–345. https://doi.org/10.1038/292344a0

Watanabe, M., & Rodieck, R. W. (1989). Parasol and midget ganglion cells of the primate retina. *Journal of Comparative Neurology*, *289*(3), 434–454. https://doi.org/10.1002/cne.902890308

Weber, A. J., Kalil, R. E., & Behan, M. (1989). Synaptic connections between corticogeniculate axons and interneurons in the dorsal lateral geniculate nucleus of the cat. *Journal of Comparative Neurology*, *289*(1), 156–164. https://doi.org/10.1002/cne.902890113

Weyand, T. G. (2007). Retinogeniculate transmission in wakefulness. *Journal of Neurophysiology*, *98*(2), 769–785. https://doi.org/10.1152/jn.00929.2006

White, A. J. R., Solomon, S. G., & Martin, P. R. (2001). Spatial properties of koniocellular cells in the lateral geniculate nucleus of the marmoset Callithriz jacchus. *Journal of Physiology*, *533*(2), 519–535. https://doi.org/10.1111/j.1469-7793.2001.0519a.x

Wilson, J. R., Friedlander, M. J., & Sherman, S. M. (1984). Fine structural morphology of identified X- and Y-cells in the cat's lateral geniculate nucleus. *Proceedings of the Royal Society of London - Biological Sciences*, *221*(1225), 411–436. https://doi.org/10.1098/rspb.1984.0042

Wilson, P. D., Rowe, M. H., & Stone, J. (1976). Properties of relay cells in cat's lateral geniculate nucleus: a comparison of W cells with X and Y cells. *Journal of Neurophysiology*, *39*(6), 1193–1209. https://doi.org/10.1152/jn.1976.39.6.1193

Wong, R. O. L., & Oakley, D. M. (1996). Changing patterns of spontaneous bursting activity of on and off retinal ganglion cells during development. *Neuron*, *16*(6), 1087–1095. https://doi.org/10.1016/S0896-6273(00)80135-X

Xu, X., Ichida, J. M., Allison, J. D., Boyd, J. D., Bonds, A. B., & Casagrande, V. A. (2001). A comparison of koniocellular, magnocellular and parvocellular receptive field properties in the lateral geniculate nucleus of the owl monkey (Aotus trivirgatus). *Journal of Physiology*, *531*(1), 203–218. https://doi.org/10.1111/j.1469-7793.2001.0203j.x

CHAPTER II

Selectivity of Excitatory, Inhibitory and Modulatory Inputs onto Geniculate Relay Cell Dendrites:

A Connectomics Approach

ABSTRACT

Relay cells in the lateral geniculate nucleus (LGN) are responsible for modifying and sending visual information from the retina to the cortex. Visual information is transformed due in part to modulatory inputs onto relay cell dendrites. Both the type of modulatory input and the location of the input on the geniculate dendrite determine how visual information is processed. I used serial blockface electron microscopy (SBEM) image stacks to reconstruct geniculate relay cell dendrites as well as all associated synapses and terminals. I then used Bayesian mixture modeling to determine the putative origin of terminals and describe their synaptic organization on relay cell dendrites. I saw that putative retinal terminals target primary and secondary dendrite segments, putative GABAergic terminals target all dendrite segments and putative cholinergic and cortical terminals target small, tertiary dendrites. I also determined the levels of association between terminals of different origins synapsing onto the same dendrite segment together and found that while cortical and cholinergic terminals synapsed on the same dendrite segments, they were not seen on the same segments as retinal terminals.

INTRODUCTION

Understanding the network properties of neuronal circuits critically benefits from characterization of distinct input axons that drive and modify the signal processed by identified neurons of the lateral geniculate nucleus (LGN). Furthermore, the patterns of axon selectivity on geniculate dendrites and interactions among various inputs inform whether there is a signature pattern for synaptic networks that impinge on functionally distinct cells (Bickford et al., 2010; Çavdar, Hacioğlu, Şirvanci, Keskinöz, & Onat, 2011; Erişir, Van Horn, Bickford, & Sherman, 1997; Erişir, Van Horn, & Sherman, 1997; Govindaiah & Cox, 2006; Guillery & Sherman, 2002; Jones, 2002; McCormick, 1992; Rovó, Ulbert, & Acsády, 2012; Sherman, 2007, 2016; Sherman & Guillery, 1996, 2001; Van Horn, Erişir, & Sherman, 2000; S. Wang, Eisenback, Datskovskaia, Boyce, & Bickford, 2002). In order to study the fine detail of input patterns onto geniculate neurons, researchers have employed 3D connectomic techniques (Chai et al., 2017; Denk & Horstmann, 2004; Hammer et al., 2014; Helmstaedter, Briggman, & Denk, 2008; Hughes, Hawes, Monteith, & Vaughan, 2014; Maco et al., 2014; Morgan, Berger, Wetzel, & Lichtman, 2016; Wilke et al., 2013). Recent efforts by Morgan, Berger, Wetzel, and Lichman used connectomics to characterize retinal ganglion cell (RGC) inputs onto geniculocortical relay cells with the aim of charting parallel visual streams through the LGN (Morgan et al., 2016). Their results demonstrated first that the retinal inputs into the LGN are more complex than were first hypothesized and second, that structurally distinct retinal input patterns onto relay cells could not be divided into distinct visual pathways. The inability to categorize geniculate relay cells into parallel pathways based on RGC input raises the following question: How do neural networks in the LGN implement specific physiological functions to different populations of relay cells? The

answer to this question may be that modulatory inputs known to synapse onto relay cell dendrites in the LGN work in conjunction with RGC inputs to shape the physiological responses displayed by LGN relay cells.

Much is known about the sizes and distributions of axon terminals in the LGN. The terminal cross-section areas in the cat and the relative contribution of input synapses to geniculate circuitry were studied with transmission electron microscopy (TEM) (Erişir, Van Horn, Bickford, et al., 1997; Erişir, Van Horn, & Sherman, 1998, 1997), resulting in the following observations: that corticothalamic axons have terminals that are the smallest in size, while cholinergic inputs are only slightly larger. Together, these two terminal populations make up about 60% of all LGN terminals (Erişir, Van Horn, Bickford, et al., 1997; Erişir, Van Horn, & Sherman, 1997; Sherman & Guillery, 2001). Further study of the LGN revealed that GABAergic terminals, including interneuron and thalamic reticular nucleus (TRN) terminals, are medium in size, making up about 33% of LGN inputs; and that retinal axons are the largest terminal boutons found in the LGN, providing 6% of synapses in the LGN (Guillery, 1969a; Montero, 1986; Sherman & Guillery, 2001; Van Horn et al., 2000). The accumulation of these knowledge has revealed a lot about LGN synaptic circuitry, but also exposed many other questions about synaptic circuitry onto relay cells in the LGN, including ones that are posed for the current experiments: Is there a specific synaptic organization of inputs from different origins onto relay cell dendrites? If there is a variability in target selectivity of geniculate inputs, do they correlate with any discernible variability in relay dendrite morphology that may allude to different synaptic circuitry properties governing different parallel pathways.

To answer these questions, I employed a connectomics approach that allowed me to study LGN circuitry in a three-dimensional space. I used serial blockface electron microscopy (SBEM) image stacks of the mouse LGN, 3D reconstructions of identified dendrite segments, and model-based classification to determine terminal patterns on specific dendrite segments, terminal selectivity for identified dendrite segments, and terminal interactions with each other on the dendrite. My results reveal direct evidence for selectivity of distinct inputs for specific compartments of the relay cell dendrites, and for interactions with other distinct terminals.

MATERIALS AND METHODS

Tissue Preparation

In order to prepare the tissue for generating SBEM image stacks, mice were deeply anesthetized and transcardially perfused with phosphate buffered saline (PBS; 0.1MPB, 0.9% NaCl) followed by a mixture of 4% paraformaldehyde and 2% glutaraldehyde made in 0.1M cacodylate buffer. Brains were then removed from the skull and cut coronally at 300μm sections on a vibratome. The LGN was then dissected from the appropriate sections and sent to Renovo Neural Inc for staining, embedding, sectioning and imaging. One LGN stack was composed of 300 41μm x 41μm sections that are 75 nm thick each and one was composed of 200 41μm x 41μm sections that are 75 nm thick each.

SBEM image tracing

Cell Bodies and dendrites: All image tracing was done using Reconstruct software (Fiala, 2005). Tracing was started by identifying all cell bodies visible in the stack. All dendrites emerging from each somata were also traced. Special care was made to identify dendrite branches and to classify each dendrite as primary (emerging from the soma), secondary, or tertiary. After all dendrites and branches associated with a soma were traced, we then looked for dendrite segments that displayed somatic organelles, identifying them as a primary branch, and traced them to the extent they spanned the image stack. Dendrites that did not display an F2 appendage, meaning they did not display a presynaptic site, were considered to belong to a relay cell and were included in this analysis. Those that displayed an F2 appendage or a presynaptic synapse, including a collection of vesicles, were classified as interneuron dendrites, and constituted the dataset for the experiments in Chapter III; those will not be considered in this chapter any further. All dendrites and cell bodies were traced until the profile of the object being traced was no longer visible in the stack (i.e. extended outside the volume of tissue represented in the stack). Dendrite lengths and volumes were measured by using the Z-length and 3D volume tools of the Reconstruct. With the assumption that dendrites are roughly cylindrical structures, the dendrite caliber (diameter) is estimated with the formula: $d=\sqrt{(volume \div (length \times \pi))}$.

Synapses and Terminals: To mark the terminals that synapse on the reconstructed dendrite, first, all synaptic zones that appeared on each already reconstructed dendrite segment were traced and reconstructed. Second, the terminal boutons that make each synapse were traced and reconstructed. We took care to capture the entire presynaptic bouton and to exclude the

thinner inter-bouton axon segments that are devoid of vesicles from the reconstructions. Terminal volumes were computed using Reconstruct software.

Model-based classification

Model-based classification calculations were done in R using the MClust package (Scrucca, Fop, Murphy, & Raftery, 2016). MClust is a package used for model-based clustering, classification, and density estimation based on normal mixture modelling. Using the Bayesian Information Criterion (BIC) strategy of MClust, I estimated the clustering of subpopulations that make up the full population of terminal volumes. This is based on the assumption that subpopulations with normal distributions partially overlap in the full population. When applied for terminal and dendrite classification, MClust yielded the number of objects in each population as well as the average and standard deviation of terminal and dendrite size in each. The confidence level for each value for belonging to any given cluster (i.e. a confidence level for each terminal volume or dendrite caliber subpopulation) was also computed. Terminal clusters computed in Mclust will be referred to as populations from this point forward.

Statistical Analysis

Analysis for association rules and network analysis were done with R using the *Arules* package version 1.6-4 and *sna* package version 2.5 respectively (Butts, 2008; Hahsler, Grun, & Hornik, 2005). All graphs, descriptive statistics, and comparative statistics (including Mann-Whitney U and Kriskal-Wallis tests) were completed using Prism software version 8. All figures were created and annotated using Adobe Photoshop 2020.

RESULTS

Datasets

Relay Cell Dendrites: In this study, we reconstructed 86 individual dendrite segments belonging to 18 distinct relay cell dendrites. Dendrite segment caliber ranged from 0.12μm to 2.68 μm+/- 0.37 μm, with an average caliber of 0.63μm3. Of the 18 relay cell dendrites, 7 of them had 3 or 4 branching points (that is, primary, secondary, tertiary dendrite segments). Of the 86 individual segments, I was able to identify 21 primary dendrite segments; 25 secondary dendrite segments and 20 tertiary dendrite segments (Figure 1). The primary dendrite segments are confirmed as such because they can be seen emerging out of cell bodies in the stack of EM images, or display morphology indicating their primary status (i.e. somatic organelles). In total, dendrites received a total of 986 synapses from 899 terminal boutons (Figure 2) .

Terminal Bouton Volumes: In this study, I used three datasets of terminal volumes from the mouse LGN. I will describe each of these datasets below:

1) Dataset A: This dataset consists of all terminal boutons that synapsed onto a relay cell dendrite reconstructed for this study. This dataset included 906 terminals. The average volume of synaptic terminal boutons was 1.23 μm3+/- 1.56, with a maximum of 23.95μm3and a minimum of 0.04μm3.
2) Dataset B: This dataset consists of all terminal boutons reconstructed in any chapter of this dissertation that synapse onto LGN dendrites. This includes terminals synapsing onto relay cell dendrites and interneuron dendrites, as well as terminal volumes collected in appendix I. This dataset includes 1448 terminals. The average terminal volume is 1.23μm3+/- 1.84, with a maximum of

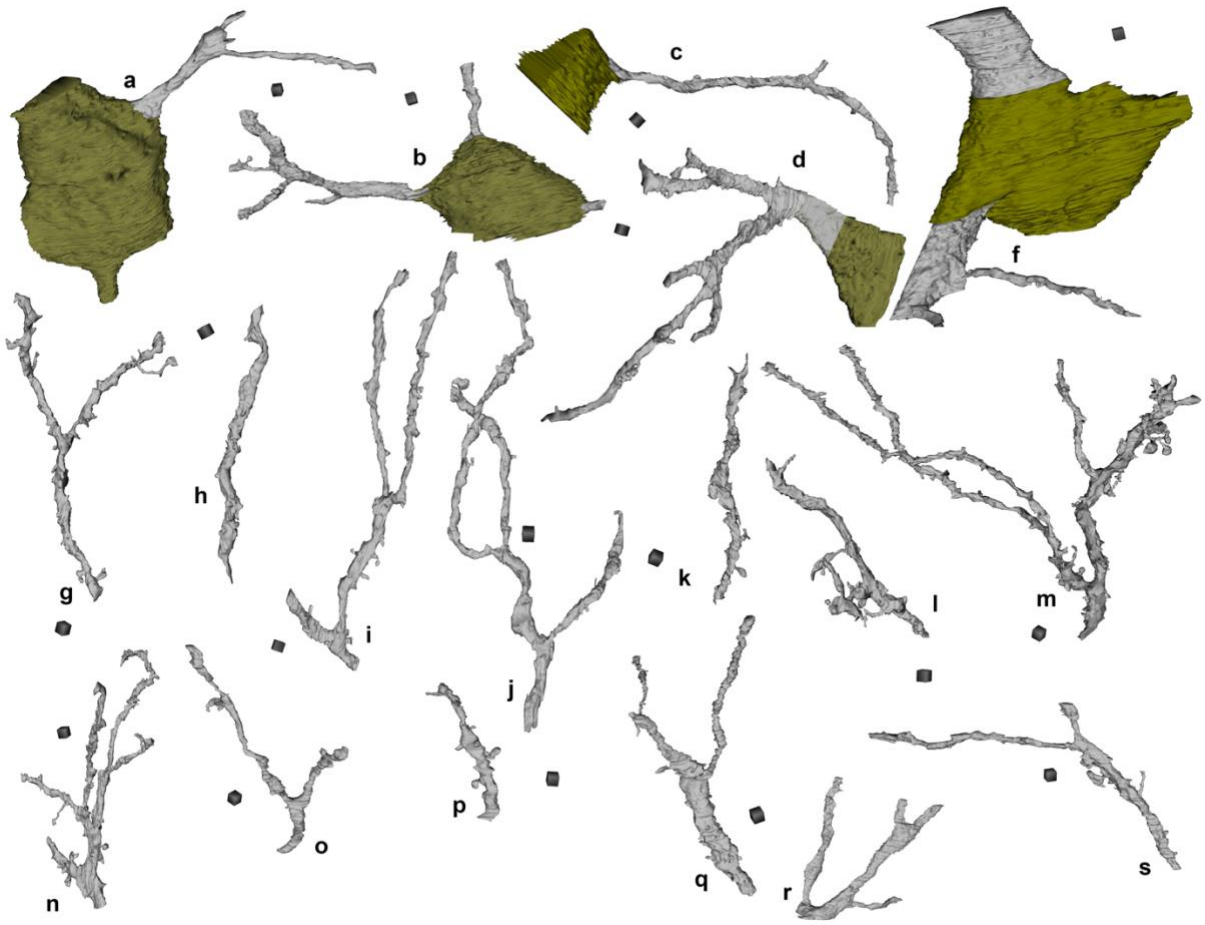

Figure 1: Reconstructions of all relay cell dendrite and cell bodies traced in the mouse LGN. Relay cell dendrites in the mouse LGN display varying shapes, sizes, and branching patterns; scale cube = 1x1x1μm

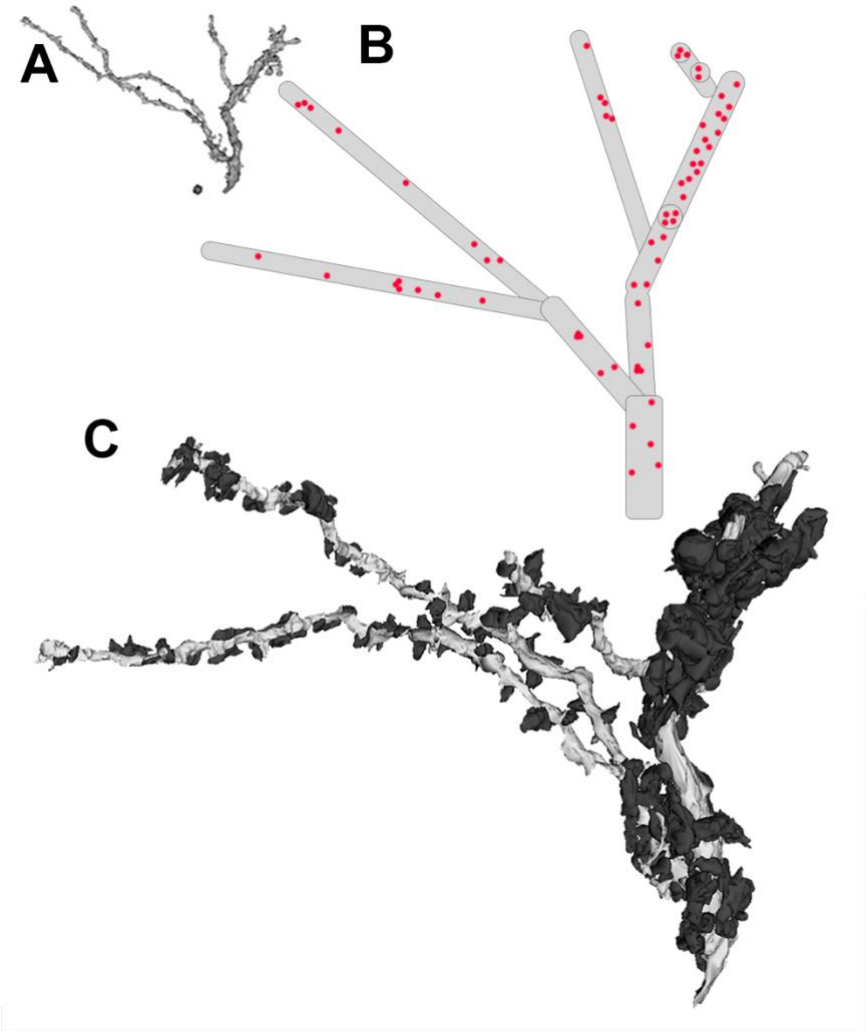

Figure 2: Example of data collection methods on a relay cell dendrite. (A) The entire length of the dendrite that is included in the image stack is traced. (B) All synapses onto the dendrite are identified and traced. (C) Terminals associated with each synapse are traced and reconstructed onto the dendrite; scale cube = 1x1x1μm

23.95µm3and a minimum of 0.02µm3. This dataset was used for terminal population modeling.

3) Dataset C: This dataset consists of an unbiased collection of terminal bouton volumes in the LGN sampled with stereological methods in appendix I. This dataset contained 408 terminals and had an average volume of 0.783 µm3 +/- 1.392 µm3 with a minimum of 0.015µm3 and a maximum of 14.69µm3.

Morphometric properties of LGN terminal boutons synapsing on relay cell dendrites

A main aim of this study was to arrive at a model that allowed for the classification of geniculate terminals from distinct origins based on a terminal's quantitative and qualitative features. In order to reveal the morphometric properties of input terminals that contribute to geniculate synaptic circuitry, I examined the volume frequency distribution of all reconstructed terminals in dataset A. The frequency distribution histogram of terminal volumes revealed a non-normal distribution with multiple peaks, many small terminals, and a few very large terminals (Figure 3c&d), suggesting that terminals captured in the dataset constitute a heterogeneous group, representing multiple origins. This is consistent with previous studies: ultrastructural surveys of the LGN have shown that inputs of different origins have distinct terminal size distributions (Erişir et al., 1998; Guillery, 1969a; Montero, 1991; Van Horn et al., 2000; Wilson, Friedlander, & Sherman, 1984).

In order to discern inputs from different origins in the SBEM dataset, I used a multivariate clustering approach to reveal the quantitative parameters of distinct populations that make up the observed distribution of terminal volumes in the LGN. The BIC analysis of the

terminal volume distribution of dataset B revealed that the best fit for my data was six different populations with unequal variances (Figure 3a). Using this model and the MClust package, the certainty of each terminal for belonging in any subpopulation was calculated. With that analysis the terminal volume cutoff points, where the certainty of any terminal volume to belong in one or the other subpopulation was equal, were computed. Gaussian mixture-based modeling sorted the mean of each terminal population with at least 80% certainty, whereas the terminal volumes close to population cutoff values had about 47-55% certainty (Figure 3b). The cutoff values collected from the BIC analysis were then used to sort terminal volumes in dataset A into different populations based on their terminal volume (Figure 3c&d). Next, in order to qualitatively evaluate synaptic selectivity of terminal populations, terminal reconstructions of boutons in dataset A were color coded based on the population identity and reconstructed onto dendrite segments (Figure 4a-f).

In order to confirm that the terminal population cutoff values determined by BIC analysis are suitable to reveal previously estimated percent contributions of distinct input terminals to the geniculate, I used dataset B (For unbiased sampling method, and more information about this dataset, see appendix I). Moving from the smallest terminals to the largest ones, I saw that the first (smallest) population comprised 40.2% of terminals, the second population comprised 26.2% of terminals, the third population was 14.9% of terminals, the fourth population was 12% of terminals, the fifth population was 4.9% of terminals, and sixth population (the largest) was 1.72% of the population.

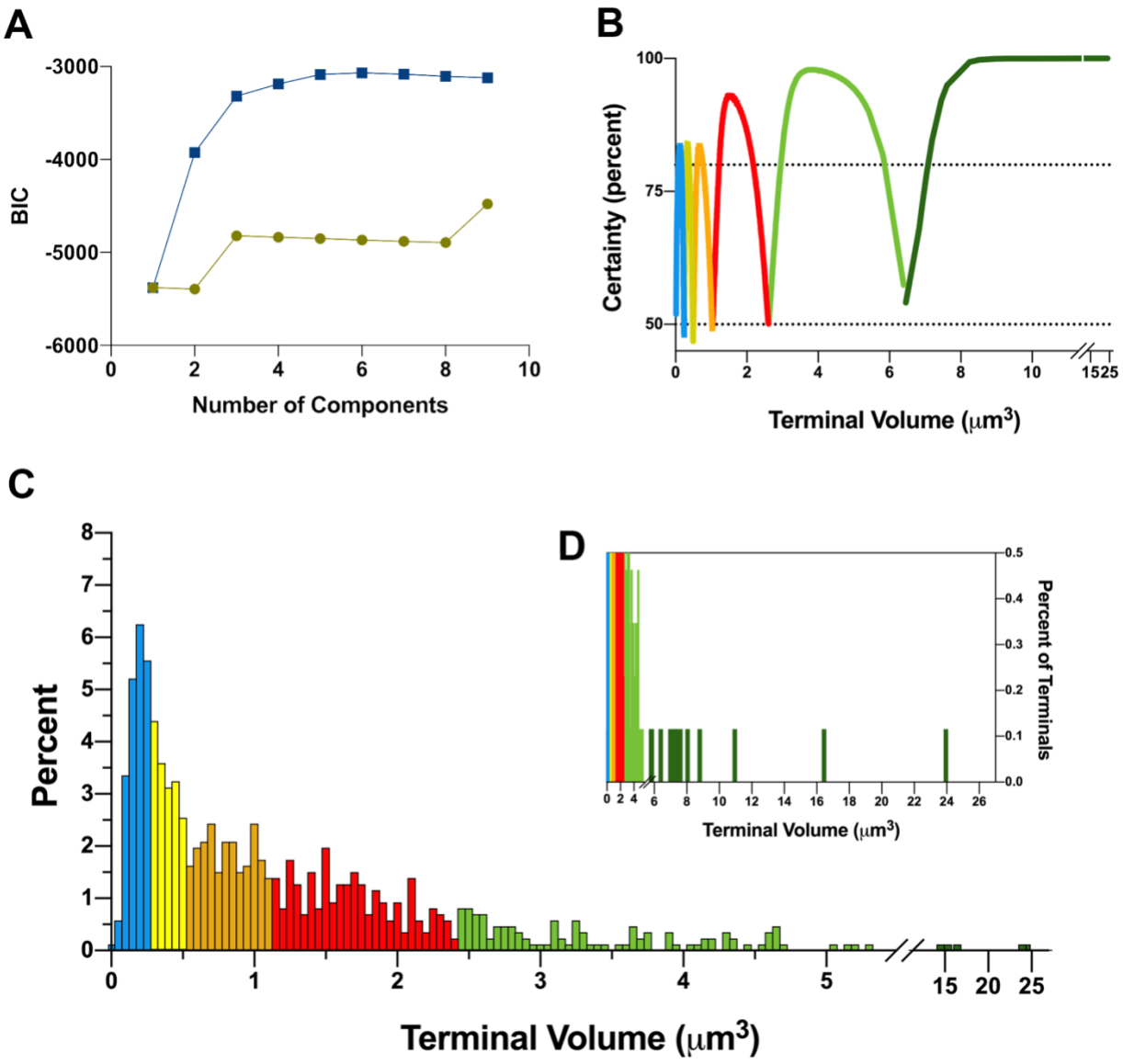

Figure 3: Gaussian finite mixture modeling of terminal volumes synapsing onto relay cell dendrites in the mouse LGN. (A) BIC analysis shows the distribution of terminal volumes in the LGN is made of 6 populations of normally distributed terminal volumes. BIC analysis demonstrates a superior fit for each population of terminals displaying unequal variance (blue line) versus equal variance (green line). (B) Certainty estimation of terminal sorting using BIC criteria for each terminal volume. The certainty of terminal sorting decreases closer to the cutoff

value between populations (C&D) Terminal volume distribution of terminals synapsing onto relay cell dendrites in the LGN. Terminal volumes can be sorted into the 6 input populations, demonstrating the contribution of each population to all terminals in the LGN. Each population is represented by a different color.

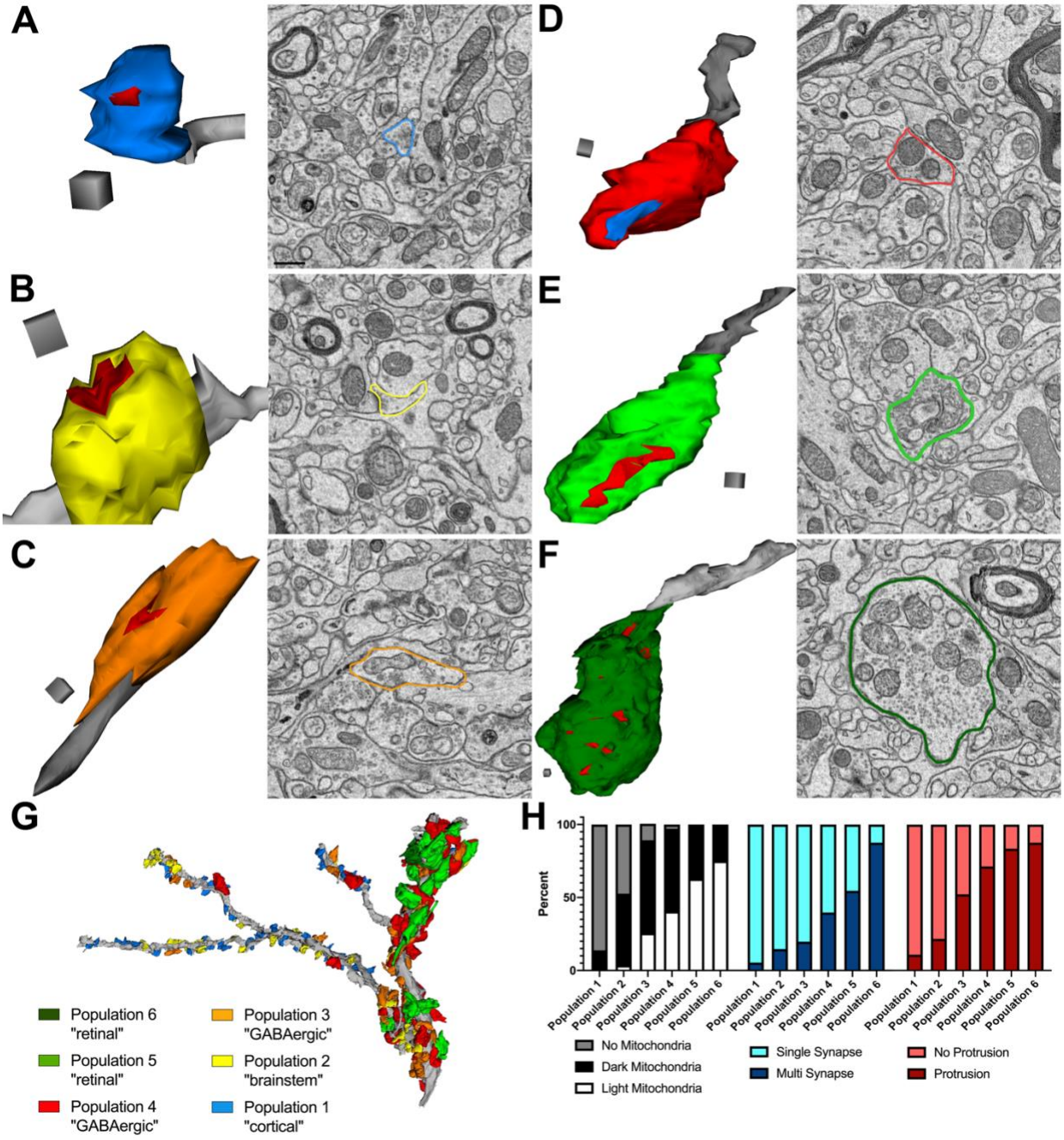

Figure 4: Representative examples of terminals in each population. The left is a 3D reconstruction of the terminal (in color) as well as the neck of the axon (grey). The right is a cross section of the same terminal from one image in the SBEM stack. (A&B) Terminals in

Populations 1 and 2 are small and contain few to no mitochondria, a single synapse and very few protrusions; Population 1 = blue, Population 2 = yellow. (C&D) Terminals in Populations 3 and 4 have a mix of light and dark mitochondria, most have a single synapse and over half contain protrusions; Population 3 = orange, Population 4 = red. (E&F) Terminals in Populations 5 and 6 contain mostly light mitochondria, the majority form multiple synapses and almost all contain protrusions; Population 5= Light green, Population 6 = dark green. (G) After terminal sorting, terminals were reconstructed onto the dendrite with appropriate color coding for qualitative descriptions of terminal targeting. (H) Quantification of morphological characteristics from each terminal population; Scale bar = 1μm, Scale cube =1x1x1μm.

The percent of the total population composed by each population of terminals was compared to those collected in previous studies using TEM in order to determine the putative origin of each population (Table 1; Erişir, Van Horn, Bickford, et al., 1997; Erişir et al., 1998; Hammer et al., 2014; Van Horn et al., 2000).

TABLE 1.

% Terminals in SBEM Stacks		% Terminals in TEM Images	
Population 1 + Population 2	66%	Cortical and Brainstem	60%
Population 3 + Population 4	27%	GABAergic	33%
Population 5 + Population 6	7%	Retinal	3-6%

These comparisons are consistent with a classification scheme in which Population 1, with smallest terminal sizes and the largest contribution to the geniculate circuitry, represents corticothalamic terminals. Similarly, Population 2, which has the second smallest terminal volumes and the second largest contribution to the geniculate circuitry, represent the cholinergic brainstem inputs. Population 3 and 4, the medium sized terminals that collectively bring ⅓ of all synapses to the LGN, represent putative GABAergic terminals, including interneuron dendritic appendages, interneuron axon terminals and axons terminals of cell located in the thalamic reticular nucleus. Population 5 and 6 are the largest sized terminals that provide <7% of the synapses in the LGN, and they largely represent retinal terminals.

Comparison of volume versus morphology terminal sorting methods

The earliest studies that described morphological properties of distinct input terminals of geniculate synaptic circuitry in minute detail did not have access to immunohistochemistry and non-degenerative tract-tracing methods. However, subsequent studies have confirmed that terminals that were described as RLP come from retina; those described as RSD come from the cortex and the brainstem; and the medium sized terminals from inhibitory cells (Erişir, Van Horn, Bickford, et al., 1997; Guillery, 1969a; Hammer et al., 2014; Morgan et al., 2016). The electron-contrast of membranes and cytoplasm of mitochondria in terminals continues to serve as a reliable criterion of terminal origin identification: retinal terminals have pale mitochondria, whereas other terminals contain dark mitochondria (Behan, 1982; Guillery, 1969b). In addition, presynaptic dendrites of interneurons can be identified as such when a terminal is observed to both receive and send a synapse.

In order to confirm whether or not the terminal volume sorting method used in this study was able to capture the morphological criteria used to sort the terminals in my dataset to their putative origins, I re-evaluated the reconstructed geniculate terminals in dataset A based on their morphological features including mitochondria, synapse and protrusions in each population (Figure 4h). Second, I compared terminal sorting based on only morphological features to sorting based on volume, and evaluated relative reliability of each method. For this, I examined terminal volumes which fell under the cutoff criterion of two adjacent distributions, and found that pale mitochondria was not exclusive to large boutons: Twenty five percent of Population 4 terminals with a volume that overlaps with the distribution of terminals in Population 5, displayed pale mitochondria. Similarly, about 13% of terminals with a volume less than 1 micron (cut off point

for Populations 3 and 4) also contained light mitochondria. Two possible scenarios would be consistent with this finding: 1) Geniculate circuitry contains really small retinal terminals, as would be evidenced by the light mitochondria in Populations 1-2 (presumed corticothalamic and brainstem terminals); or 2) mitochondria density is not a reliable criterion to sort terminals in SBEM images. I find scenario 2 more plausible because TEM morphology tissue preparation approaches (which coined the pale mitochondria terminology and criteria) rarely yield identification of very small terminals with light mitochondria. In those studies, small terminals display dark mitochondria exclusively. I posit that instances of pale mitochondria detected in SBEM material is a function of the capacity of different embedding and contrasting agents used in SBEM and TEM processes to differentiate electron density gradations in the respective tissues. Also to speaking to the unreliability of morphological criteria of mitochondria electron-density in SBEM stack images, we observed several terminals containing mitochondria with ambiguous opacity that could not be confirmed to be pale or dark, confirmed interneuron presynaptic dendrites with pale mitochondria, and a few terminals that contained both pale and dark mitochondria (Figure 5). Overall I conclude that although some terminals can be missorted based on volume (those remain under the cut-off criteria), still more others would have been missorted if only based on morphological characteristics. This is especially true when using mitochondria opacity as a terminal identifier as we observed some mitochondria opacity that did not agree with known terminal origin and other mitochondria opacities to be ambiguous.

On the other hand, of the terminals sorted into Population 5 (putative retinal) by volume, only 3% were confirmed to be interneuron dendrite terminals by their morphology, suggesting

that cut-off criteria for Population 4 and 5 is reliable for differentiating retinal terminals from interneuron dendritic terminals.

Terminal targeting of LGN relay cell dendrite segments

After identifying putative terminal input origins, I next asked if there was targeting of specific dendrite segments by terminals from different origins. To answer this question, I first had to determine what characteristics could be used to define differences between dendrite segments. Previous studies made the assumption that dendrites with smaller calibers represented more distal dendrites, while dendrites with larger calibers represented proximal dendrites (Erişir, Van Horn, Bickford, et al., 1997; Wilson et al., 1984). However, I observed that this was not always the case. In order to classify relay dendrite segments by size, I again employed a BIC-based gaussian distribution to sort dendrites based on dendrite caliber (Figure 6b&c). The analysis determined that there were three populations of dendrite sizes, and thus they will be referred to as small, medium and large dendrites. My data showed that of 17 primary dendrite segments, two are small in size and 12 are medium sized (Figure 6a). Overall, the distribution of primary dendrite calibers showed significant overlap with calibers of secondary and tertiary dendrites. Because of this, I treated dendrite order and dendrite caliber as two independent variables. A non-parametric regression test showed that calibers of primary, secondary, and tertiary dendrites were statistically different; however, it should be noted that there was a large variance in size of primary and secondary dendrites, which may contribute to this significance (Figure 6d). Although a larger sample size is needed to make large predictions about the relationship between dendrite order and caliber, overall I conclude that dendrite caliber is not predictive of branch

order, and it is not accurate to make the assumptions that smaller caliber dendrites are always distal, and larger caliber dendrites are always proximal. TEM studies have shown there is a selectivity for smaller terminals to synapse onto smaller caliber dendrites in the thalamus (Erişir, Van Horn, Bickford, et al., 1997; Wilson et al., 1984). Here, I again asked if there was a terminal selectivity onto dendrite segments, and further asked if this selectivity was more strongly correlated to dendrite caliber or dendritic branch order. First, I asked if there was a direct correlation between terminal volume and dendrite caliber. To answer this, I did a linear regression on paired terminal volume and dendrite caliber data points. The regression of this data showed that there was no linear relationship between these two variables (R_2=0.01, Figure 7a).

Next, I compared percent of terminals synapsing onto dendrite segments categorized first by branch order and then by size. My results showed that terminals from different dendrite origins targeted specific dendrite segments. The smallest terminals in Populations 1 and 2 primarily synapsed on tertiary dendrites; medium-sized terminals from Populations 3 and 4 synapsed on all dendrite orders but showed a slight preference for secondary dendrites; and large terminals from Populations 5 and 6 synapsed the most on primary and secondary dendrites, with a stronger preference for primary dendrites (Figure 7b-d). In order to determine if dendrite order or size were more predictive of terminal targeting, I ran a two-tailed ANOVA for each terminal population versus either dendrite order or size. I also ran a factor analysis to determine if the variables of dendrite order and size could be combined for more accurate terminal targeting predictions. The results of this statistical testing is shown in table 2. For terminal Populations 1, 2, and 4, dendrite order was predictive of terminal targeting. However, factoring in both dendrite size and order created a stronger prediction for Population 1 terminal targeting. Terminal

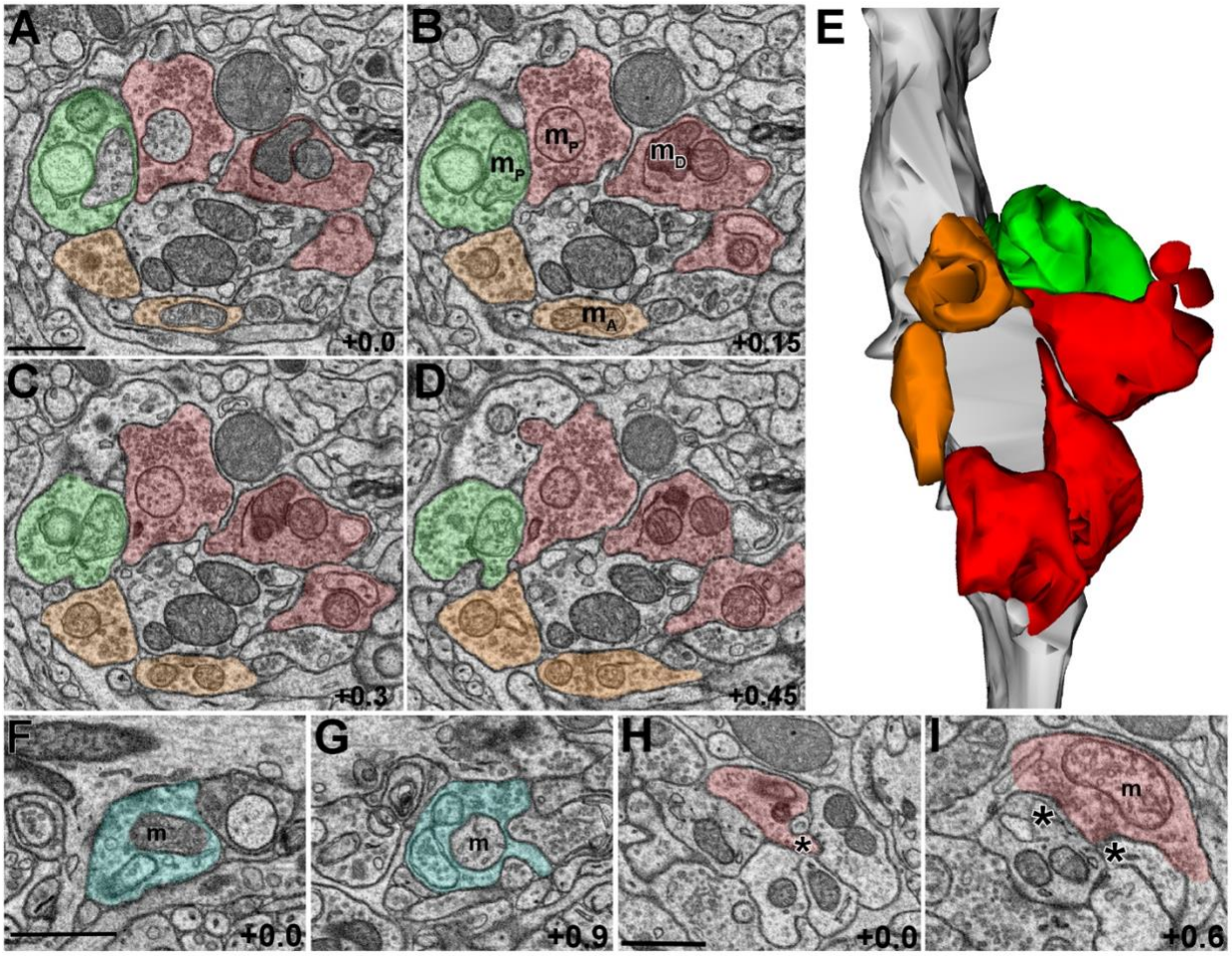

Figure 5: Varying mitochondria opacity in geniculate terminals. (A-D) A group of 6 terminals synapsing onto a relay cell dendrite. (B) Mitochondria in some terminals can be identified as pale (mP) some are dark (mD) but others have ambiguous coloring and cannot reliably be classified as pale or dark (mA). (E) A 3D reconstruction of terminals in A-D. (F-G) A geniculate terminal with both dark (F) and pale (G) mitochondria (m). (H-I) An identified presynaptic interneuron dendrite with pale mitochondria (m), postsynaptic cleft marked with asterisk; scale bar = 1μm.

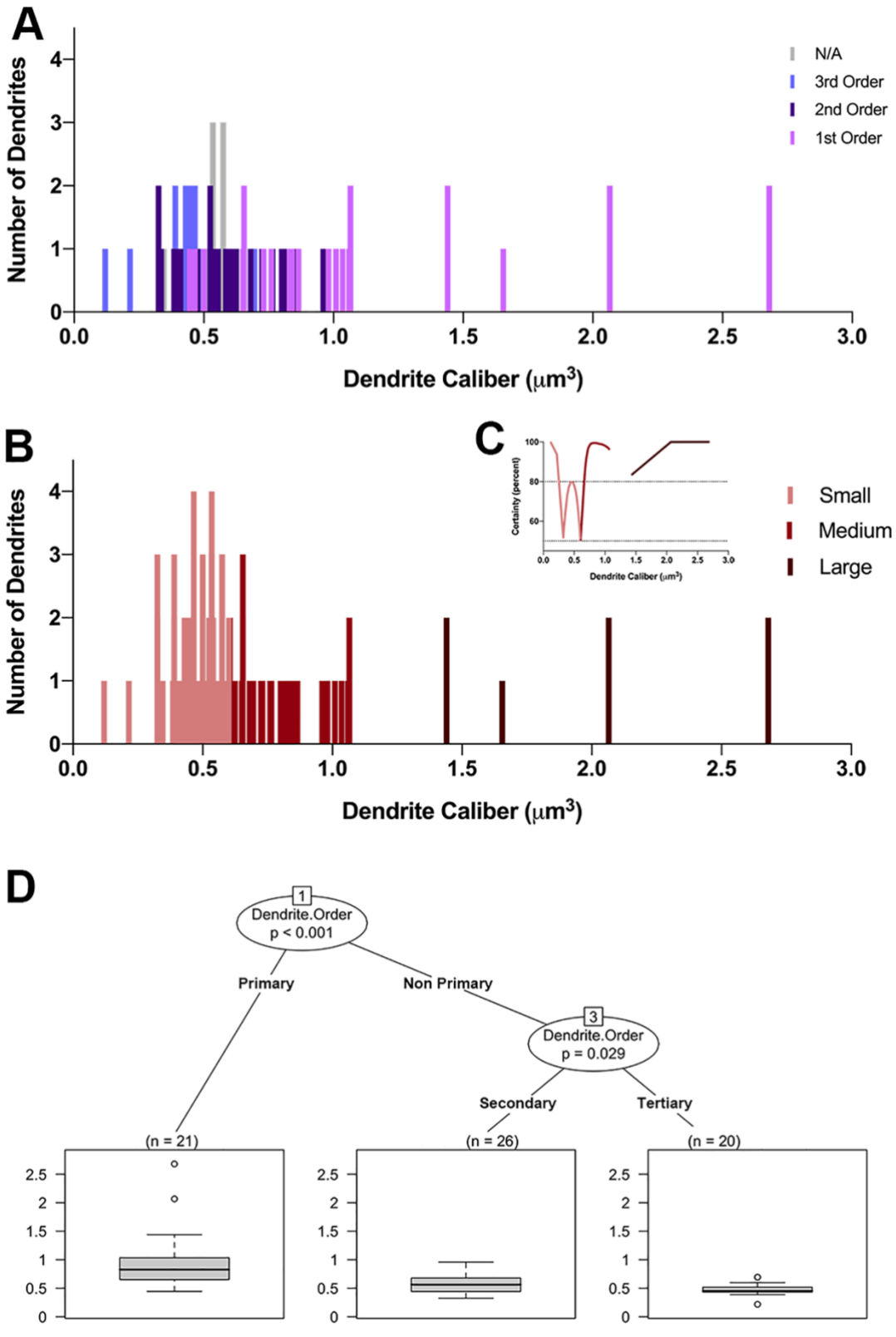
A
Number of Dendrites
Dendrite Caliber (μm³)
N/A
3rd Order
2nd Order
1st Order
B
Number of Dendrites
Dendrite Caliber (μm³)
Small
Medium
Large
C
Certainty (percent)
Dendrite Caliber (μm³)
D
1
Dendrite.Order
p < 0.001
Primary
Non Primary
3
Dendrite.Order
p = 0.029
Secondary
Tertiary
(n = 21)
(n = 26)
(n = 20)

Figure 6: Dendrite caliber distributions categorized either by branch order or size. (A) Dendrite caliber distribution color coded for dendrite order. (B&C) Dendrite caliber distribution color coded for dendrite size based on BIC analysis (inset). (D) Nonparametric regression tree shows that primary, secondary, and tertiary dendrites have significantly different dendrite calibers.

Population 5 targeting may also be predicted by the combined factors, but this had low significance. Terminal Populations 3 and 6 targeting was not predicted by dendrite order, size, or a combination of the two factors.

In addition to asking about dendrite targeting by specific input populations, I also asked if triadic arrangements have specificity for dendrite segments. Triads were sparse and selective in my dataset: only 15 (out of 81) dendrite segments from 9 dendrites contained triads. While some dendrites had only one triad, four dendrites had multiple triads on different dendrite segments, suggesting that triads can be more prominent features of selective relay cell types. Dendrites that contained triads showed variability in their morphology. The average dendrite diameter of segments containing triads was 0.65μm, with 60% medium sized and 40% small sized. I asked whether triadic arrangements are selective for dendrite branch order. My results showed that 40% of dendrite segments (6) with triads were primary, 20% (3) were secondary, and 40% (6) were tertiary branches.

In order to determine if terminal targeting differed between different relay cell types in the LGN, I studied terminal targeting onto primary dendrites. My data set contained 20 primary dendrites. These were identified as such because they were either seen emerging from the soma, or they displayed morphological characteristics known to markers of primary dendrites (i.e. dark cytoplasm, somatic organelles). I first separated primary dendrites into small, medium, and large, based on my earlier dendrite size criteria. Out of the 20 primary dendrite segments, one was small, 16 were medium, and 3 were large. The sizes of terminals synapsing onto different sized primary segments were significantly different from each other (Kruskal-Wallis, $p=0.042$). I also observed that the small primary dendrite was the only one to have terminals from the

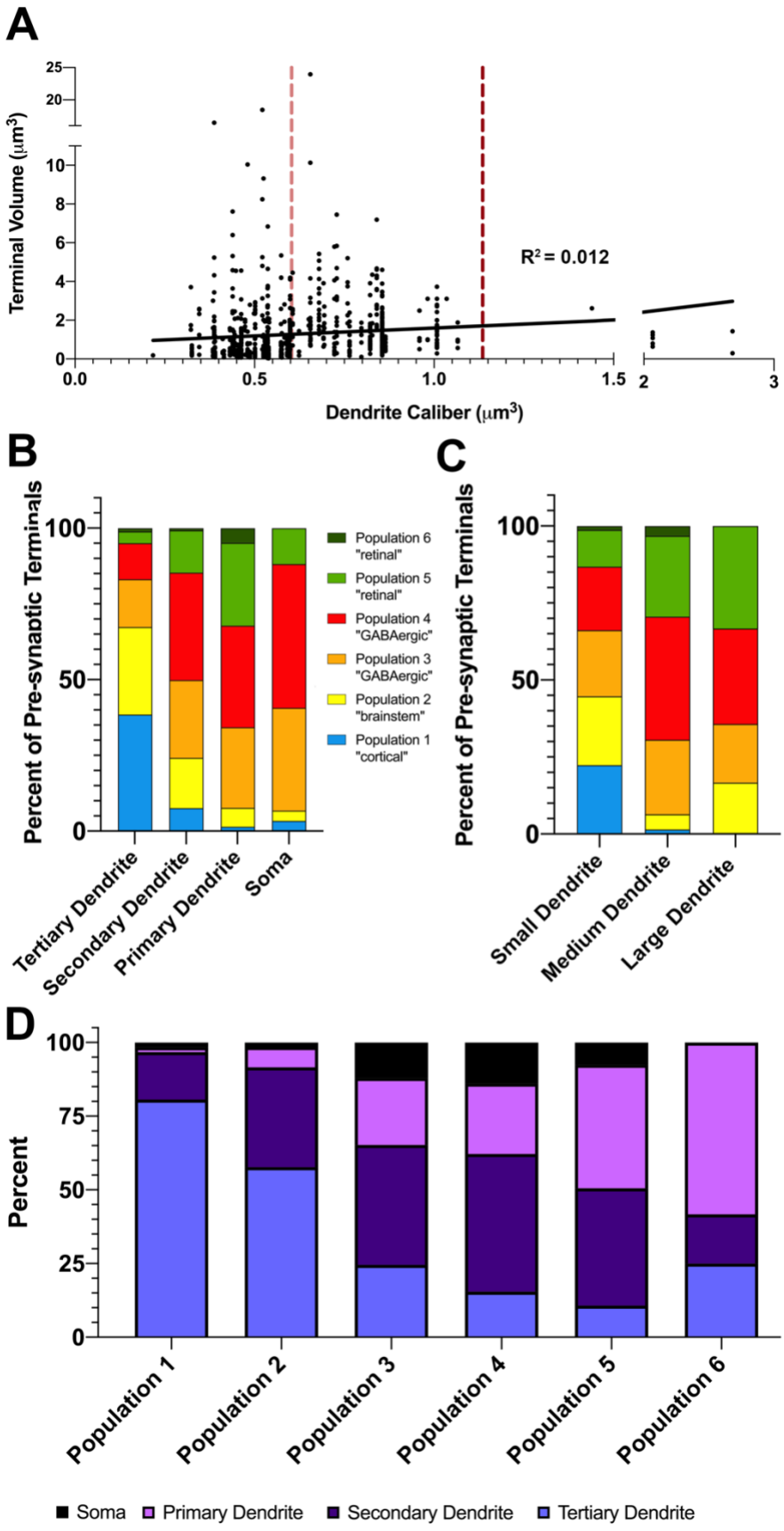
A
Terminal Volume (μm³)
25
20
10
8
6
4
2
0
0.0
0.5
1.0
1.5
2
3
R² = 0.012
Dendrite Caliber (μm³)
B
Percent of Pre-synaptic Terminals
100
50
0
Population 6 "retinal"
Population 5 "retinal"
Population 4 "GABAergic"
Population 3 "GABAergic"
Population 2 "brainstem"
Population 1 "cortical"
Tertiary Dendrite
Secondary Dendrite
Primary Dendrite
Soma
C
Percent of Pre-synaptic Terminals
100
50
0
Small Dendrite
Medium Dendrite
Large Dendrite
D
Percent
100
75
50
25
0
Population 1
Population 2
Population 3
Population 4
Population 5
Population 6
Soma
Primary Dendrite
Secondary Dendrite
Tertiary Dendrite

Figure 7: Terminal targeting onto relay cell dendrites in the LGN. (A) A paired linear regression between dendrite caliber and terminal volume show that the two variables are not directly correlated. Dotted lines represent cutoff values between small, medium and large dendrite sizes. (B) Percent of terminals from each population synapsing onto dendrite segments categorized by branch order. (C) Percent of terminals from each population synapsing onto dendrite segments categorized by size. (D) Percent each dendrite branch order is targeted by different terminals populations.

Table 2.			
Terminal Population	Dendrite Order p value	Dendrite Diameter p value	Factor Combining Order and Diameter p value
1	<0.001**	0.414	<0.001***
2	0.008**	0.5	0.039*
3	0.396	0.76	0.569
4	0.018**	0.876	0.023*
5	0.291	0.478	0.068
6	0.143	0.278	0.692

smallest-size population synapsing onto it. This small dendrite also had a large percent of terminals from Population 2 synapsing onto it. In contrast, the medium and large primary dendrites had very few terminals from Population 1 or 2, and the majority of terminals were from the larger sized terminal populations (Populations 3-6). Although my sample size of primary dendrites proved too small to be differentiated into relay cell types, these results show that primary dendrites of different sizes receive different input organizations and suggest that primary dendrite diameter could be a feature of a specific type of relay cell.

I next asked if there was selectivity for different populations of terminals synapsing onto the same dendrite segments together. For this, I used a basket analysis to determine association rules between different terminal populations on the same dendrite segment (Hahsler et al., 2005). Results from this test showed the confidence of the “if” terminal synapsing onto the same dendrite segment as the “then” terminal (Figure 8a). Confidence values showed that terminals of similar size show a strong association to each other and terminals in Populations 3 and 4 show a

strong association with most other terminal populations. In order to probe associations between terminals, I used the centrality measure of out-strength. Out-strength determines the centrality of a node (terminal population) by summing the weights coming from one node contacting all other nodes in the network. My results showed that Population 6 had the largest out-strength (Figure 8b). The topology of association confidence values and out-strength are summarized in a network map (Figure 8c). These results suggest that retinal terminals were closely associated with each other but rarely synapse onto the same dendrite segment as cortical or brainstem terminals whereas inhibitory inputs associate will all other terminal types.

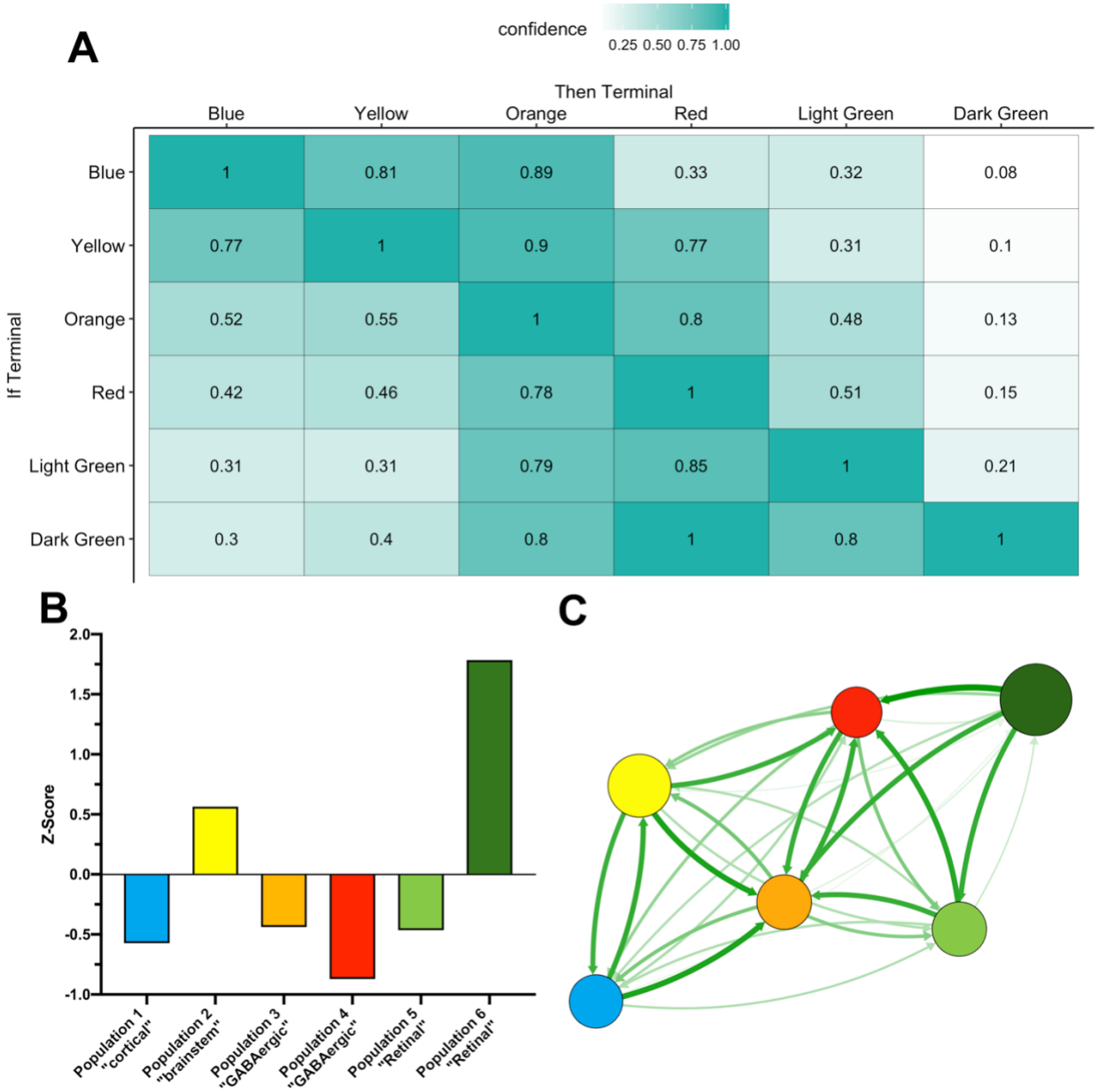

Figure 8: Associations between terminals of different populations synapsing onto the same dendrite segments. (A) A Heat map of terminal association rules. When the ”If terminal” is present on a dendrite the square represents the confidence that the “then terminal” will synapse on the same dendrite segment. (B) Z-scores of the out-strength of each terminal population. This

measures which terminal population is the most influential when determining which terminal populations are more likely to synapse together on the same dendrite segment. (C) Network map of terminal associations. Nodes and their colors represent different terminal populations. The size of the node represents out-score, the larger the node, the larger the out-score. The opacity of the arrow represents confidence of association and the direction of the arrow illustrates the directionality of the association.

DISCUSSION

The aim of this study was twofold. The first was to devise a strategy for determining putative origin of terminals synapsing onto relay cell dendrites in the LGN. My results showed that terminal volumes could be used to accurately determine terminal subpopulations and that these subpopulations reflected the origin of terminals synapsing in the LGN.

The second aim of this study was to characterize patterns of driving and modulatory synaptic inputs onto LGN relay cell dendrite segments. Results showed that 1) putative retinogeniculate terminals synapse onto primary dendrite segments or larger caliber secondary dendrite segments; 2) putative modulatory inputs from the brainstem and inputs that bring feedback excitation form cortex synapse onto tertiary dendrite segments, or small caliber dendrites even if they are primary dendrites; and 3) putative GABAergic inputs synapse onto all dendrite segments indiscriminately. I also show that terminals from the cortex and brainstem very rarely synapse on the same dendritic segments as the retinal terminals. These results suggest that while there is somewhat of a selectivity of distinct terminal types for dendrites with certain characteristics, there is an almost complete segregation of corticothalamic and brainstem inputs from the retinal inputs on the relay cell dendrites. . The level of segregation of inputs that bring feedforward (retinal) and feedback (corticothalamic) excitation on relay cells reported in this study is novel, and implies compartmentalization of network influences on relay cells.

Methodological Considerations

Recent advances in 3D serial imaging technology made up for several shortcomings of 2D TEM: 1) Quantitative approaches used with 2D material provide estimated inferences for the

terminal size, while 3D material allows for direct volume measurements for terminal boutons. 2) In theory, the terminal size (cross-section area) frequency distributions for 2D material yield a non-normal distribution even if the population is normally distributed. This introduces an unresolvable factor for computations using multi-population data, and ambiguates potential size-separation of subpopulations. Volume distributions obtained with 3D material do not have this confound. 3) 3D reconstructions are the only way to reliably visualize complex synaptic interactions. 4) Questions that involve organization in 3D space (such as the selectivity of inputs to primary secondary or tertiary dendrite branches) can only be addressed by using 3D EM. Because of these advantages offered by SBEM, I was able to collect an accurate representation of the distribution of terminal sizes in the LGN and to characterize the organization of inputs onto geniculate relay cell dendrite segments. These results do not contain confounds or assumptions that can be introduced by TEM methods. Although SBEM offered several advantages to me in the course of this work, collecting data for this study also brought to light some disadvantages that should be considered before using this technique. The first is that mitochondria opacity, although used accurately to identify terminals in TEM tissue, may not be as suitable a criteria for terminal identification in SBEM images. Second, although the size of the image stack used in this study was sufficient to answer the questions I posed here, larger and wider image stacks would be necessary to study long distance properties.

Terminal Sorting and Putative Origin Identification

In order to fully understand how inputs from terminals affect relay cell firing, it is important to know from where in the brain these terminals originate. However, one of the biggest

drawbacks of using SBEM to study synaptic circuitry is the current inability to use immunohistochemical methods to identify input origin. To approach this obstacle from an alternative angle, I employed distribution modeling combined with knowledge of terminal size distribution data from past TEM studies to estimate a range of terminal volumes for each input into the LGN. I showed that using Gaussian-based normal distribution modeling is a reliable way to determine the putative origin of terminals given a large set of terminal volume data.

Populations of terminals can be divided by input origin based on the overall contribution to the total number of terminals in the brain region. Previous tEM studies have shown that retinal terminals in the LGN are the largest but most sparse, inhibitory terminals are medium sized and constitute about a third of LGN terminals, and cortical and brainstem inputs are the smallest but most numerous terminals in the LGN (Erişir, Van Horn, & Sherman, 1997; Guillery, 1969a; Van Horn et al., 2000). With this information in mind, I was able to assign putative origin of terminals in SBEM stacks using only terminal volume. The largest and most sparse terminals from Population 5 and 6 were putative retinal terminals, medium sized terminals in Populations 3 and 4 were putative GABAergic terminals from interneurons and the thalamic reticular nucleus, and the smallest and most abundant terminals in Populations 1 and 2 were putative cortical and brainstem inputs respectively.

Apart from immunohistochemical techniques, there are some morphological features of terminals that can be used to identify terminal origin. Retinal terminals are often described as having an "RLP" morphology, meaning they have **r**ound vesicles, are **l**arge, and have **p**ale mitochondria (Behan, 1982; Guillery, 1969b). Mitochondrial color in particular is used to identify retinal terminals in these instances. Presynaptic interneuron dendrites are easily

identified by the presence of a terminal that both sends and receives a synapse (Bickford, Carden, & Patel, 1999; Casagrande, Royal, & Sáry, 2006; Guillery, 1966; Krahe, El-Danaf, Dilger, Henderson, & Guido, 2011; Parnavelas, Sullivan, Lieberman, & Webster, 1977; Rafols & Valverde, 1973). In TEM preparations, inhibitory synapses can be differentiated by junctional properties: GABA immunopositive terminals often display symmetrical synapses (the pre and postsynaptic membranes are equal thickness; versus excitatory synapses that have asymmetric morphology with thick postsynaptic densities). However, this property is not easily detected in SBEM images, which have lower resolution value than the images that can be achieved with TEM. Therefore, no morphological characteristics can be used to differentiate GABAergic terminals of axonal origin (i.e. from the axons of interneurons or from the thalamic reticular nucleus) in SBEM stacks. Similarly, TEM studies using track-tracing and immunohistochemistry have revealed that the terminals formed by corticothalamic and brainstem axons are similar in size, with brainstem terminals being slightly larger.

The volume sorting approach designed in the current study was able to differentiate two distinct populations that fell in the smaller range of the all terminals, speaking for the utility value of my approach. In order to further evaluate the accuracy of my terminal sorting technique, I compared my assigned putative terminal origin to those morphological features used by others to identify terminal origin. I demonstrated that, although many terminals with pale mitochondria fit the morphological criteria of a retinal terminal (also large with many protrusions), I also observed some small terminals and confirmed interneuron dendrite terminals with pale mitochondria. In addition, there were some mitochondria that were too ambiguous to be considered pale or dark and thus were not suitable to be used for terminal origin

identification. I also saw a few instances of terminals that contained both pale and dark mitochondria. Although defining terminal origin by volume did not sort every terminal perfectly, I was able to identify putative terminal origin with little mis-sorting while also being able to identify putative origin of previously ambiguous terminals with no distinct morphological properties (i.e. terminals from the cortex, brainstem, and inhibitory axons).

Dendrite Characteristics

Past studies using TEM have made the assumption that postsynaptic dendrites with a large caliber belong exclusively to primary dendrites and that terminals synapsing onto these dendrites are closer to the soma (Erişir, Van Horn, Bickford, et al., 1997; Wilson et al., 1984). Here I show that these assumptions about dendrite caliber are not correct. My results demonstrate that, although relay cell dendrites do indeed decrease in caliber as they branch, this does not speak to the initial caliber of the primary dendrite. The caliber of some primary dendrites traced in this study can be considered small, while others are medium or large. I also demonstrate that the assumption cannot be made that terminals synapsing onto dendrites with thicker calibers are closer to the cell body than those synapsing onto thinner dendrites. Cable properties still apply to dendrite caliber in that thicker dendrites will have less resistance and therefore will propagate a stronger signal than that of thinner dendrites. However, it is no longer accurate to make the assumption using TEM that dendrite caliber is indicative of branch order or distance from the soma. Because of this, when studying terminal targeting onto dendrite segments, I considered dendrite caliber and branch order as two separate variables.

Terminal Targeting of LGN Relay Cell Dendrite Segments

The majority of work describing synaptic circuitry in the LGN focuses on retinal inputs onto relay cell dendrites (Dacey, Peterson, Robinson, & Gamlin, 2003; Kaas, Huerta, Weber, & Harting, 1978; Kaas, Ling, & Casagrande, 1976; Morgan et al., 2016; Perry, Oehler, & Cowey, 1984; Usrey, Reppas, & Reid, 1999). These studies are very informative, but do not give the full picture of synaptic inputs onto relay cells. Modulatory inputs onto relay cells play important roles in shaping the information sent to the visual cortex by relay cells. Glutamatergic cortical terminals bring feedback from the cortex, while cholinergic terminals from the brainstem cause relay cell firing to switch between burst and tonic modes (McCormick, 1992; McCormick & Prince, 1987). GABAergic terminals from the thalamic reticular nucleus provide feedback inhibition, and GABAergic interneuron dendrites provide feedforward inhibition (Augustinaite & Heggelund, 2018; Crandall & Cox, 2013; Famiglietti, 1970; Famiglietti & Peters, 1972; X. Wang et al., 2008). In order to understand the full impact of inputs onto relay cell dendrites, I characterized input patterns of all terminals onto dendrite segments.

My results show that cortical and brainstem synaptic targeting can be predicted by dendrite order and that terminals from these areas primarily target tertiary dendrite segments. Small GABAergic terminals synapsed onto all dendrite segments relatively equally, and indeed I show that synapsing by these terminals could not be predicted by either dendrite caliber nor by dendrite branching pattern. I do find that large GABAergic terminal targeting can be predicted by dendrite order and these terminals preferentially synapsed onto secondary dendrites. Large GABAergic terminals were also more likely to be found forming triads in glomerular

arrangements, and thus it can be speculated that small GABAergic terminals may be from the reticular nucleus, whereas large GABAergic terminals come from interneurons.

In addition to studying terminal targeting of modulatory inputs into the LGN, I also characterized targeting patterns of the driving terminals from the retina onto LGN dendrite segments. Although statistical analysis showed that dendrite order and caliber are both not predictive of retinal terminal targeting, this may be due to the fact that retinal terminals target primary and secondary terminals at the same rate, whereas they target tertiary dendrites very rarely. In most instances in which retinal terminals were targeting tertiary dendrites, it was in a triadic arrangement with other large terminals.

Differential targeting of dendrite segments by axon terminals from different origins is more nuanced than was originally found by TEM studies, and I show that this targeting is driven by different dendrite characteristics depending on their origin. It is possible that there are more factors in play than those I have studied here. For instance, neurotransmitter receptors on postsynaptic targets play a large role in signal transduction and I can then assume they may play a role in axon targeting. Future studies should continue to gain a more complete picture of the factors that influence terminal targeting of LGN axons in order to gain a fuller understanding of how information is processed in the LGN before reaching the cortex.

Terminal Targeting Association Rules

Spatial summation of neuronal inputs down a dendrite can have a large impact on firing in the postsynaptic cell (Bloomfield, Hamos, & Sherman, 1987). Thus, it is important to understand how different inputs interact on dendrite segments and how close the association is

between terminals from different origins. My results showed that terminals from different origins have varying associations with each other. Terminals from the cortex and brainstem were closely associated with each other and synapse onto the same dendrite segment a majority of the time. Retinal terminals were closely associated with each other but rarely synapse onto the same dendrite segment as cortical or brainstem terminals. All terminal populations were closely associated with GABAergic terminals. This makes sense considering the diverse functions that GABAergic terminals have on LGN synaptic circuitry. Overall, small terminals that act in a modulatory capacity (i.e. terminals from the brainstem and cortex) synapsed onto smaller, higher-order dendrites, GABAergic terminals synapsed onto all dendrite segments, and retinal terminals synapsed onto larger, lower-order dendrites.

Although I determined terminal targeting associations, I also wanted to determine what terminals were driving these associations. My results showed that, based on out-strength, retinal terminals and cholinergic terminals had the greatest impact on where cortical and inhibitory terminals were synapsing. The implications of this are that more information about terminals synapsing onto a dendrite segment can be inferred if a confirmed retinal or cholinergic terminal is seen on that dendrite segment.

Considerations on Parallel Pathways in the Mouse LGN

The results of this study characterized in detail the targeting properties of inputs onto relay cell dendrites in the LGN. However, none of my analyses were able to separate dendrites into distinct parallel pathways. This result, combined with the results found by Morgan et al., lead us to consider why I have been unsuccessful in my attempts to characterize input differences

in different parallel pathways in the LGN of the mouse (Morgan et al., 2016). It is possible that parallel pathways through the mouse LGN are not as cut and dried as those in the cat, tree shrew, or primate. It may be prudent for future studies focusing on parallel pathways in the LGN to consider an animal model with clearly defined and spatially segregated parallel pathways through the LGN in order to fully understand how inputs differ between separate visual streams.

Acknowledgments

I thank all of the research assistants that contributed to the tracing and reconstruction in this study including: Alisson Baya, **Alex Briegel,** Kaya Burn, Alex Coffin, Elif Keskinoz, Melissa Liu, L Waller, and Sydney Rohlwing. I also thank Robert Moulder and Hudson Golino for assistance with R coding.

LITERATURE CITED

Augustinaite, S., & Heggelund, P. (2018). Short-term Synaptic Depression in the Feedforward Inhibitory Circuit in the Dorsal Lateral Geniculate Nucleus. *Neuroscience*, *384*, 76–86. https://doi.org/10.1016/j.neuroscience.2018.05.022

Behan, M. (1982). A quantitative analysis of the ipsilateral retinocollicular projection in the cat: An EM degeneration and EM autoradiographic study. *Journal of Comparative Neurology*, *206*(3), 253–258. https://doi.org/10.1002/cne.902060305

Bickford, M. E., Carden, W. B., & Patel, N. C. (1999). Two types of interneurons in the cat visual thalamus are distinguished by morphology, synaptic connections, and nitric oxide synthase content. *Journal of Comparative Neurology*, *413*(1), 83–100. https://doi.org/10.1002/(SICI)1096-9861(19991011)413:1<83::AID-CNE6>3.0.CO;2-E

Bickford, M. E., Slusarczyk, A. S., Dilger, E. K., Krahe, T. E., Kucuk, C., & Guido, W. (2010). Synaptic development of the mouse dorsal lateral geniculate nucleus. *Journal of Comparative Neurology*, *518*(5), 622–635. https://doi.org/10.1002/cne.22223

Bloomfield, S. A., Hamos, J. E., & Sherman, S. M. (1987). Passive cable properties and morphological correlates of neurones in the lateral geniculate nucleus of the cat. *The Journal of Physiology*, *383*(1), 653–692. https://doi.org/10.1113/jphysiol.1987.sp016435

Butts, C. T. (2008). Social network analysis with sna. *Journal of Statistical Software*, *24*(6). https://doi.org/10.18637/jss.v024.i06

Casagrande, V. A., Royal, D. W., & Sáry, G. (2006). Extraretinal Inputs and Feedback Mechanisms to the Lateral Geniculate Nucleus (LGN). *The Primate Visual System: A Comparative Approach*. https://doi.org/10.1002/0470868112.ch7

Çavdar, S., Hacioğlu, H., Şirvanci, S., Keskinöz, E., & Onat, F. (2011). Synaptic organization of

the rat thalamus: A quantitative study. *Neurological Sciences*, *32*(6), 1047–1056. https://doi.org/10.1007/s10072-011-0606-4

Chai, H., Diaz-Castro, B., Shigetomi, E., Monte, E., Octeau, J. C., Yu, X., … Khakh, B. S. (2017). Neural Circuit-Specialized Astrocytes: Transcriptomic, Proteomic, Morphological, and Functional Evidence. *Neuron*, *95*(3), 531-549.e9. https://doi.org/10.1016/j.neuron.2017.06.029

Crandall, S. R., & Cox, C. L. (2013). Thalamic microcircuits: Presynaptic dendrites form two feedforward inhibitory pathways in thalamus. *Journal of Neurophysiology*, *110*(2), 470–480. https://doi.org/10.1152/jn.00559.2012

Dacey, D. M., Peterson, B. B., Robinson, F. R., & Gamlin, P. D. (2003). Fireworks in the primate retina: In vitro photodynamics reveals diverse LGN-projecting ganglion cell types. *Neuron*, *37*(1), 15–27. https://doi.org/10.1016/S0896-6273(02)01143-1

Denk, W., & Horstmann, H. (2004). Serial block-face scanning electron microscopy to reconstruct three-dimensional tissue nanostructure. *PLoS Biology*, *2*(11). https://doi.org/10.1371/journal.pbio.0020329

Erişir, A., Van Horn, S. C., Bickford, M. E., & Sherman, S. M. (1997). Immunocytochemistry and distribution of parabrachial terminals in the lateral geniculate nucleus of the cat: A comparison with corticogeniculate terminals. *Journal of Comparative Neurology*, *377*(4), 535–549. https://doi.org/10.1002/(SICI)1096-9861(19970127)377:4<535::AID-CNE5>3.3.CO;2-Q

Erişir, A., Van Horn, S. C., & Sherman, S. M. (1997). Relative numbers of cortical and brainstem inputs to the lateral geniculate nucleus. *Proceedings of the National Academy of Sciences of the United States of America*, *94*(4), 1517–1520.

https://doi.org/10.1073/pnas.94.4.1517

Erişir, A., Van Horn, S. C., & Sherman, S. M. (1998). Distribution of synapses in the lateral geniculate nucleus of the cat: Differences between laminae A and A1 and between relay cells and interneurons. *Journal of Comparative Neurology*, *390*(2), 247–255. https://doi.org/10.1002/(SICI)1096-9861(19980112)390:2<247::AID-CNE7>3.0.CO;2-1

Famiglietti, E. V. (1970). Dendro-dendritic synapses in the lateral geniculate nucleus of the cat. *Brain Research*, *20*(2), 181–191. https://doi.org/10.1016/0006-8993(70)90287-8

Famiglietti, E. V., & Peters, A. (1972). The synaptic glomerulus and the intrinsic neuron in the dorsal lateral geniculate nucleus of the cat. *Journal of Comparative Neurology*, *144*(3), 285–333. https://doi.org/10.1002/cne.901440304

Fiala, J. C. (2005). Reconstruct: A free editor for serial section microscopy. *Journal of Microscopy*, *218*(1), 52–61. https://doi.org/10.1111/j.1365-2818.2005.01466.x

Govindaiah, G., & Cox, C. L. (2006). Excitatory actions of synaptically released catecholamines in the rat lateral geniculate nucleus. *Neuroscience*, *137*(2), 671–683. https://doi.org/10.1016/j.neuroscience.2005.09.021

Guillery, R. W. (1966). A study of Golgi preparations from the dorsal lateral geniculate nucleus of the adult cat. *Journal of Comparative Neurology*, *128*(1), 21–49. https://doi.org/10.1002/cne.901280104

Guillery, R. W. (1969a). A quantitative study of synaptic interconnections in the dorsal lateral geniculate nucleus of the cat. *Zeitschrift Für Zellforschung Und Mikroskopische Anatomie*, *96*(1), 39–48.

Guillery, R. W. (1969b). The organization of synaptic interconnections in the laminae of the dorsal lateral geniculate nucleus of the cat. *Zeitschrift Für Zellforschung Und*

Mikroskopische Anatomie, *96*(1), 1–38.

Guillery, R. W., & Sherman, S. M. (2002). Thalamic relay functions and their role in corticocortical communication: Generalizations from the visual system. *Neuron*, *33*(2), 163–175. https://doi.org/10.1016/S0896-6273(01)00582-7

Hahsler, M., Grun, B., & Hornik, K. (2005). arules – A Computational Environment for Mining Association Rules and Frequent Item Sets. *Journal of Statistical Software*, *14*(15), 1–6. Retrieved from papers2://publication/uuid/388D2132-AF39-463F-8D87-91A45FA1E26D

Hammer, S., Carrillo, G. L., Govindaiah, G., Monavarfeshani, A., Bircher, J. S., Su, J., … Fox, M. A. (2014). Nuclei-specific differences in nerve terminal distribution, morphology, and development in mouse visual thalamus. *Neural Development*, *9*(1), 1–20. https://doi.org/10.1186/1749-8104-9-16

Helmstaedter, M., Briggman, K. L., & Denk, W. (2008). 3D structural imaging of the brain with photons and electrons. *Current Opinion in Neurobiology*, *18*(6), 633–641. https://doi.org/10.1016/j.conb.2009.03.005

Hughes, L., Hawes, C., Monteith, S., & Vaughan, S. (2014). Serial block face scanning electron microscopy-the future of cell ultrastructure imaging. *Protoplasma*, *251*(2), 395–401. https://doi.org/10.1007/s00709-013-0580-1

Jones, E. G. (2002). Thalamic organization and function after Cajal. *Progress in Brain Research*, *136*, 333–357. https://doi.org/10.1016/S0079-6123(02)36029-1

Kaas, J. H., Huerta, M. F., Weber, J. T., & Harting, J. K. (1978). Patterns of retinal terminations and laminar organization of the lateral geniculate nucleus of primates. *Journal of Comparative Neurology*, *182*(3), 517–553. https://doi.org/10.1002/cne.901820308

Kaas, J. H., Ling, C. S., & Casagrande, V. A. (1976). The relay of ipsilateral and contralateral

retinal input from the lateral geniculate nucleus to striate cortex in the owl monkey: a transneuronal transport study. *Brain Research, 106*(2), 371–378. https://doi.org/10.1016/0006-8993(76)91032-5

Krahe, T. E., El-Danaf, R. N., Dilger, E. K., Henderson, S. C., & Guido, W. (2011). Morphologically distinct classes of relay cells exhibit regional preferences in the dorsal lateral geniculate nucleus of the mouse. *Journal of Neuroscience, 31*(48), 17437–17448. https://doi.org/10.1523/JNEUROSCI.4370-11.2011

Maco, B., Cantoni, M., Holtmaat, A., Kreshuk, A., Hamprecht, F. A., & Knott, G. W. (2014). Semiautomated correlative 3D electron microscopy of in vivo-imaged axons and dendrites. *Nature Protocols*, *9*(6), 1354–1366. https://doi.org/10.1038/nprot.2014.101

McCormick, D. A. (1992). Neurotransmitter actions in the thalamus and cerebral cortex and their role in neuromodulation of thalamocortical activity. *Progress in Neurobiology*, *39*(4), 337–388. https://doi.org/10.1016/0301-0082(92)90012-4

McCormick, D. A., & Prince, D. A. (1987). Actions of acetylcholine in the guinea-pig and cat medial and lateral geniculate nuclei, in vitro. *The Journal of Physiology*, *392*(1), 147–165. https://doi.org/10.1113/jphysiol.1987.sp016774

Montero, V. M. (1986). Localization of γ-aminobutyric acid (GABA) in type 3 cells and demonstration of their source to f2 terminals in the cat lateral geniculate nucleus: A golgi-electron-microscopic GABA-immunocytochemical study. *Journal of Comparative Neurology*, *254*(2), 228–245. https://doi.org/10.1002/cne.902540207

Montero, V. M. (1991). A quantitative study of synaptic contacts on interneurons and relay cells of the cat lateral geniculate nucleus. *Experimental Brain Research*, *86*(2), 257–270.

Morgan, J. L., Berger, D. R., Wetzel, A. W., & Lichtman, J. W. (2016). The Fuzzy Logic of

Network Connectivity in Mouse Visual Thalamus. *Cell*, *165*(1), 192–206. https://doi.org/10.1016/j.cell.2016.02.033

Parnavelas, J. G., Sullivan, K., Lieberman, A. R., & Webster, K. E. (1977). Neurons and their synaptic organization in the visual cortex of the rat. *Cell and Tissue Research*, *183*(4), 499–517.

Perry, V. H., Oehler, R., & Cowey, A. (1984). Retinal ganglion cells that project to the dorsal lateral geniculate nucleus in the macaque monkey. *Neuroscience*, *12*(4), 1101–1123. https://doi.org/10.1016/0306-4522(84)90006-X

Rafols, J. A., & Valverde, F. (1973). The structure of the dorsal lateral geniculate nucleus in the mouse. A golgi and electron microscopic study. *Journal of Comparative Neurology*, *150*(3), 303–331. https://doi.org/10.1002/cne.901500305

Rovó, Z., Ulbert, I., & Acsády, L. (2012). Drivers of the primate thalamus. *Journal of Neuroscience*, *32*(49), 17894–17908. https://doi.org/10.1523/JNEUROSCI.2815-12.2012

Scrucca, L., Fop, M., Murphy, T. B., & Raftery, A. E. (2016). mclust 5: Clustering, Classification and Density Estimation Using Gaussian Finite Mixture Models. *The R Journal*, *8*(1), 289.

Sherman, S. M. (2007). The thalamus is more than just a relay. *Current Opinion in Neurobiology*, *17*(4), 417–422. https://doi.org/10.1016/j.conb.2007.07.003

Sherman, S. M. (2016). Thalamus plays a central role in ongoing cortical functioning. *Nature Neuroscience*, *19*(4), 533–541. https://doi.org/10.1038/nn.4269

Sherman, S. M., & Guillery, R. W. (1996). Functional Organization of Thalamocortical Relays. *Journal of Neurophysiology*, *76*(3), 1367–1395. https://doi.org/10.1074/jbc.271.4.1849

Sherman, S. M., & Guillery, R. W. (2001). *Exploring the thalamus*. Elsevier.

Usrey, W. M., Reppas, J. B., & Reid, R. C. (1999). Specificity and strength of retinogeniculate connections. *Journal of Neurophysiology*, *82*(6), 3527–3540. https://doi.org/10.1152/jn.1999.82.6.3527

Van Horn, S. C., Erişir, A., & Sherman, S. M. (2000). Relative distribution of synapses in the A-laminae of the lateral geniculate nucleus of the cat. *Journal of Comparative Neurology*, *416*(4), 509–520. https://doi.org/10.1002/(SICI)1096-9861(20000124)416:4<509::AID-CNE7>3.0.CO;2-H

Wang, S., Eisenback, M., Datskovskaia, A., Boyce, M., & Bickford, M. E. (2002). GABAergic pretectal terminals contact GABAergic interneurons in the cat dorsal lateral geniculate nucleus, *323*, 141–145.

Wang, X., Wei, Y., Vaingankar, V., Wang, Q., Koepsell, K., Friedrich, T., & Hirsch, J. A. (2008). Feedforward Excitation and Inhibition Evoke Dual Modes of Firing in the Cat's Visual Thalamus during Naturalistic Viewing. *Neuron*, *55*(3), 465–478. https://doi.org/10.1016/j.neuron.2007.06.039.Feedforward

Wilke, S. A., Antonios, J. K., Bushong, E. A., Badkoobehi, A., Malek, E., Hwang, M., … Ghosh, A. (2013). Deconstructing complexity: Serial block-face electron microscopic analysis of the hippocampal mossy fiber synapse. *Journal of Neuroscience*, *33*(2), 507–522. https://doi.org/10.1523/JNEUROSCI.1600-12.2013

Wilson, J. R., Friedlander, M. J., & Sherman, S. M. (1984). Fine structural morphology of identified X- and Y-cells in the cat's lateral geniculate nucleus. *Proceedings of the Royal Society of London - Biological Sciences*, *221*(1225), 411–436. https://doi.org/10.1098/rspb.1984.0042

CHAPTER III

Inputs onto Geniculate Interneuron Dendrites, and Synaptic Motifs involving Triads and Glomeruli

ABSTRACT

Presynaptic interneuron dendrites play a central role in triadic arrangements in glomeruli in the lateral geniculate nucleus (LGN). Inputs onto geniculate interneurons dictate the level of inhibition released from interneurons onto relay cells. The present study aims to describe the organization of inputs onto geniculate interneurons and to determine how these inputs contribute to triadic motifs in glomeruli to modulate interneuron firing. I used serial blockface electron microscopy (SBEM) image stacks to reconstruct geniculate interneuron dendrites. We then reconstructed all synapses and terminals associated with these dendrites. Interneuron dendrites receive their primary input from large and medium sized terminals that are putative retinal and GABAergic inputs. Most inputs onto interneuron dendrites occurred in glomerular arrangements. Glomeruli contained several different triadic motifs between terminals from different origins. I also saw varying degrees of convergence and divergence of retinal input, interneuron dendrites, and relay cell dendrites between different glomeruli, indicating that interneuron dendrites may play several roles in modification of visual information depending on the other neurites involved in the glomeruli.

INTRODUCTION

The lateral geniculate nucleus (LGN) of the thalamus, which relays visual information from the retina to the cortex, consists of two major cell types: thalamocortical relay cells and inhibitory interneurons (Bickford, Carden, & Patel, 1999; Casagrande, Royal, & Sáry, 2006; Guillery, 1966; Krahe, El-Danaf, Dilger, Henderson, & Guido, 2011; Parnavelas, Sullivan, Lieberman, & Webster, 1977; Rafols & Valverde, 1973). Interneurons provide strong feed forward inhibition to the relay cells in the LGN, refining the signals from the retina before they reach the cortex (Augustinaite & Heggelund, 2018; Crandall & Cox, 2013; Famiglietti, 1970; Famiglietti & Peters, 1972; X. Wang et al., 2008). Interneurons are especially interesting because unlike traditional neurons, their dendrites can send and receive inputs (Bickford et al., 1999; Casagrande et al., 2006; Guillery, 1966; Krahe et al., 2011; Parnavelas et al., 1977; Rafols & Valverde, 1973). It is speculated that interneuron dendrites and axons are functionally isolated from one another because signals from synapses onto these dendrites do not reach the soma (Bloomfield, Hamos, & Sherman, 1987; Briska, Uhlrich, & Lytton, 2003; Grimes, Zhang, Graydon, Kachar, & Diamond, 2010; Halnes, Augustinaite, Heggelund, Einevoll, & Migliore, 2011; Perreault & Raastad, 2006). Because of this, dendrites of interneurons can be thought of as participating in their own local circuits that function to inhibit relay cells and are separate from the functions of interneuron somas and axons.

A specific interneuron dendritic circuit that has been described in abundance in visual literature is called a triadic arrangement. As the name suggests, these arrangements consist of three synapses. A retinal axon terminal synapses onto both an interneuron dendrite and onto a thalamocortical relay cell dendrite. To complete the triad, the interneuron dendrite then synapses onto the same relay cell dendrite as the retinal terminal, thus creating a mechanism of

feedforward inhibition onto the relay cell dendrite (Famiglietti & Peters, 1972; Hamos, Van Horn, Raczkowski, & Sherman, 1987; Hamos, Van Horn, Raczkowski, Uhlrich, & Sherman, 1985; Lam, Cox, Varela, & Sherman, 2005; reviewed in Sherman, 2004). All of the terminals involved in the arrangement are wrapped in an astrocytic sheath (Famiglietti & Peters, 1972). The interneuron dendrite can have different effects on the relay cell dendrite depending on the nature of the input from the retinal terminal. At low levels of retinal terminal firing, ionotropic receptors on the interneuron dendrite are activated and the resulting inhibitory postsynaptic potential onto the relay cell dendrite opposes the excitatory retinal input linearly (Cox & Sherman, 2000). At higher levels of retinal firing, metabotropic mGlu5 receptors on the interneuron dendrite are activated, resulting in an increase in GABAergic inhibition onto the relay cell dendrite that increases and persists after input from the retina has stopped (Cox & Sherman, 2000; Cox, Zhou, & Sherman, 1998; Errington, di Giovanni, Crunelli, & Cope, 2011; Liu, Petrof, & Sherman, 2015).

Although the functional implication of triadic arrangements for visual processing in the LGN remains to be proven, the main hypothesis is that triadic arrangements play a key role in contrast gain control of LGN relay cells (Errington et al., 2011). Contrast gain control is an important method of visual adaptation and helps adjust neuronal activity to ambient stimulation; as contrast of the stimulus increases, retinal firing increases. As discussed above, an increase in retinal firing increases GABAergic input and thus decreases relay cell firing, reducing the contrast gain.

In order to fully understand the influence of interneuron dendrites onto corticothalamic dendrites, it is important to have a full picture of all of the inputs synapsing onto relay cells in a glomerulus. To date, transmission electron microscopy (TEM) is the method used to study the

synaptic circuitry of triadic arrangements in the LGN (reviewed in Bickford, 2019). While these studies have revealed the basic synaptic circuitry of triadic arrangements, they lack the ability to describe the organization of all terminals and synapses involved in this complex circuitry. In this study, I use serial electron microscopy to partially trace 6 interneuron dendrites and identify all synapses and terminals associated with these dendrites with a particular emphasis on triadic arrangements in glomeruli. The results reveal that triadic arrangements associated with interneuron dendrites consist of several retinal terminals and interneuron terminals and there are several variations of interactions between terminals and these different terminal motifs may have different functional effects on signals relayed to the cortex from the LGN.

METHODS

Tissue Preparation

2 stacks collected from the LGN of adult mice were used for data collection in this study. Mice were transcardially perfused with PBS followed by 4% paraformaldehyde/2% glutaraldehyde made in 0.1M cacodylate buffer. Brains were then immediately dissected and cut coronally at 300μm sections on a vibratome. The LGN was then dissected from the appropriate section and sent to Renovo Neural Inc for staining, embedding, sectioning and imaging. Both LGN stacks were composed of 200 or 300 41μm x 41μm sections that are 75 nm thick each.

Serial Blockface Electron Microscopy (SBEM) image tracing

Interneuron Dendrites: All image tracing was done using Reconstruct software (Fiala, 2005). Tracing was started by identifying potential interneuron dendrites. These dendrites could

be readily identified by finding a terminal that forms a presynaptic and postsynaptic terminal. Specifically, interneuron presynaptic dendrites contain a thin postsynaptic density, frequently contain mitochondria and have a collection of vesicles gathered at the presynaptic site. After an interneuron dendrite was identified, it was traced through the stack until the dendrite came to a natural ending or continued out of the area of the image. Dendrite length and volume were computed using the Reconstruct software.

Terminals: To mark the terminals that synapse on the reconstructed dendrite, first all synaptic zones that appeared on the dendrite segment were marked and reconstructed as a slab-like object. Following this, the terminal boutons that make each synapse were traced and reconstructed. We paid care to capture the entire presynaptic bouton and to exclude the thinner interbouton axon segments that are devoid of vesicles from the reconstructions. Retinal terminals can be putatively identified because they contain pale mitochondria, whereas other terminals contain dark mitochondria (Behan, 1982; Guillery, 1969). In addition, interneuron dendritic terminals can be identified as such when a terminal is observed to be both a presynaptic and postsynaptic terminal (Bickford et al., 1999; Guillery, 1966; Parnavelas et al., 1977; Rafols & Valverde, 1973). Terminal volumes were computed using Reconstruct software.

Glomeruli Identification: In order to identify glomeruli in our image stacks, I first identified synaptic triadic arrangements. Next, I looked for astrocytic appendages that wrapped around the entire synaptic motif. Astrocytic wrappings could be identified first from the light cytoplasm that does not contain any organelles and second from their shape, which is amorphous and fills irregular shapes in the neuropil. Once an astrocytic wrapping was identified, every terminal and dendrite within the borders of the astrocytic sheath were considered to be a part of the glomerulus.

Model-based classification

Model-based classification calculations were all completed in R using the MClust package (Scrucca, Fop, Murphy, & Raftery, 2016). MClust is a package used for model-based clustering, classification, and density estimation based on normal mixture modelling. MClust uses the Bayesian Information Criterion (BIC) strategy for clustering and density estimation analysis. For terminal and dendrite classification, MClust yielded the number of objects in each population as well as the average and standard deviation of terminal and dendrite size in each. The confidence level for each value given (i.e. a confidence level for each terminal volume or dendrite caliber) was also computed.

Statistical Analysis

All graphs, descriptive statistics and comparative statistics (including Mann-Whitney U and Kriskal-Wallis tests) were completed using Prism software version 8. 3D reconstructions of dendrites and terminals were generated in Reconstruct. All figures were organized and annotated using Adobe Photoshop 2020.

RESULTS

In the LGN, interneuron dendrites function both as a presynaptic and postsynaptic compartment (Bickford et al., 1999; Casagrande et al., 2006; Guillery, 1966; Krahe et al., 2011; Parnavelas et al., 1977; Rafols & Valverde, 1973). In addition to this unique synaptic morphology, interneuron dendrites have been described to have the appearance of a “string of beads”, a morphology that is different from relay cells (Bickford et al., 1999; Friedlander, Lin,

Stanford, & Sherman, 1981; Guillery, 1966; Rafols & Valverde, 1973). Previous studies have characterized the morphology of interneuron dendrites and synaptic inputs onto them with light microscopy and TEM but were insufficient in revealing potential complex interactions among those inputs. In this study, I used SBEM image stacks and a sample of dendrite segments, to characterize the selectivity and convergence of distinct input types on geniculate interneurons and the motifs of connectivity in triads and glomerular structures.

Qualitative Observations of Interneuron Dendrite Morphology

In order to characterize inputs onto specialized morphological features of interneuron dendrites, I reconstructed 6 interneuron dendrite segments (referred to as IDS1- IDS6) in the mouse LGN from SBEM image stacks (Figure 1). The length of the dendrite segments traced ranged from 16.8μm to 55.4μm. Collectively, these interneuron dendrites received 141 synapses from 130 terminals. Interneuron dendrites display various morphological properties that differentiate them from relay cell dendrites studies in Chapter II (Figure 1). There are five major characteristics of note:

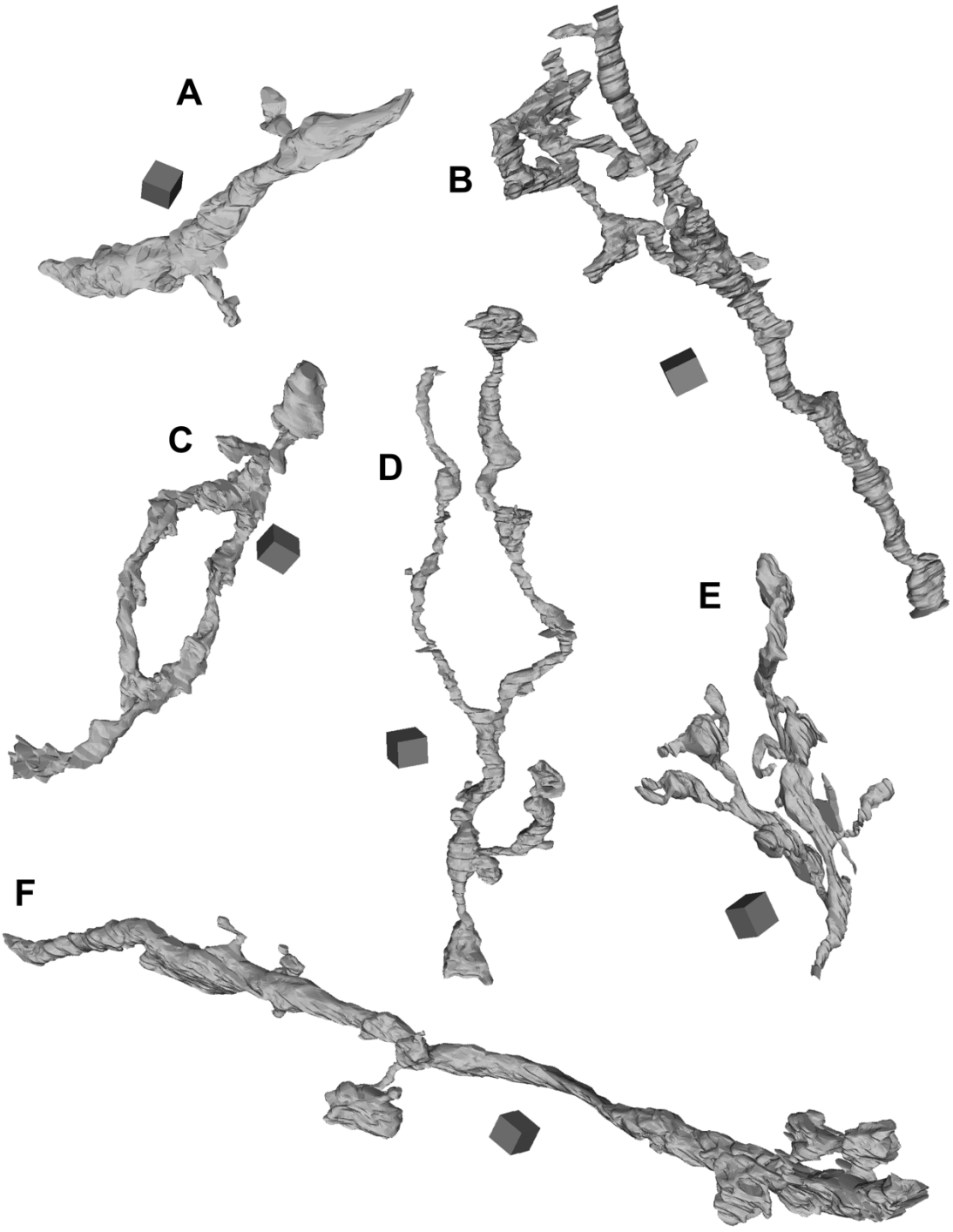

Figure 1: Reconstructions of all interneuron dendrites traced in the mouse LGN. Interneuron dendrites in the mouse LGN display varying shapes, sizes, and branching patterns; scale cube = 1x1x1mm

1) *Dendrite Shape:* Interneuron dendrites were generally thin and the dendrite caliber varied even on lengths of dendrite between branch points. The dendrite looked like an irregularly shaped string punctuated with swellings, appendages, and filopodia that emerged at uneven intervals. Archetypal properties of neuronal dendrite branching seemed not to apply to interneurons: when a branch point occurred, the caliber of the daughter segments, when possible to discern, did not differ noticeably from the parent segment.

2) *Appendages and swellings.* Most interneuron dendrite segments gave out thin protrusions that displayed filopodia morphology. Some of the thin protrusions turned into large end-swellings. These end-swellings could become larger than the diameter of the dendrite shaft it emerged from. Swellings also occurred within the dendrite shaft without the typical thin filopodia stalk of the appendages, giving the dendrite its 'beady' appearance (Figure 1d & f).

3) *Postsynaptic regions:* All portions of the interneuron dendrite segment (that is shaft, appendage, swelling and filopodia) could receive a synapse, although a great majority of synapses are found on appendages and swellings (also see below).

4) *Presynaptic regions:* Only appendages and dendrite swellings displayed collections of vesicles in varying amounts, and formed synapses on other neuropil. Almost all of the appendages and swellings participated in triadic arrangements. The filopodia (appendages without swellings) did not form synapses or participate in triadic arrangements.

5) *Glial Wrapping:* As described previously (Famiglietti & Peters, 1972) glomerular structures that involve interneuron dendrites are wrapped in a glial sheath. Glial wrapping was also present around synapse-sparse dendrite shafts, an interesting interneuron dendrite characteristic that was not seen on relay cell dendrites. Thin interneuron dendrite segments could be completely encapsulated by a glial sheath, which is a flattened and irregularly shaped

astrocytic process displaying light cytoplasm, few mitochondria and no cytoskeletal filaments (Figure 2). The glia encapsulated the interneuron dendrite exclusively but occasionally wrapped around single, small terminals that were not involved in triadic arrangements (not shown). This glial encapsulation of interneuron dendrites persisted in between the regions of triadic arrangements (Figure 2). In my dataset, the length of dendrite segments that were wrapped in astrocytic processes was as long as 37μm. The glial ensheathment of dendritic segments, which provides electrical isolation of the dendrite segment, may help with signal propagation toward the cell body or between localized circuits in glomeruli.

Selectivity of Inputs onto Interneuron Dendrites

Interneuron dendrites in the LGN receive input from several areas of the brain including: the retina, the thalamic reticular nucleus, the brainstem, other LGN interneurons, and the cortex (Hamos et al., 1987; McCormick & Pape, 1988; Weber, Kalil, & Behan, 1989). Several studies have described the number and organization of inputs onto interneuron dendrites using light microscopy and TEM methods (Bickford et al., 1999; Famiglietti & Peters, 1972; Guillery, 1966; Hamos et al., 1987; Lam et al., 2005; S. Wang, Eisenback, Datskovskaia, Boyce, & Bickford, 2002).

Selectivity of terminal types onto interneuron dendrites: In order to find out whether or not there is a selectivity of geniculate inputs on interneuron dendrites, I examined a total of 134 terminals that synapsed onto reconstructed segments (IDS1-IDS6). Synapses onto interneuron dendrites display a wide range of morphological and morphometric features (Figure 3a-c). The average volume of synaptic boutons synapsing onto interneuron dendrites is 1.68 μm^3 +/- 1.22μm^3 with a maximum of 6.92μm^3 and a minimum of 0.07μm^3 (Figure 3d). The terminal

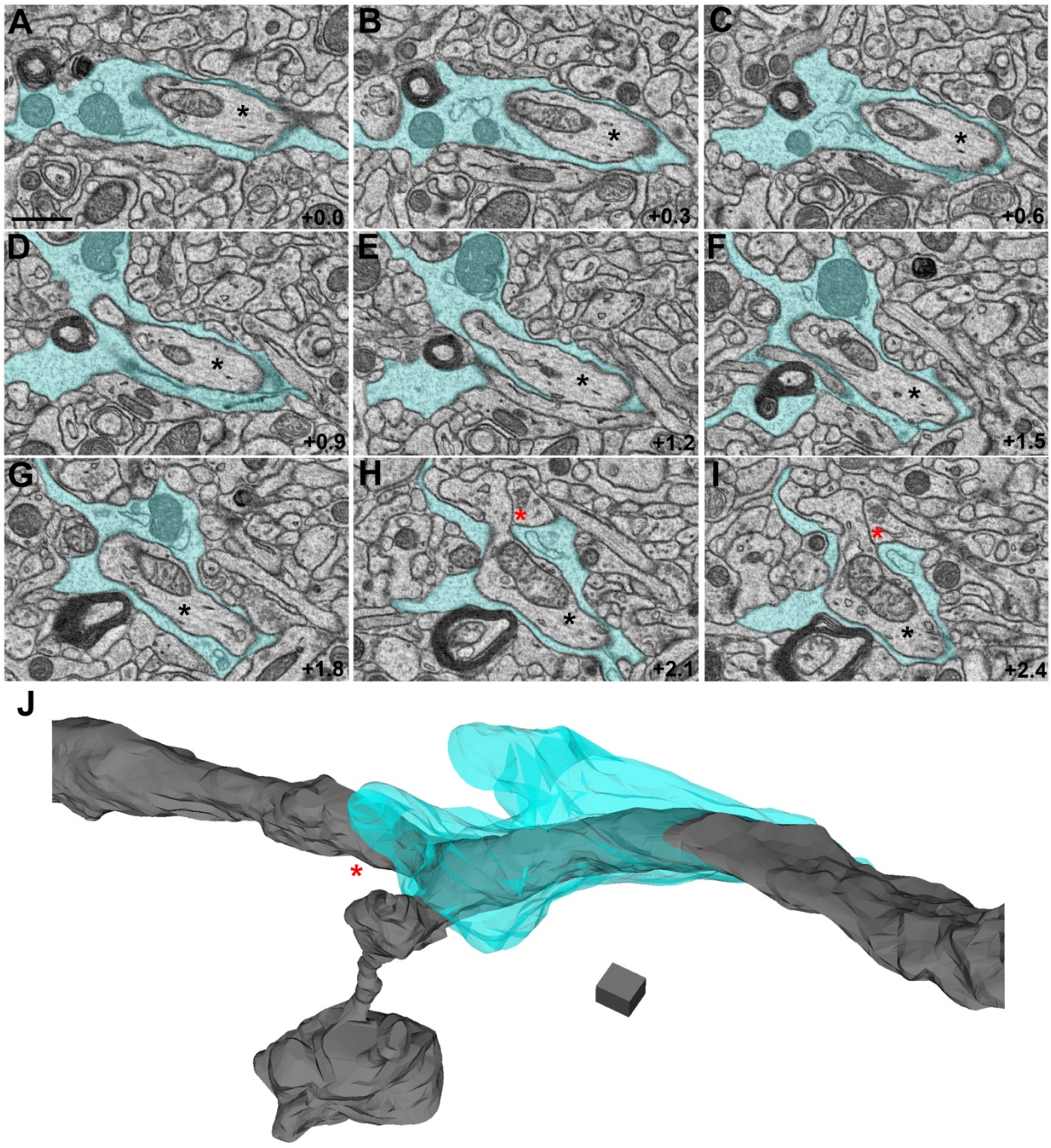

Figure 2: Glial wrapping around a length of interneuron dendrite. (A-I) EM images of glia wrapping (blue) around an segment of interneuron dendrite (black asterisk). While it is wrapped in the glia, the dendrite receives no input and does not synapse onto another neurite. Part of the dendrite leaves the glial

ensheathment to participate in synaptic arrangements (red asterisk). (J) A 3D reconstruction of the same interneuron dendrite segment (grey) surrounded by glia (blue). The location of the dendrite leaving the ensheathment is again marked with a red asterisk; scale bar= 1μm; scale cube = 1x1x1μm.

volume distribution in this dataset was significantly different than the terminals in the relay cell dendrite dataset analyzed in Chapter II, with the interneuron dataset containing more of the larger size terminals and less of the smaller size terminals (Mann-Whitney U, $r<0.0001$).

In order to identify putative origins of terminals synapsing onto interneurons dendrites in this study, I primarily relied on morphological characteristics. However, in cases where morphology was ambiguous, incorporating volumetric data (as described in Chapter II) for terminal origin identification led to the best possible estimate of terminal origin without the use of immunohistochemical techniques. As described in Chapter II, I used a randomly sampled volumetric terminal dataset of terminals found in LGN and used the multivariate clustering analysis to classify the terminals on interneuron dendrites into populations. These populations of terminals then inform on putative origins (Figure 3d). The terminals that fell into Populations 5-6 (i.e., large terminals) often displayed morphological characteristics attributed to axon terminals from the retina, including pale mitochondria, many protrusions, and round vesicles filling the bouton (Figure 3a). Similar to the relay cell data (Chapter II), I also observed large and medium sized terminals with dark mitochondria and some small terminals (Populations 1-2) that had few or no mitochondria (Figure 3b&c). Some of the large and medium sized terminals could be identified as belonging to interneuron dendrites because they were both pre-and postsynaptic, a unique criteria for interneuron dendrites. Small sized terminals (putative brainstem or cortical origin) constituted 15% all terminals synapsing onto interneuron dendrites. This is a notably small number, compared to the findings that ~60% of terminals of synapsing on relay cell dendrites are of brainstem and cortical origin), suggesting that corticothalamic feedback excitation and brainstem modulation do not play an as large role on interneurons. The majority (75%) of these small terminals synapsed outside of glomeruli. The Population 6 terminals, the

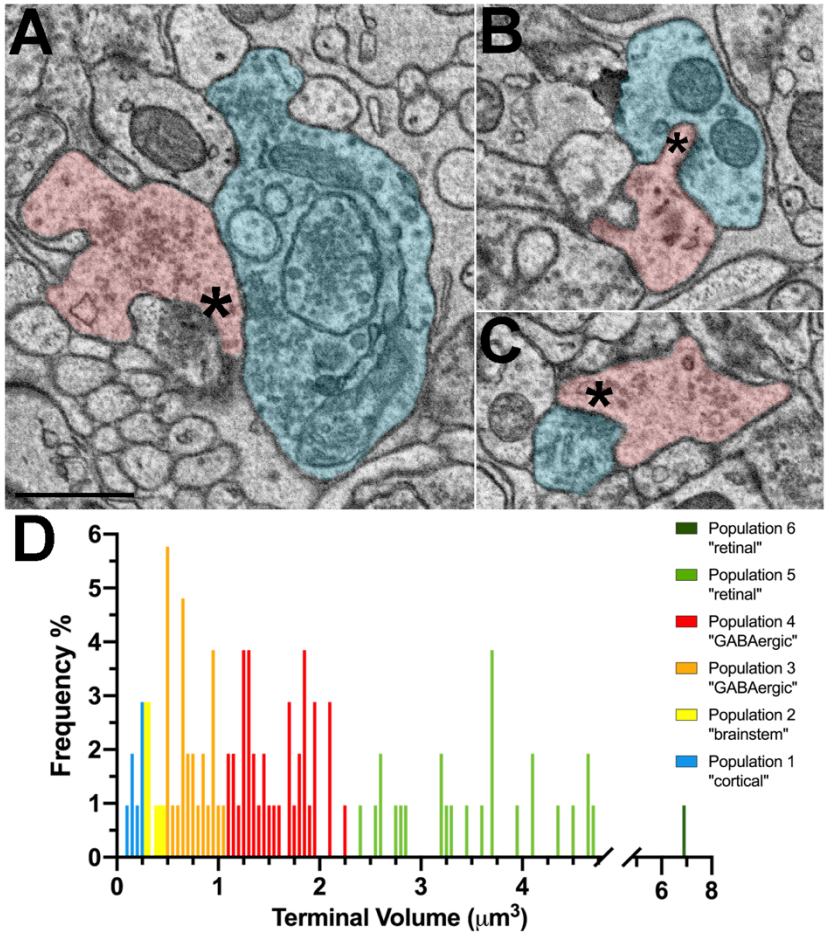

Figure 3: Morphological feature of terminals synapsing onto interneuron dendrites. (A) Some terminals (blue) were large, filed with vesicles, contained protrusions and had light mitochondria. (B) Other terminals (blue) were medium sized and contained dark mitochondria. (C) Few terminals (blue) synapsing onto interneuron dendrites were small and did not contain any mitochondria; interneuron dendrites are in red, black asterisks indicate the area postsynaptic to the cleft. (D) Terminal volume distribution of all terminals synapsing onto interneuron dendrites demonstrates that most terminals synapsing onto LGN interneurons are medium to large in size. Colors correspond to terminal populations described in chapter II; scale bar = 1μm

largest terminals seen synapsing on relay cell dendrites described in Chapter II, were not represented on interneuron dendrites in this dataset. This is not surprising because Population 6 terminals were not found synapsing in glomeruli on relay cell dendrites, and almost all terminals with large volumes were located in glomeruli of the interneurons.

Selectivity of terminal types in glomeruli: The majority (85%) of input onto interneuron dendrites occurred within glomeruli and a few (15%) terminals synapsed onto interneuron dendrites outside of glomeruli. Terminals synapsing onto interneurons in glomeruli were significantly larger than those synapsing onto interneurons outside of glomeruli (Mann Whitney U, $p<0.001$). The average volume of terminals synapsing onto interneurons in glomeruli was 1.8μm +/- 1.2μm and the average volume of terminals synapsing onto interneuron dendrites outside of glomeruli was 0.79μm +/- 0.89μm. These suggest that the larger inputs (putative retinal and GABAergic axon terminals from interneurons and thalamic reticular nucleus) onto interneurons are selective for dendrite segments in glomeruli, and that smaller terminals (corticothalamic and cholinergic brainstem) are selective for dendrite segments that are outside of glomeruli.

Triad and Glomerulus Motifs

Inhibitory interneurons provide a feedforward inhibition onto relay cells via triadic arrangements that are located in glomeruli (Augustinaite & Heggelund, 2018; Crandall & Cox, 2013; Famiglietti, 1970; Famiglietti & Peters, 1972; X. Wang et al., 2008). This inhibition is thought to filter out excess noise from retinal terminals, or to suppress the retinal excitation on relay cells in a temporal fashion, thereby refining the visual information before it is sent to the cortex (Augustinaite & Heggelund, 2018; Crandall & Cox, 2013; Famiglietti, 1970; Famiglietti

& Peters, 1972; X. Wang et al., 2008). This view emphasizes a localized function for triads, and de-emphasizes a potential network function of interneurons in generating lateral inhibition via their dendrites by summating receptive field or parallel pathway specific information. The 3D reconstruction dataset now allows me to reveal local and network properties of interneuron dendrites. To that aim, I first examine the patterns of connectivity in triads (that is, the triadic motifs), and reveal that the retinal terminal is not the ubiquitous partner of triads. Second, I look at the glomerular motifs to reveal the extent of the retinal convergence in these structures. Finally, I examine if and how glomeruli are connected to each other via the sharing of synaptic partners.

Triad Motifs

This data set included 81 triads. Complete reconstruction of all terminals that contributed to each triad allowed identification of triadic motifs that eluded 2D EM studies.

Retina-Interneuron-Relay Cell Motifs: The most common motif encountered is that of a stereotypical triadic arrangement: A retinal terminal synapses onto an interneuron dendrite and a relay cell dendrite. The interneuron dendrite then synapses onto the same relay cell dendrite as the retinal terminal (Figure 4). 63 out of 81 triads are this type. This triadic motif may be responsible for the rapid (two synaptic delays apart) inhibition of the relay cell dendrite induced by the excitation from retinal terminals.

Interneuron-Interneuron-Relay Cell Motifs: The dataset included 14 examples of triads formed among an appendage or swelling of a dendrite that is presynaptic to a second presynaptic dendrite. Both presynaptic terminals also synapse onto a relay cell dendrite (Figure 5). Notice that in this configuration the retinal terminal is replaced by an interneuron dendritic terminal that

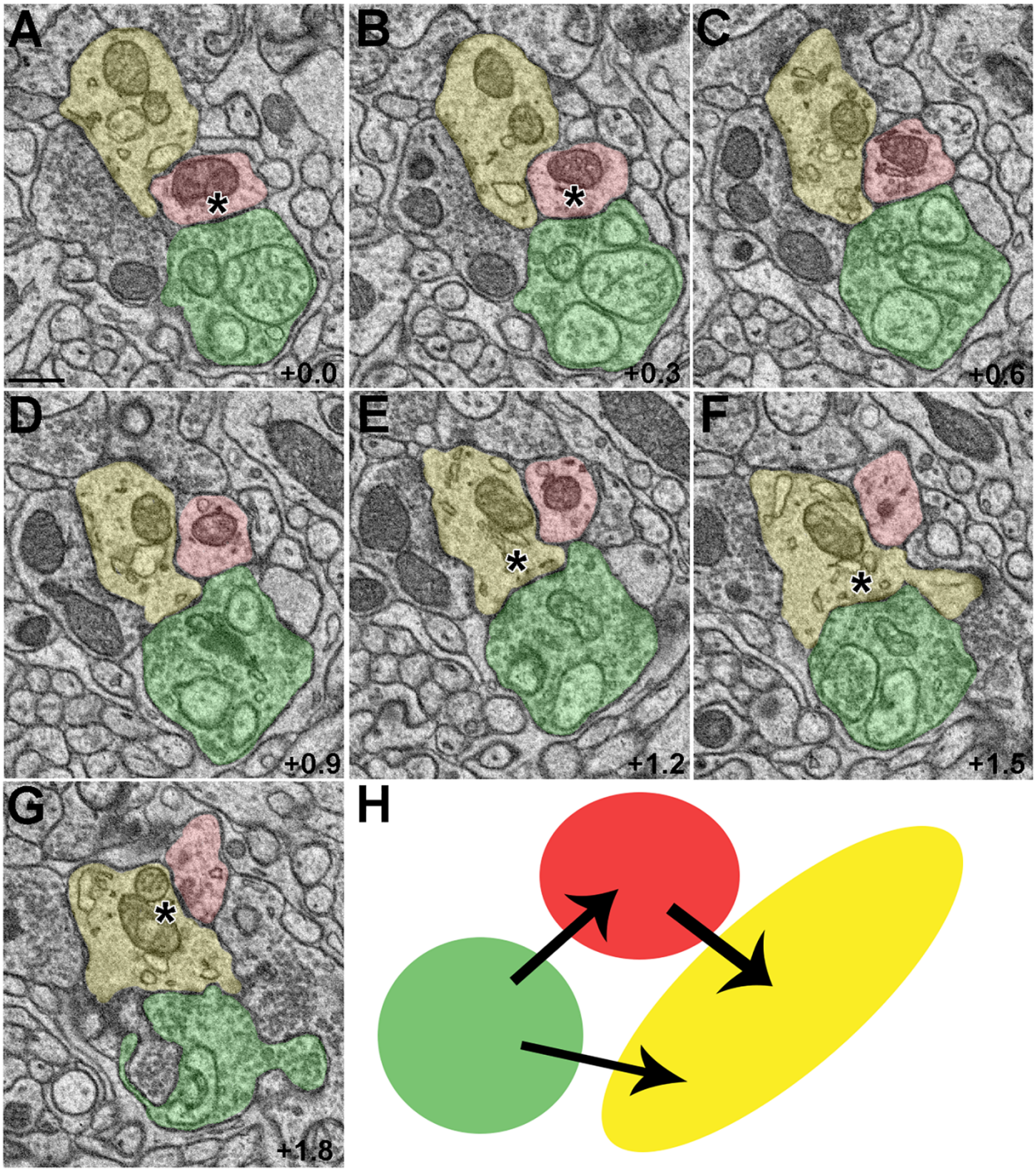

Figure 4: An example of a retinal-interneuron-relay cell motif. (A,B) A retinal input (green) synapses onto an interneuron dendrite (red). (E,F) The same retinal input (green) synapses onto a relay cell dendrite (yellow). (G) The interneuron dendrite (red) synapses onto the same relay cell dendrite (yellow) as the

retinal input; asterisks indicate area postsynaptic to the cleft. (H) Schematic of the retinal-interneuron-relay cell motif. Colors correspond to those in EM images; retinal terminal in green, interneuron dendrite in red, relay cell dendrite in yellow. Arrows indicate directionality of synapses. Scale bar = 0.5μm

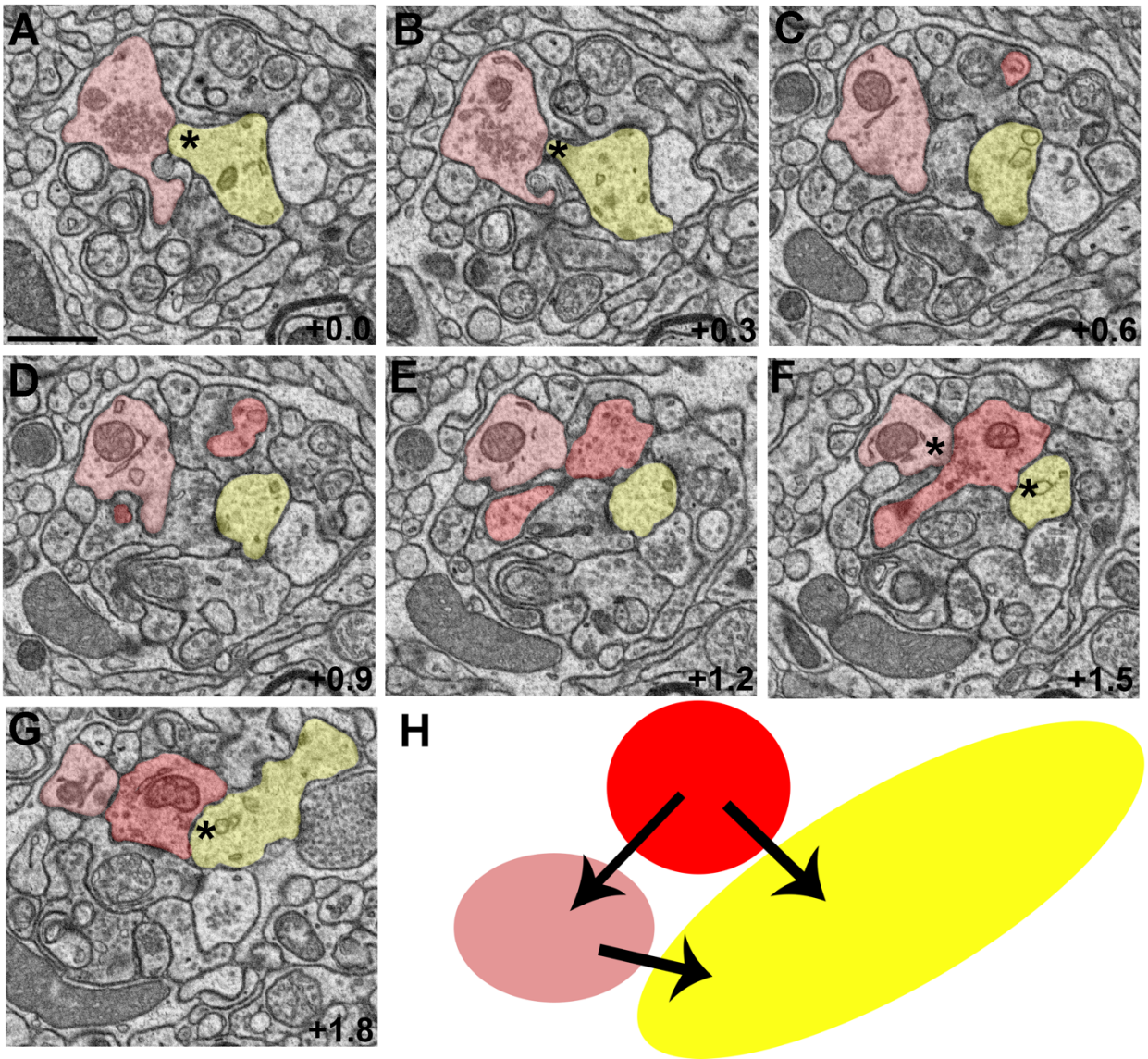

Figure 5: An example of an interneuron-interneuron-relay cell motif. (A,B) An interneuron dendrite (pink) synapses onto a relay cell dendrite (yellow). (F) A different interneuron dendrite (red) synapses both onto a relay cell dendrite (yellow) and onto the first interneuron dendrite (pink). (G) the second interneuron dendrite (red) continues to synapse onto the relay cell dendrite (yellow); asterisks indicate area postsynaptic to the cleft. (H) Schematic of the interneuron-interneuron-relay cell motif. Colors correspond to those in EM images; first interneuron dendrite in pink, second interneuron dendrite in red, relay cell dendrite in yellow. Arrows indicate directionality of synapses. Scale bar = 1μm

makes two presynaptic contacts in the triad. It is interesting that the interneuron making two presynaptic contacts can also take part in another triad in the same glomerulus, but this time as the interneuron dendrite that is postsynaptic to a retinal terminal. The interneuron-interneuron-relay triads clearly indicate complex interactions, including a tri-synaptic-delay of local disinhibition of relay cell dendrites, perhaps to facilitate the recovery of the feedforward inhibition generated via the retinal/interneuron triad.

Small Terminal-Interneuron-Relay Cell Motifs: The least common motif (2 of 81) I encountered in the LGN is that of a small terminal that does not display the morphological features of retinal terminals (i.e., pale mitochondria) synapsing onto a relay cell dendrite and an interneuron dendrite which then synapses onto the same relay cell dendrite (Figure 6). The small terminals mentioned here may be akin to the cholinergic terminals (with small boutons and dark mitochondria) that are described to make synapses in glomeruli (McCormick & Pape, 1988). Physiology studies have demonstrated that cholinergic input decreases GABA release from interneuron dendrites while increasing firing of relay cell dendrites (Carden & Bickford, 1999; Cox & Sherman, 2000; McCormick, 1992; McCormick & Pape, 1988; Plummer, Manning, Levey, Rees, & Uhlrich, 1999). With the assumption that these non-retinal small terminals are cholinergic, my data provide evidence that cholinergic input to glomeruli is formed both directly onto interneurons and relay cell dendrites, suggesting that brainstem modulation of glomerulus action is done via facilitation of disinhibition (via suppressive cholinergic receptors at the brainstem synapse on interneurons) as well as increased excitation of relay cell dendrites (via faciliatory receptors at this synapse) (Carden & Bickford, 1999; McCormick, 1992; McCormick & Pape, 1988). The arrangement described above is a true triad however, I also saw a few (4) instances of putative cholinergic terminals that synapse onto presynaptic interneuron dendrites in

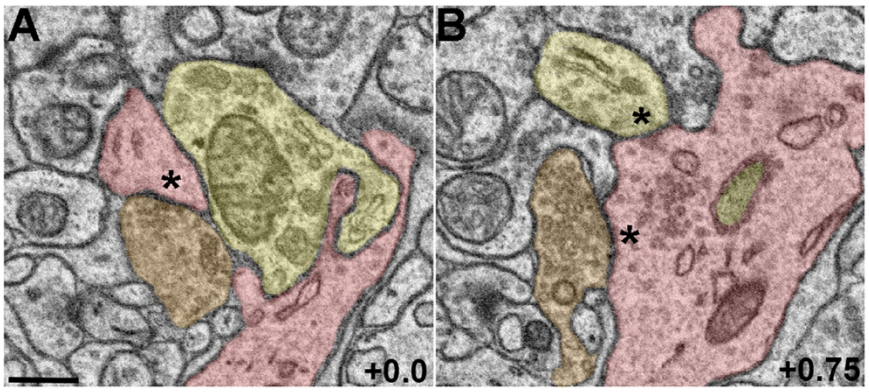

Figure 6: An example of a brainstem-interneuron-relay cell motif. (A) A brainstem terminal (orange) synapses onto a relay cell dendrite (red). (B) The brainstem terminal (orange) continues to synapse onto the interneuron dendrite (red). The same interneuron dendrite can also be seen synapsing onto a relay cell dendrite (yellow); asterisk indicate area postsynaptic to the cleft, scale bar = 0.5μm

glomeruli, but not onto relay cell dendrites. This arrangement may also contribute to the disinhibition of relay cell dendrites without direct synaptic connections between the cholinergic terminals and the relay cell dendrite.

Glomerular Motifs:

We traced a total of 7 distinct glomeruli of various sizes. Some glomeruli were large and contained over 20 terminals and dendrites while some were much smaller and only contained 5 total terminals and dendrites (Figure 7).

Number of retinal boutons in the glomerulus: Glomeruli in my data set receive input from between 1 and 20 distinct retinal terminals (Table 1). For most boutons, the axon was also reconstructed so that I would have the information for whether or not the same axon provided a second bouton into the same glomerulus, or onto another portion of the reconstructed interneuron dendrite. However, the volume of the reconstructed axon was not included in the volume calculation of the bouton. I did not encounter any instance of a retinal axon providing more than one bouton to an individual glomerulus. Therefore, I am able to state that the retinal terminals that enter a single glomerulus are from different retinal ganglion cells[1], suggesting that multiple retinal ganglion axons may converge in a single glomerulus.

Number of Interneuron Dendrites in Glomeruli: Of the 7 glomeruli I characterized in this study, 1 contained 3 presynaptic interneuron dendrites, 2 contained 2 presynaptic interneuron dendrites, and 4 of them contained only 1 presynaptic interneuron dendrite (Table 1). Involvement of more than one interneuron dendrite in a glomerulus (which is centered around a

[1] The certainty of this finding is limited by the extent of reconstructions that can be performed in the volume of tissue that is represented in a stack. If a retinal axon had a collateral or branching point outside of the stack, and the branches traveled to the exact location of the glomerulus, I would not be able to identify those two boutons as coming from the same retinal ganglion cell. However, I assume the probability of the scenario above is negligible.

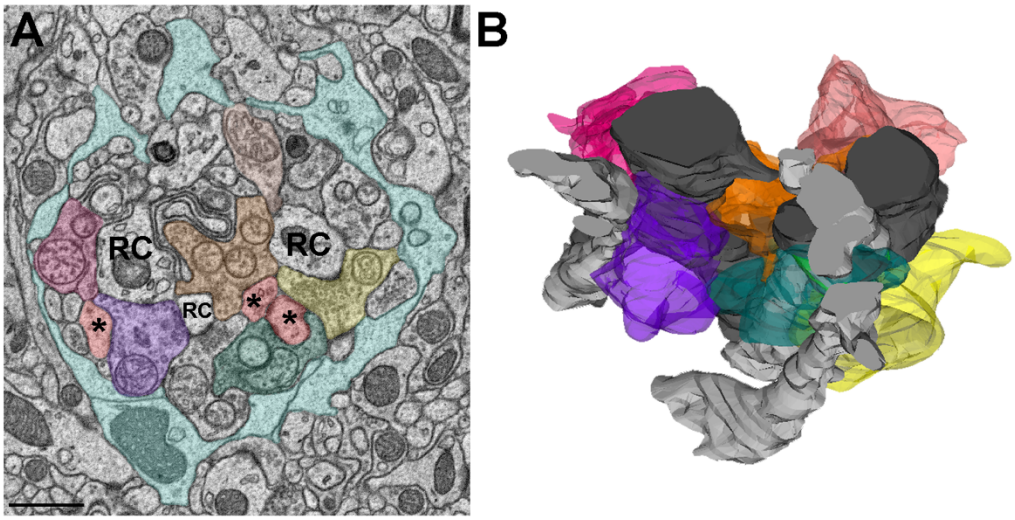

Figure 7: Synaptic arrangements in glomeruli are complex and involve several terminals and dendrites. (A) An EM image of what a glomerular arrangement looks like with a single two dimensional image. Although some terminals can be synapsing onto relay cell dendrites (RC) and interneuron dendrites (red, asterisk), many more synaptic interactions are missed; glomerular sheath = blue. (B) A 3D reconstruction of the same glomeruli. Some terminals have been reconstructed and their colors correspond to those in panel (A). The 2D reconstruction of the glomerulus is able to give a more accurate representation of the complexity of synaptic arrangements around interneuron dendrites in glomeruli; dark grey = relay cell dendrites, light grey = interneuron dendrites, scale bar = 1μm.

Table 1.				
Glomerulus Name	Number of Interneuron Dendrites	Number of Relay Cell Dendrites	Number of Triads	Number of Retinal Terminals
G1	3	1	20	10
G2	1	1	3	3
G3	2	1	28	20
G4	1	2	15	13
G5	1	1	3	1
G6	2	1	4	2
G7	1	1	9	9

single relay cell dendrite-- although for an exception, see below) implies a convergence of inhibitory influences on a single relay cell dendrite within the localized circuit. Also of note and as mentioned above, my dataset included instances where the interneuron dendrites in the same glomerulus interacted with each other via interneuron-interneuron-relay type triads. This arrangement sets the stage for modulation of localized circuits by other localized circuits, perhaps enabling adaptive response properties of geniculate parallel pathways.

Finally, although most interactions between interneuron dendrites were limited to a one-way interaction, I observed three interneuron dendrites in my sample making reciprocal synapses with each other in a glomeruli (Figure 8). These synapses are small and only span 0.15 microns in depth (one or two SBEM images) each. Although the two interneuron dendrites do not show vesicles docking in the same section, they do appear to share the same extrasynaptic space.

Number of Relay Cell Dendrites in Glomeruli: Of the 7 glomeruli described in this study, 6 of them contained one relay cell dendrite segment and 1 contained two relay cell dendrite segments (Table 1). The relative paucity of multi-relay glomeruli confirms the standing notion

that the relay dendrite is the central element of glomeruli, and the main purpose of the other components of triads the in the glomerulus is to modulate or modify the temporal activity in that particular relay cell. On the other hand, the clear evidence for the presence of multi-relay glomeruli I provide in this study, suggests that glomeruli can also be the site of divergence of receptive-field specific inputs that converged on interneurons. An example of the observations that lead to this conclusion is described below.

One glomerulus I characterized (G4) was unique in that it involved two different relay cell dendrites (R1 and R2), whereas all other glomeruli only centered around one relay cell dendrite. The G4 glomerulus involved a portion of the IDS3 interneuron dendrite that synapsed onto two different relay cell dendrites in the same astrocytic sheet. G4 was a large glomerulus with 15 terminals synapsing onto IDS3. Of these 15 terminals, 13 were from the retina and 2 were other interneuron dendrite terminals that act only in a presynaptic capacity. In addition to all terminals synapsing onto IDS3, 8 terminals (all retinal) synapsed onto R1, 3 terminals (all retinal) synapsed onto R2, and 3 terminals (two retinal and one interneuron) synapsed onto both R1 and R2. One interneuron dendrite terminal formed a synapse onto IDS3, but did not synapse onto a relay cell in the glomerulus. This glomerulus was the only example of two relay cell dendrites in the same glomerulus that received input from the same interneuron and the same set of retinal inputs.

G4 is an example of convergence of retinal terminals onto one interneuron dendrite that will in turn affect the firing of two relay cells. The broad effect of this interneuron is an economical way for an interneuron to modulate firing of several retinal inputs onto relay cells. This also suggests that this interneuron has a powerful influence over the firing of these two relay cells because there are many retinal terminals that cause it to inhibit relay cell firing.

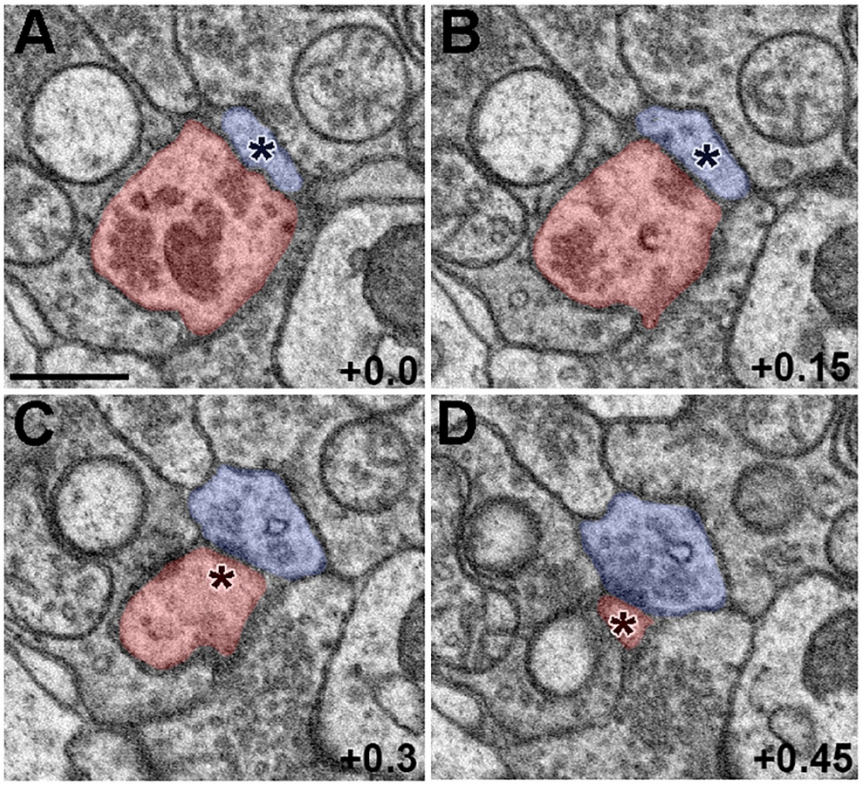

Figure 8: Reciprocal synapse between two interneuron dendrites. (A,B) One interneuron dendrite (red) synapses onto a second interneuron dendrite (blue). (C,D) The second interneuron dendrite (blue) then synapses onto the first interneuron dendrite (red) creating a reciprocal synapse between the two interneurons; asterisk indicate area postsynaptic to the cleft, scale bar = 0.5μm

G4 also gave us an example of lateral inhibition by interneurons in the LGN. A retinal input that synapsed onto IDS3 can cause inhibition onto a relay cell dendrite that did not receive input from that same retinal terminal. These inhibitory characteristics can sharpen the response properties of relay cell dendrites in the LGN. Whether or not multi-relay glomeruli can form on selective relay cell-types will require a larger data set or an approach that yields cell-type identified geniculate tissue that is also suitable for connectomics analysis.

Intraglomerular interaction motifs:

In order to reveal, if any, repeated connections between an interneuron dendrite and another neuropil (a relay cell, a retinal terminal, or another interneuron dendrite), I reconstructed each neuropil that appeared in a glomerulus with a interneuron dendrite, and looked for other instances of interaction between the two neuropils. This way, I was able to determine if each of these elements pair up or interact multiple times, or in other words, they are selective for each other.

Relay Cells: The dataset included an interneuron (IDS6) that had selectivity for a single relay cell dendrite (R3) and interacted with R3 through multiple synapses. IDS6 and R3 traverse through the neuropil in close proximity and IDS6 synapses multiple times along the length of the R3 dendrite at swellings in glomeruli and once outside of a glomerulus (Figure 9). This indicates that any excitatory input that the interneuron receives will inhibit the same relay cell, that is the interneuron's local interactions can be amplified by its network properties. In addition, this selectivity also represents a convergence of different RGC axons onto an interneuron to inhibit a single relay cell. That is, visual activity evoked at various visual field representations can inhibit

a single relay cell, perhaps sharpening its receptive field properties. This arrangement may provide a substrate for lateral inhibition via interneuron dendrites.

I cannot comment whether or not the motif described above is a common property of all interneurons. All other reconstructed segments did not reveal selectivity for a relay dendrite within the confounds of the stack. In the IDS6 example, paired interactions occur in close proximity. It is possible that paired interactions occur in distant segments of an interneurons. It is also a possibility that interneuron-relay paired interactions (selectivity) is a characteristic of a distinct geniculate relay cell type, or of a distinct geniculate interneuron type.

This reconstruction also confirmed that relay cells can receive inhibitory inputs from multiple interneurons. The dataset includes a total of 8 relay cell dendrites that receive input from interneurons in reconstructed glomeruli. Five of these relay dendrites receive input from one interneuron in a single glomerulus, two receive input from two interneurons in two different glomerulus, and one relay cell dendrite receive input from three interneurons in three separate glomeruli. These results demonstrate that relay cell dendrites are not under the control of one interneuron, but can be influenced by several different interneurons in separate glomeruli.

Retinal Terminals: In my dataset, I see examples of retinal input divergence in which terminals originating from the same retinal axon synapse onto different interneuron segments and relay cells in different glomeruli. For example, RGC1 synapsed onto IDS3 and IDS1. In terms of visual maps, divergence implies broadening of the receptive field tuning in the target cells. Because in this case the target cell is an inhibitory interneuron, which induces local inhibition via its own divergence and convergence on relay cells, this motif can be a substrate of lateral inhibition on relay cells to to sharpen their receptive field responses, or enable the ON/OFF

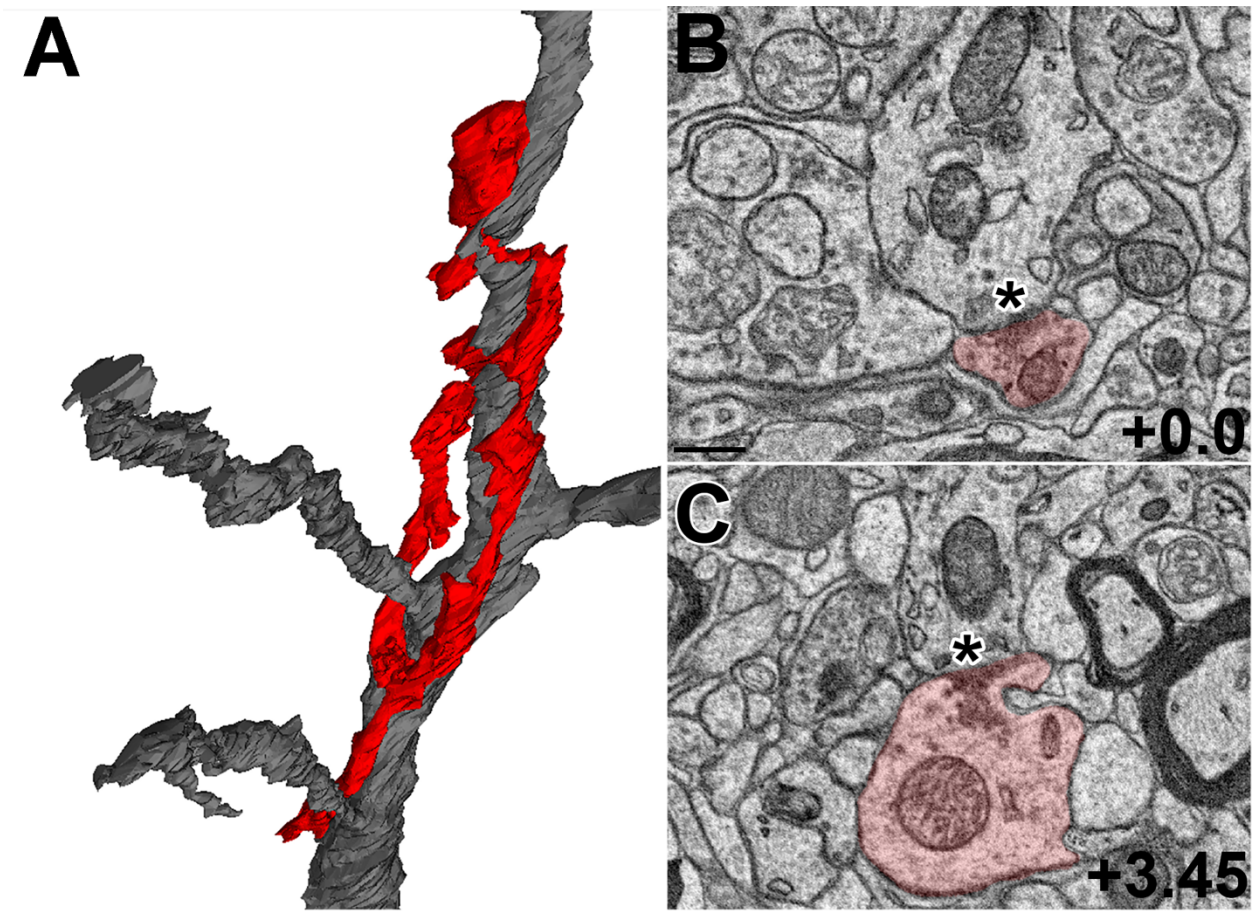

Figure 9: (A) Example of a relay cell dendrite (grey) traversing the neuropil in close proximity to an interneuron dendrite (red). Although this interneuron synapses onto the relay cell, the synapses are formed far apart and not at every point where the two dendrites come into contact. Synapses occur both in glomeruli (B) and outside of glomeruli (C); postsynaptic cleft marked by an asterisk; scale bar= 1μm.

phenotype of the interneurons. This motif can also be a substrate for adaptive regulation of interneurons' ON or OFF type response properties.

I also noted that reconstructed RGC axons synapse on more than one relay dendrite in an example of RGC divergence on relay cells. It is possible that one RGC is providing input onto two different relay cells that belong to the same parallel pathways and therefore receive the same level of inhibition from the interneuron dendrite. However, given that the current approach does not allow for the reliable identification of relay cell types that belong to distinct parallel pathways, this question remains unanswered.

Interneuron Dendrites: My dataset contained four interneuron dendrite segments that participate in a glomerulus, where other interneuron dendrites are also present. While indirect interneuron-interneuron interactions are common (by definition of the glomerulus), interneuron dendrites located in the same glomerulus can have direct synaptic contacts (see Glomerular Motifs/ Interneurons above). None of the interneuron-interneuron pairs that took part in a glomerular motif did not appear to have another interaction together. Again, my dataset only speaks for interactions that take place within the span of the reconstructions in the limited volume of the SBEM stack. The lack of evidence in my dataset for multiple interneuron-interneuron paired interactions suggests that, if present at all, interneuron selectivity for another interneuron takes place via synapses located at distant branches of these cells.

DISCUSSION

Inhibitory interneurons in the LGN have been a topic of study for decades and their morphology and physiology has been characterized in several species (Bickford et al., 1999; Blitz & Regehr, 2005; Casale & McCormick, 2011; Cox et al., 1998; Errington et al., 2011;

Famiglietti & Peters, 1972; Kaas, Huerta, Weber, & Harting, 1978; Lam et al., 2005). Here, I describe in detail the synaptic circuitry of interneurons in the mouse LGN using SBEM image stacks. Overall, the results from my study are consistent with past conclusions while also adding novel information about how interneurons are connected to LGN circuitry. I found that inhibitory interneuron dendrites in the LGN display a variety of morphological characteristics. Some portions of interneuron dendrites had small calibers and were enveloped by a glial sheath while other portions formed varicosities where it formed and received several synapses. I also saw a great diversity in synaptic motifs formed onto and by interneuron dendrites, which I will discuss below. My results indicate that interneurons play a variety of roles in synaptic circuitry in the LGN, with the foremost role being the inhibition of relay cells in order to refine visual information sent to the cortex.

Glomeruli exhibit a diversity of synaptic motifs

The results demonstrate that synaptic circuitry in glomeruli of the LGN is complex and individual glomeruli have a large degree of variability in their composition. Almost all input onto interneuron dendrites in triadic arrangements originate from the retina. My data show that there may be up to 13 retinal terminals synapsing onto one interneuron dendrite in a glomerulus. The large amount of retinal input being modulated by one interneuron dendrite terminal suggests some degree of consolidation of interneuron function. It could be that input coming from all retinal terminals in a glomerulus have the same receptive field properties and thus can be modulated in the same way however, this remains speculative. I also demonstrate that while most retinal axon terminals converging onto interneurons originate from separate RGCs, I saw some instances of terminals originating from separate branches of the same RGC synapsing onto the

same interneuron dendrite and the same relay cell dendrite. This is a very interesting retinal axon specificity and may function to increase the amount of inhibition in the case of extra noise from one type of RGC.

While the majority of interneuron dendrites receive input from retinal terminals, I also see evidence of modulatory inputs in glomeruli. The first of these inputs is from putative cholinergic terminals from the brainstem. Input from cholinergic terminals causes a decrease in GABA release from interneuron dendrites and these cholinergic terminals are more active when the animal is in an alert state (McCormick & Pape, 1988; McCormick & Prince, 1987; Steriade & Contreras, 1995; Steriade & McCarley, 2013). Therefore, it can be theorized that in a sleep state, not only do relay cells receive less excitatory input form cholinergic axons, but also not have a decrease in inhibition from interneuron dendrites, thus decreasing the overall responsiveness of relay cell dendrites. These small terminals only make up a small number of total the total inputs synapsing onto interneuron dendrites and therefore are not expected to play a large role in interneuron firing.

It should be considered that terminals synapsing onto interneuron dendrites may be axon terminals from interneurons or inhibitory terminals from the thalamic reticular nucleus. Because input from the thalamic reticular nucleus has been shown to target more distal dendrites, it is more likely for inhibitory axon terminal in glomeruli to be from the axons of interneurons. Without additional methods such as transgenic identification of different inhibitory inputs, it is not possible for us to reliably identify the origin of these GABAergic terminals.

The Role of Interneurons in the Flow of Visual Information to the Cortex

The results of this study bring us closer to understanding of how interneuron dendrites influence visual information that is sent to the cortex by LGN relay cells. Unlike traditional neurons in which the entire cell works as a unified, multistep computational unit, my data supports the hypothesis that inhibitory interneurons dendrites in the LGN are more accurately thought of as separate microcircuits and each individual mico circuit does not affect the response of the entire interneuron. This is especially true for glomeruli that are formed around appendages of interneuron dendrites. Past evidence of this comes from physiological modeling studies of interneurons. These studies demonstrate that inputs onto distal interneuron dendrites can be attenuated up to 99% by the time it reaches the interneuron soma (Bloomfield et al., 1987; Briska et al., 2003; Grimes et al., 2010; Halnes et al., 2011; Perreault & Raastad, 2006). It has also been shown in amacrine cells in the retina, a population of cells that behave similarly to interneurons, that activity of one dendrite terminal only affected other terminals if they were within 20μm of each other (Grimes et al., 2010). This suggests that interneuron dendrite influence is restricted to individual glomeruli. However, it may be the case that glomeruli formed around swellings of the main interneuron dendrite shaft facilitate the diffusion of EPSPs from one glomerulus to the other. This is supported by the result demonstrating that portions of interneuron dendrites between glomeruli are encased in a glial sheath. This interneuron characteristic strongly suggests that dendritic transmission can occur between glomeruli on the same dendrite shaft, effecting more than just local dendrite dynamics.

The diversity of synaptic motifs seen in glomeruli suggests that interneurons may have several different functions in the LGN. One of the leading ideas of interneuron function is decreasing visual noise from the LGN to the cortex (Sherman, 2004). Retinal, inhibitory, and

cholinergic inputs all modulate the amount of inhibition exerted onto relay cells by interneuron dendrites. When there is an increase in visual stimulation in the retina, retinal terminals increase firing onto relay cell dendrites but also onto interneuron dendrites. Inhibition onto a relay cell dendrite from an interneuron prevents an excess of visual information from the retina being passed by that relay cell to the visual cortex. On the other hand, inhibitory and cholinergic inputs onto interneuron dendrites decrease inhibition onto relay cells. My findings show that there are few of these synaptic arrangements in glomeruli. However, this indicates that only a few cholinergic and inhibitory inputs onto interneuron dendrites are necessary to change the firing pattern of a relay cell dendrite regardless of the number of RGC inputs in the glomerulus. This mechanism of rapid disinhibition may allow for relay cells to rapidly adapt to changes in the visual environment.

Although retinal input onto relay cell dendrites shows little convergence, my results suggest that some convergence and divergence of retinal inputs happen via interneuron dendrites. This study demonstrates that not only do interneuron dendrites participate in feedforward inhibition onto relay cells in glomeruli, but also contribute lateral inhibition onto relay cell dendrites. It is reasonably speculated that lateral inhibition allows for relevant information to be passed through one relay cell and inhibited in another. This may have implications for adaptations in ON and OFF parallel pathways through the LGN. Relay cells in ON versus OFF center parallel pathways have opposite responses to luminance (Martinez, Molano-Mazón, Wang, Sommer, & Hirsch, 2014). Because of this, it makes sense that when a relay cell in one pathway is excited, the relay cell in the other pathway is inhibited. My results suggest that it could be input from interneuron dendrites that strengthens this firing contrast through lateral inhibition.

It is interesting to note that studies in the cat LGN show that the vast majority of glomeruli are found on type X relay cells and very few, if any can be found on Y cells (Wilson, Friedlander, & Sherman, 1984). Given that X type relay cells in the LGN are known to have higher spatial but lower temporal frequency then Y relay cells, triadic arrangements may play a crucial role in decreasing visual noise for spatial information over temporal information. In this study, I was unable to discriminate between X and Y relay cells in the mouse LGN and my attempts to sort relay cells into parallel pathways using input patterns proved unsuccessful. The reason for this may be because of a large amount of divergence of retinal inputs in the mouse LGN. This study and the results from Chapter II show a large amount of retinal divergence onto relay cell dendrites and interneuron dendrites and this result is in alignment with previous studies that show varying amounts of retinal divergence onto dendrites in the mouse LGN. In order to probe how glomeruli function to modify visual information in different parallel pathways, studies of glomeruli and triadic motifs should be studied in a species where X and Y relay cells can be easily distinguished with minimal divergence of retinal input into the LGN.

Acknowledgments

I thank Shahrozia Imtiaz and Alex Briegel for their assistance in data collection in this study.

LITERATURE CITED

Augustinaite, S., & Heggelund, P. (2018). Short-term Synaptic Depression in the Feedforward Inhibitory Circuit in the Dorsal Lateral Geniculate Nucleus. *Neuroscience*, *384*, 76–86. https://doi.org/10.1016/j.neuroscience.2018.05.022

Behan, M. (1982). A quantitative analysis of the ipsilateral retinocollicular projection in the cat: An EM degeneration and EM autoradiographic study. *Journal of Comparative Neurology*, *206*(3), 253–258. https://doi.org/10.1002/cne.902060305

Bickford, M. E. (2019). Synaptic organization of the dorsal lateral geniculate nucleus. *European Journal of Neuroscience*, *49*(7), 938–947. https://doi.org/10.1111/ejn.13917

Bickford, M. E., Carden, W. B., & Patel, N. C. (1999). Two types of interneurons in the cat visual thalamus are distinguished by morphology, synaptic connections, and nitric oxide synthase content. *Journal of Comparative Neurology*, *413*(1), 83–100. https://doi.org/10.1002/(SICI)1096-9861(19991011)413:1<83::AID-CNE6>3.0.CO;2-E

Blitz, D. M., & Regehr, W. G. (2005). Timing and specificity of feed-forward inhibition within the LGN. *Neuron*, *45*(6), 917–928. https://doi.org/10.1016/j.neuron.2005.01.033

Bloomfield, S. A., Hamos, J. E., & Sherman, S. M. (1987). Passive cable properties and morphological correlates of neurones in the lateral geniculate nucleus of the cat. *The Journal of Physiology*, *383*(1), 653–692. https://doi.org/10.1113/jphysiol.1987.sp016435

Briska, A. M., Uhlrich, D. J., & Lytton, W. W. (2003). Computer model of passive signal integration based on whole-cell in vitro studies of rat lateral geniculate nucleus. *European Journal of Neuroscience*, *17*(8), 1531–1541. https://doi.org/10.1046/j.1460-9568.2003.02579.x

Carden, W. B., & Bickford, M. E. (1999). The location of muscarinic type 2 receptors within the synaptic circuitry of the cat lateral posterior nucleus. *Neuroscience Letters*, *276*(3), 153–156. https://doi.org/10.1016/S0304-3940(99)00812-5

Casagrande, V. A., Royal, D. W., & Sáry, G. (2006). Extraretinal Inputs and Feedback Mechanisms to the Lateral Geniculate Nucleus (LGN). *The Primate Visual System: A Comparative Approach*.

https://doi.org/10.1002/0470868112.ch7

Casale, A. E., & McCormick, D. A. (2011). Active action potential propagation but not initiation in thalamic interneuron dendrites. *Journal of Neuroscience*, *31*(50), 18289–18302. https://doi.org/10.1523/JNEUROSCI.4417-11.2011

Cox, C. L., & Sherman, S. M. (2000). Control of dendritic outputs of inhibitory interneurons in the lateral geniculate nucleus. *Neuron*, *27*(3), 597–610. https://doi.org/10.1016/S0896-6273(00)00069-6

Cox, C. L., Zhou, Q., & Sherman, S. M. (1998). Glutamate locally activates dendritic outputs of thalamic internuerons. *Nature*, *394*, 478–481. https://doi.org/10.1038/246170a0

Crandall, S. R., & Cox, C. L. (2013). Thalamic microcircuits: Presynaptic dendrites form two feedforward inhibitory pathways in thalamus. *Journal of Neurophysiology*, *110*(2), 470–480. https://doi.org/10.1152/jn.00559.2012

Errington, A. C., di Giovanni, G., Crunelli, V., & Cope, D. W. (2011). mGluR control of interneuron output regulates feedforward tonic GABAA inhibition in the visual thalamus. *Journal of Neuroscience*, *31*(23), 8669–8680. https://doi.org/10.1523/JNEUROSCI.0317-11.2011

Famiglietti, E. V. (1970). Dendro-dendritic synapses in the lateral geniculate nucleus of the cat. *Brain Research*, *20*(2), 181–191. https://doi.org/10.1016/0006-8993(70)90287-8

Famiglietti, E. V., & Peters, A. (1972). The synaptic glomerulus and the intrinsic neuron in the dorsal lateral geniculate nucleus of the cat. *Journal of Comparative Neurology*, *144*(3), 285–333. https://doi.org/10.1002/cne.901440304

Fiala, J. C. (2005). Reconstruct: A free editor for serial section microscopy. *Journal of Microscopy*, *218*(1), 52–61. https://doi.org/10.1111/j.1365-2818.2005.01466.x

Friedlander, M. J., Lin, C. S., Stanford, L. R., & Sherman, S. M. (1981). Morphology of functionally identified neurons in lateral geniculate nucleus of the cat. *Journal of Neurophysiology*, *46*(1), 80–129. https://doi.org/10.1152/jn.1981.46.1.80

Grimes, W. N., Zhang, J., Graydon, C. W., Kachar, B., & Diamond, J. S. (2010). Retinal Parallel Processors: More than 100 Independent Microcircuits Operate within a Single Interneuron. *Neuron*,

65(6), 873–885. https://doi.org/10.1016/j.neuron.2010.02.028

Guillery, R. W. (1966). A study of Golgi preparations from the dorsal lateral geniculate nucleus of the adult cat. *Journal of Comparative Neurology*, *128*(1), 21–49. https://doi.org/10.1002/cne.901280104

Guillery, R. W. (1969). The organization of synaptic interconnections in the laminae of the dorsal lateral geniculate nucleus of the cat. *Zeitschrift Für Zellforschung Und Mikroskopische Anatomie*, *96*(1), 1–38.

Halnes, G., Augustinaite, S., Heggelund, P., Einevoll, G. T., & Migliore, M. (2011). A multi-compartment model for interneurons in the dorsal lateral geniculate nucleus. *PLoS Computational Biology*, *7*(9). https://doi.org/10.1371/journal.pcbi.1002160

Hamos, J. E., Van Horn, S. C., Raczkowski, D., & Sherman, S. M. (1987). Synaptic circuits involving an individual retinogeniculate axon in the cat. *Journal of Comparative Neurology*, *259*(2), 165–192. https://doi.org/10.1002/cne.902590202

Hamos, J. E., Van Horn, S. C., Raczkowski, D., Uhlrich, D. J., & Sherman, S. M. (1985). Synaptic connectivity of a local circuit neurone in lateral geniculate nucleus of the cat. *Nature*, *317*(6038), 618–621. https://doi.org/10.1038/317618a0

Kaas, J. H., Huerta, M. F., Weber, J. T., & Harting, J. K. (1978). Patterns of retinal terminations and laminar organization of the lateral geniculate nucleus of primates. *Journal of Comparative Neurology*, *182*(3), 517–553. https://doi.org/10.1002/cne.901820308

Krahe, T. E., El-Danaf, R. N., Dilger, E. K., Henderson, S. C., & Guido, W. (2011). Morphologically distinct classes of relay cells exhibit regional preferences in the dorsal lateral geniculate nucleus of the mouse. *Journal of Neuroscience*, *31*(48), 17437–17448. https://doi.org/10.1523/JNEUROSCI.4370-11.2011

Lam, Y., Cox, C. L., Varela, C., & Sherman, S. M. (2005). Morphological correlates of triadic circuitry in the lateral geniculate nucleus of cats and rats. *Journal of Neurophysiology*, *93*(2), 748–757. https://doi.org/10.1152/jn.00256.2004

Liu, T., Petrof, I., & Sherman, S. M. (2015). Modulatory effects of activation of metabotropic glutamate

receptors on GABAergic circuits in the mouse thalamus. *Journal of Neurophysiology*, *113*(7), 2646–2652. https://doi.org/10.1152/jn.01014.2014

Martinez, L. M., Molano-Mazón, M., Wang, X., Sommer, F. T., & Hirsch, J. A. (2014). Statistical wiring of thalamic receptive fields optimizes spatial sampling of the retinal image. *Neuron*, *81*(4), 943–956. https://doi.org/10.1016/j.neuron.2013.12.014

McCormick, D. A. (1992). Neurotransmitter actions in the thalamus and cerebral cortex and their role in neuromodulation of thalamocortical activity. *Progress in Neurobiology*, *39*(4), 337–388. https://doi.org/10.1016/0301-0082(92)90012-4

McCormick, D. A., & Pape, H. C. (1988). Acetylcholine inhibits identified interneurons in the cat lateral geniculate nucleus. *Nature*, *334*(6179), 246–248. https://doi.org/10.1038/334246a0

McCormick, D. A., & Prince, D. A. (1987). Actions of acetylcholine in the guinea-pig and cat medial and lateral geniculate nuclei, in vitro. *The Journal of Physiology*, *392*(1), 147–165. https://doi.org/10.1113/jphysiol.1987.sp016774

Parnavelas, J. G., Sullivan, K., Lieberman, A. R., & Webster, K. E. (1977). Neurons and their synaptic organization in the visual cortex of the rat. *Cell and Tissue Research*, *183*(4), 499–517.

Perreault, M. C., & Raastad, M. (2006). Contribution of morphology and membrane resistance to integration of fast synaptic signals in two thalamic cell types. *Journal of Physiology*, *577*(1), 205–220. https://doi.org/10.1113/jphysiol.2006.113043

Plummer, K. L., Manning, K. A., Levey, A. I., Rees, H. D., & Uhlrich, D. J. (1999). Muscarinic receptor subtypes in the lateral geniculate nucleus: A light and electron microscopic analysis. *Journal of Comparative Neurology*, *404*(3), 408–425. https://doi.org/10.1002/(SICI)1096-9861(19990215)404:3<408::AID-CNE9>3.0.CO;2-Y

Rafols, J. A., & Valverde, F. (1973). The structure of the dorsal lateral geniculate nucleus in the mouse. A golgi and electron microscopic study. *Journal of Comparative Neurology*, *150*(3), 303–331. https://doi.org/10.1002/cne.901500305

Scrucca, L., Fop, M., Murphy, T. B., & Raftery, A. E. (2016). mclust 5: Clustering, Classification and

Density Estimation Using Gaussian Finite Mixture Models. *The R Journal*, *8*(1), 289.

Sherman, S. M. (2004). Interneurons and triadic circuitry of the thalamus. *Trends in Neurosciences*, *27*(11), 670–675. https://doi.org/10.1016/j.tins.2004.08.003

Steriade, M., & Contreras, D. (1995). Relations between cortical and thalamic cellular events during transition from sleep patterns to paroxysmal activity. *Journal of Neuroscience*, *15*(1 II), 623–642. https://doi.org/10.1523/jneurosci.15-01-00623.1995

Steriade, M., & McCarley, R. W. (2013). *Brainstem control of wakefulness and sleep*. Springer Science & Business Media.

Wang, S., Eisenback, M., Datskovskaia, A., Boyce, M., & Bickford, M. E. (2002). GABAergic pretectal terminals contact GABAergic interneurons in the cat dorsal lateral geniculate nucleus, *323*, 141–145.

Wang, X., Wei, Y., Vaingankar, V., Wang, Q., Koepsell, K., Friedrich, T., & Hirsch, J. A. (2008). Feedforward Excitation and Inhibition Evoke Dual Modes of Firing in the Cat's Visual Thalamus during Naturalistic Viewing. *Neuron*, *55*(3), 465–478. https://doi.org/10.1016/j.neuron.2007.06.039.Feedforward

Weber, A. J., Kalil, R. E., & Behan, M. (1989). Synaptic connections between corticogeniculate axons and interneurons in the dorsal lateral geniculate nucleus of the cat. *Journal of Comparative Neurology*, *289*(1), 156–164. https://doi.org/10.1002/cne.902890113

Wilson, J. R., Friedlander, M. J., & Sherman, S. M. (1984). Fine structural morphology of identified X- and Y-cells in the cat's lateral geniculate nucleus. *Proceedings of the Royal Society of London - Biological Sciences*, *221*(1225), 411–436. https://doi.org/10.1098/rspb.1984.0042

CHAPTER IV

DISCUSSION

DISCUSSION

The organization of synaptic circuits in the LGN determines the information that is passed to the visual cortex from the retina. The purpose of this dissertation was to characterize inputs onto relay cells and interneuron dendrites in the LGN to reveal the organizational principles of synaptic inputs on different geniculate cell types to a degree that was previously unfeasible by using connectomic approaches. Previous studies of LGN synaptic circuitry use TEM methods to identify and describe inputs into the LGN (Çavdar, Hacioğlu, Şirvanci, Keskinöz, & Onat, 2011; Erişir, Van Horn, Bickford, & Sherman, 1997; Erişir, Van Horn, & Sherman, 1998, 1997; Famiglietti, 1970; Guillery, 1969; Hammer et al., 2014; Montero, 1986; Smith, O'Leary, Harris, & Gay, 1964; Van Horn, Erişir, & Sherman, 2000; Wilson, Friedlander, & Sherman, 1984). These foundational studies provide the basic principles of synaptic organization in the LGN. However, measuring three dimensional objects in the two dimensional space leads to sampling confounds that introduce ambiguity for the findings. Here, we aimed to answer several questions about LGN synaptic circuitry that are unable to be answered using TEM methods. These questions include: How are axon terminals from different origins organized on relay cell and interneuron dendrite segments? Do terminals from different origins synapse on the same dendrite segment as other inputs preferentially? How do terminals in the same glomeruli organize and interact? To answer these questions, I studied the synaptic circuitry onto dendrite segments in the LGN using SBEM image stacks and connectomics.

Identification of Terminal input origin:

In order to study the organization of different inputs onto LGN relay cell dendrites, I first devised a method to infer terminal origin without the use of immunohistochemical methods. Previously, different morphological features have been used to assign putative origin to unlabeled terminals (Behan, 1982; Bickford, Carden, & Patel, 1999; Casagrande, Royal, & Sáry, 2006; Guillery, 1966, 1969; Krahe, El-Danaf, Dilger, Henderson, & Guido, 2011; Parnavelas, Sullivan, Lieberman, & Webster, 1977; Rafols & Valverde, 1973). In this dissertation, I demonstrate how terminal volume can be used alone or in conjunction with other morphological features to give a more accurate assumption of terminal origin. Previous studies have shown that terminals from the same brain region create a distinct size distribution (Erişir, Van Horn, Bickford, et al., 1997; Erişir et al., 1998; Erişir, Van Horn, & Sherman, 1997; Van Horn et al., 2000). I used this knowledge, as well as known relative terminal sizes from TEM studies of the LGN to classify terminals into putative terminal origin using Gaussian Mixture Modelling. There are several advantages of using model based clustering of terminal volume to sort terminals by axon origin. One advantage is the speed in which terminals can be sorted. Terminal volumes are easily collected from tissue reconstruction software and unlike using only morphological features, each terminal does not need to be individually studied and described in order to determine terminal origin. This method is also a reliable way to identify putative terminal origin of terminals who do not have distinct morphological correlates, like input from the cortex or brainstem. I also demonstrate that this method of terminal sorting is just as accurate and possibly more accurate than using morphology alone and combining these two methods can increase

sorting accuracy. Finally, this method can be applied to brain regions other than the LGN in order to classify terminal input and study the patterns of innervation with SBEM methods.

Input Targeting onto LGN relay cell dendrites

Relay cell dendrite segments can be defined in several ways. In this dissertation, we studied terminal targeting of dendrite segments based on two variables that may contribute to their passive cable properties: dendrite branching order and dendrite diameter. These two variables are related to each other, and thus our data is in agreement that as dendrites branch the caliber decreases. However, I also show that dendrite caliber is not predictive of branch order and thus caliber and order should be considered as two different variables with each influencing terminal targeting in varying amounts. This results has implications for conclusions of earlier TEM studies. Previous TEM studies made the assumption that dendrites with larger calibers are primary dendrites that are more proximal to the cell body (Erişir, Van Horn, Bickford, et al., 1997; Wilson et al., 1984). In these dissertation studies, I show that dendrite caliber cannot reliably predict distance from the some or the order of a dendrite. Because of this finding, future studies of synaptic circuitry using TEM should supplement their findings with some type of spatial data (for example, light microscopy or SBEM) in order to draw conclusions about the exact location of a terminal on a dendrite in relation to the soma. My results also have implications for neuromodeling studies for which knowing the parameters for the cable properties of neurites is essential. Lastly, the variability of the primary dendrite caliber, as demonstrated in Chapter 2, can constitute one of the criteria for identifying different relay cell

types by their ultrastructural morphology, although more parameters have to be discovered to reach a certainty for sorting relay cell types.

Most populations of terminals synapsing onto relay cell dendrites in the LGN show specificity for the dendrite segment they synapse onto. Some of our results are consistent with what has been described in previous literature. For example, large terminals from the retina synapse onto larger caliber dendrites where as small terminals from the cortex and brainstem synapse onto small caliber dendrites (Erişir, Van Horn, Bickford, et al., 1997; Wilson et al., 1984). Through this experiment, I was able to establish the frequency of terminals from specific origins synapsing onto dendrite segments based on dendrite size and branch order. This experiment also provides definitive evidence that retinal and corticothalamic excitation exerted on relay cells occupy completely segregated domains of these cells, suggesting that the integration of feedforward and feedback excitation of relay cells is not summative. Instead, the corticothalamic input that clusters on tertiary dendrite segments, which potentially extend out of the receptive field center watershed area of the geniculate visual map, may have the substrate of bringing in surround information on the relay cells, and mediating the retinal input mediated information processing based on center-surround integration that occurs in cortex.

Input Targeting onto LGN Interneuron Dendrites

Interneurons play an important role in shaping the visual information sent to the cortex. One way interneurons accomplish this is through triadic arrangements in which interneuron dendrites provide feedforward inhibition onto relay cell dendrites (Famiglietti & Peters, 1972; Hamos, Van Horn, Raczkowski, & Sherman, 1987; Hamos, Van Horn, Raczkowski, Uhlrich, &

Sherman, 1985; Lam, Cox, Varela, & Sherman, 2005). In order to obtain a detailed description of inputs onto interneuron dendrites in the LGN, we reconstructed several interneuron dendrites and measured every terminal synapsing onto them. I describe synaptic motifs for triads and glomerular arrangements similar to those alluded to in TEM studies, as well as several novel motifs that were not described before. Using connectomics, I was able to characterize several glomeruli on the same interneuron dendrite and detail the motifs that substantiate the convergence and divergence of interneuron output on relay dendrites.

My results build on existing evidence that interneuron dendrite segments in glomeruli act as individual microcircuits as opposed to one cohesive cellular unit (Bloomfield, Hamos, & Sherman, 1987; Briska, Uhlrich, & Lytton, 2003; Crandall & Cox, 2013; Grimes, Zhang, Graydon, Kachar, & Diamond, 2010; Halnes, Augustinaite, Heggelund, Einevoll, & Migliore, 2011; Perreault & Raastad, 2006). In addition, my results demonstrate that triadic arrangements display an even greater degree of complexity than what is shown with TEM methods and these triadic arrangements show varying degrees of convergence and divergence. In particular, my results reveal convergence of retinal inputs onto interneuron presynaptic segments, a level that was previously unappreciated. This arrangement, that is, the divergent inhibition of relay cells via interneuron appendages that has the capacity to collect information from retinal axons potentially representing a wide variety of receptive fields, may outline a substrate for ON or OFF response properties of interneurons and relays cells. My results also suggest that geniculate interneurons provide multiple types of inhibition onto relay cells via their dendrites, including local and temporal inhibition that occurs at triads, and receptive-field relevant feedforward inhibition that is substantiated via complex motifs found in the glomeruli.

Future Directions:

The results of this dissertation provide a detailed account of patterns of innervation onto both relay cell and interneuron dendrite segments in the LGN. This was done in an effort to understand how information is transformed in the thalamus before reaching the cortex. Although my results contributed to this understanding, I was unable to answer any questions in regard to parallel pathways of visual information in the LGN. Similarly to what was reported in Morgan 2016, several attempts to differentiate different parallel pathways based on input patterns onto dendrites were unsuccessful (Morgan, Berger, Wetzel, & Lichtman, 2016). One possible reason for this is because we used the mouse as an animal model. Not all inputs into the mouse LGN are segregated neatly into parallel pathways like is seen in other species. Studies have demonstrated RCG input into the rodent LGN are more convergent than was first thought and studies that aim to segregate the mouse LGN into anatomically distinct parallel pathways lack confirmatory evidence (Godement, Salaün, & Imbert, 1984; Howarth, Walmsley, & Brown, 2014; Morgan et al., 2016; Reese, 1988).

In order to overcome the limitations of using the mouse LGN as a model of parallel pathways, future research on this topic should utilize an animal model that has known parallel pathways that are anatomically segregated in the LGN. Although there are several examples of animal models that fit this criteria, tree shrews offer unique advantages that cannot be found in other species. Tree shrews are a non-primate species that are considered to represent a prototype of prosimian primates (Murphy et al., 2001). This includes anatomically segregated parallel pathways through the LGN that are organized into layers (Balaram, Isaamullah, Petry, Bickford, & Kaas, 2015; Campbell, Jane, & Yashon, 1967; Conway & Schiller, 1983; Holdefer & Norton,

1995; Hutchins & Casagrande, 1988). Tree shrews have already been used in several studies of the visual system and have shown to be uniquely situated to answer questions about vision in primates (Cruz-Martín et al., 2014; Godement et al., 1984; Hammer, Monavarfeshani, Lemon, Su, & Fox, 2015; Huberman et al., 2009; Marshel, Kaye, Nauhaus, & Callaway, 2012; Petry, Fox, & Casagrande, 1984; Piscopo, El-Danaf, Huberman, & Niell, 2013; Reese, 1988; Rompani et al., 2017).

Our lab has planned several follow up studies to this dissertation with the aim of describing the differences and similarities in synaptic circuitry between different layers in the tree shrew LGN. We will achieve this by generating SBEM image stacks of tree shrew LGN tissue collected from different layers followed by reconstruction of dendrites and terminals using the methods described in this dissertation. The results of these planned studies will show the differences in input pattern onto relay cells that process different visual characteristics and will allow us to speculate how the differences in input patterns lead to this differential visual processing.

Conclusion:

This dissertation provided a detailed analysis of axon terminal patterns onto dendrites in the LGN. Here, I have provided important details of how synapses are organized onto dendrite segments and speculate as to how this organization may be affecting how visual information is modified before reaching the cortex. The findings of this dissertation have important implications for how EM image stacks can be used to study synaptic circuitry throughout the brain, and inform future electrophysiological and neuromodeling studies.

LITERATURE CITED

Balaram, P., Isaamullah, M., Petry, H. M., Bickford, M. E., & Kaas, J. H. (2015). Distributions of vesicular glutamate transporters 1 and 2 in the visual system of tree shrews (Tupaia belangeri). *Journal of Comparative Neurology*, *523*(12), 1792–1808. https://doi.org/10.1002/cne.23727

Behan, M. (1982). A quantitative analysis of the ipsilateral retinocollicular projection in the cat: An EM degeneration and EM autoradiographic study. *Journal of Comparative Neurology*, *206*(3), 253–258. https://doi.org/10.1002/cne.902060305

Bickford, M. E., Carden, W. B., & Patel, N. C. (1999). Two types of interneurons in the cat visual thalamus are distinguished by morphology, synaptic connections, and nitric oxide synthase content. *Journal of Comparative Neurology*, *413*(1), 83–100. https://doi.org/10.1002/(SICI)1096-9861(19991011)413:1<83::AID-CNE6>3.0.CO;2-E

Bloomfield, S. A., Hamos, J. E., & Sherman, S. M. (1987). Passive cable properties and morphological correlates of neurones in the lateral geniculate nucleus of the cat. *The Journal of Physiology*, *383*(1), 653–692. https://doi.org/10.1113/jphysiol.1987.sp016435

Briska, A. M., Uhlrich, D. J., & Lytton, W. W. (2003). Computer model of passive signal integration based on whole-cell in vitro studies of rat lateral geniculate nucleus. *European Journal of Neuroscience*, *17*(8), 1531–1541. https://doi.org/10.1046/j.1460-9568.2003.02579.x

Campbell, C. B. G., Jane, J. A., & Yashon, D. (1967). The retinal projections of the tree shrew and hedgehog. *Brain Research*, *5*, 406–418. https://doi.org/10.1136/bmj.3.5565.607

Casagrande, V. A., Royal, D. W., & Sáry, G. (2006). Extraretinal Inputs and Feedback Mechanisms to the Lateral Geniculate Nucleus (LGN). *The Primate Visual System: A*

Comparative Approach. https://doi.org/10.1002/0470868112.ch7

Çavdar, S., Hacioğlu, H., Şirvanci, S., Keskinöz, E., & Onat, F. (2011). Synaptic organization of the rat thalamus: A quantitative study. *Neurological Sciences*, *32*(6), 1047–1056. https://doi.org/10.1007/s10072-011-0606-4

Conway, J. L., & Schiller, P. H. (1983). Laminar organization of tree shrew dorsal lateral geniculate nucleus. *Journal of Neurophysiology*, *50*(6), 1330–1342. https://doi.org/10.1152/jn.1983.50.6.1330

Crandall, S. R., & Cox, C. L. (2013). Thalamic microcircuits: Presynaptic dendrites form two feedforward inhibitory pathways in thalamus. *Journal of Neurophysiology*, *110*(2), 470–480. https://doi.org/10.1152/jn.00559.2012

Cruz-Martín, A., El-Danaf, R. N., Osakada, F., Sriram, B., Dhande, O. S., Nguyen, P. L., … Huberman, A. D. (2014). A dedicated circuit links direction-selective retinal ganglion cells to the primary visual cortex. *Nature*, *507*(7492), 358–361. https://doi.org/10.1038/nature12989

Erişir, A., Van Horn, S. C., Bickford, M. E., & Sherman, S. M. (1997). Immunocytochemistry and distribution of parabrachial terminals in the lateral geniculate nucleus of the cat: A comparison with corticogeniculate terminals. *Journal of Comparative Neurology*, *377*(4), 535–549. https://doi.org/10.1002/(SICI)1096-9861(19970127)377:4<535::AID-CNE5>3.3.CO;2-Q

Erişir, A., Van Horn, S. C., & Sherman, S. M. (1997). Relative numbers of cortical and brainstem inputs to the lateral geniculate nucleus. *Proceedings of the National Academy of Sciences of the United States of America*, *94*(4), 1517–1520. https://doi.org/10.1073/pnas.94.4.1517

Erişir, A., Van Horn, S. C., & Sherman, S. M. (1998). Distribution of synapses in the lateral geniculate nucleus of the cat: Differences between laminae A and A1 and between relay cells and interneurons. *Journal of Comparative Neurology*, *390*(2), 247–255. https://doi.org/10.1002/(SICI)1096-9861(19980112)390:2<247::AID-CNE7>3.0.CO;2-1

Famiglietti, E. V. (1970). Dendro-dendritic synapses in the lateral geniculate nucleus of the cat. *Brain Research*, *20*(2), 181–191. https://doi.org/10.1016/0006-8993(70)90287-8

Famiglietti, E. V., & Peters, A. (1972). The synaptic glomerulus and the intrinsic neuron in the dorsal lateral geniculate nucleus of the cat. *Journal of Comparative Neurology*, *144*(3), 285–333. https://doi.org/10.1002/cne.901440304

Godement, P., Salaün, J., & Imbert, M. (1984). Prenatal and postnatal development of retinogeniculate and retinocollicular projections in the mouse. *Journal of Comparative Neurology*, *230*(4), 552–575. https://doi.org/10.1002/cne.902300406

Grimes, W. N., Zhang, J., Graydon, C. W., Kachar, B., & Diamond, J. S. (2010). Retinal Parallel Processors: More than 100 Independent Microcircuits Operate within a Single Interneuron. *Neuron*, *65*(6), 873–885. https://doi.org/10.1016/j.neuron.2010.02.028

Guillery, R. W. (1966). A study of Golgi preparations from the dorsal lateral geniculate nucleus of the adult cat. *Journal of Comparative Neurology*, *128*(1), 21–49. https://doi.org/10.1002/cne.901280104

Guillery, R. W. (1969). The organization of synaptic interconnections in the laminae of the dorsal lateral geniculate nucleus of the cat. *Zeitschrift Für Zellforschung Und Mikroskopische Anatomie*, *96*(1), 1–38.

Halnes, G., Augustinaite, S., Heggelund, P., Einevoll, G. T., & Migliore, M. (2011). A multi-compartment model for interneurons in the dorsal lateral geniculate nucleus. *PLoS*

Computational Biology, *7*(9). https://doi.org/10.1371/journal.pcbi.1002160

Hammer, S., Carrillo, G. L., Govindaiah, G., Monavarfeshani, A., Bircher, J. S., Su, J., … Fox, M. A. (2014). Nuclei-specific differences in nerve terminal distribution, morphology, and development in mouse visual thalamus. *Neural Development*, *9*(1), 1–20. https://doi.org/10.1186/1749-8104-9-16

Hammer, S., Monavarfeshani, A., Lemon, T., Su, J., & Fox, M. A. (2015). Multiple Retinal Axons Converge onto Relay Cells in the Adult Mouse Thalamus. *Cell Reports*, *12*(10), 1575–1583. https://doi.org/10.1016/j.celrep.2015.08.003

Hamos, J. E., Van Horn, S. C., Raczkowski, D., & Sherman, S. M. (1987). Synaptic circuits involving an individual retinogeniculate axon in the cat. *Journal of Comparative Neurology*, *259*(2), 165–192. https://doi.org/10.1002/cne.902590202

Hamos, J. E., Van Horn, S. C., Raczkowski, D., Uhlrich, D. J., & Sherman, S. M. (1985). Synaptic connectivity of a local circuit neurone in lateral geniculate nucleus of the cat. *Nature*, *317*(6038), 618–621. https://doi.org/10.1038/317618a0

Holdefer, R. N., & Norton, T. T. (1995). Laminar organization of receptive field properties in the dorsal lateral geniculate nucleus of the tree shrew (Tupaiaglis belangeri). *Journal of Comparative Neurology*, *358*(3), 401–413. https://doi.org/10.1002/cne.903580307

Howarth, M., Walmsley, L., & Brown, T. M. (2014). Binocular integration in the mouse lateral geniculate nuclei. *Current Biology*, *24*(11), 1241–1247. https://doi.org/10.1016/j.cub.2014.04.014

Huberman, A. D., Wei, W., Elstrott, J., Stafford, B. K., Feller, M. B., & Barres, B. A. (2009). Genetic Identification of an On-Off Direction- Selective Retinal Ganglion Cell Subtype Reveals a Layer-Specific Subcortical Map of Posterior Motion. *Neuron*, *62*(3), 327–334.

https://doi.org/10.1016/j.neuron.2009.04.014

Hutchins, J. B., & Casagrande, V. A. (1988). Development of acetylcholinesterase activity in the lateral geniculate nucleus. *Journal of Comparative Neurology*, *275*(2), 241–253. https://doi.org/10.1002/cne.902750206

Krahe, T. E., El-Danaf, R. N., Dilger, E. K., Henderson, S. C., & Guido, W. (2011). Morphologically distinct classes of relay cells exhibit regional preferences in the dorsal lateral geniculate nucleus of the mouse. *Journal of Neuroscience*, *31*(48), 17437–17448. https://doi.org/10.1523/JNEUROSCI.4370-11.2011

Lam, Y., Cox, C. L., Varela, C., & Sherman, S. M. (2005). Morphological correlates of triadic circuitry in the lateral geniculate nucleus of cats and rats. *Journal of Neurophysiology*, *93*(2), 748–757. https://doi.org/10.1152/jn.00256.2004

Marshel, J. H., Kaye, A. P., Nauhaus, I., & Callaway, E. M. (2012). Anterior-Posterior Direction Opponency in the Superficial Mouse Lateral Geniculate Nucleus. *Neuron*, *76*(4), 713–720. https://doi.org/10.1016/j.neuron.2012.09.021

Montero, V. M. (1986). Localization of γ-aminobutyric acid (GABA) in type 3 cells and demonstration of their source to f2 terminals in the cat lateral geniculate nucleus: A golgi-electron-microscopic GABA-immunocytochemical study. *Journal of Comparative Neurology*, *254*(2), 228–245. https://doi.org/10.1002/cne.902540207

Morgan, J. L., Berger, D. R., Wetzel, A. W., & Lichtman, J. W. (2016). The Fuzzy Logic of Network Connectivity in Mouse Visual Thalamus. *Cell*, *165*(1), 192–206. https://doi.org/10.1016/j.cell.2016.02.033

Murphy, W. J., Eizirik, E., O'Brien, S. J., Madsen, O., Scally, M., Douady, C. J., … Springer, M. S. (2001). Resolution of the early placental mammal radiation using bayesian phylogenetics.

Science, *294*(5550), 2348–2351. https://doi.org/10.1126/science.1067179

Parnavelas, J. G., Sullivan, K., Lieberman, A. R., & Webster, K. E. (1977). Neurons and their synaptic organization in the visual cortex of the rat. *Cell and Tissue Research*, *183*(4), 499–517.

Perreault, M. C., & Raastad, M. (2006). Contribution of morphology and membrane resistance to integration of fast synaptic signals in two thalamic cell types. *Journal of Physiology*, *577*(1), 205–220. https://doi.org/10.1113/jphysiol.2006.113043

Petry, H. M., Fox, R., & Casagrande, V. A. (1984). Spatial contrast sensitivity of the tree shrew. *Vision Research*, *24*(9), 1037–1042. https://doi.org/10.1016/0042-6989(84)90080-4

Piscopo, D. M., El-Danaf, R. N., Huberman, A. D., & Niell, C. M. (2013). Diverse visual features encoded in mouse lateral geniculate nucleus. *Journal of Neuroscience*, *33*(11), 4642–4656. https://doi.org/10.1523/JNEUROSCI.5187-12.2013

Rafols, J. A., & Valverde, F. (1973). The structure of the dorsal lateral geniculate nucleus in the mouse. A golgi and electron microscopic study. *Journal of Comparative Neurology*, *150*(3), 303–331. https://doi.org/10.1002/cne.901500305

Reese, B. E. (1988). “Hidden lamination” in the dorsal lateral geniculate nucleus: the functional organization of this thalamic region in the rat. *Brain Research Reviews*, *13*(2), 119–137. https://doi.org/10.1016/0165-0173(88)90017-3

Rompani, S. B., Müllner, F. E., Wanner, A., Zhang, C., Roth, C. N., Yonehara, K., & Roska, B. (2017). Different Modes of Visual Integration in the Lateral Geniculate Nucleus Revealed by Single-Cell-Initiated Transsynaptic Tracing. *Neuron*, *93*(4), 767-776.e6. https://doi.org/10.1016/j.neuron.2017.01.028

Smith, J. M., O’Leary, J. L., Harris, A. B., & Gay, A. J. (1964). Ultrastructural features of the

lateral geniculate nucleus of the cat. *Journal of Comparative Neurology*, *123*(3), 357–377. https://doi.org/10.1002/cne.901230305

Van Horn, S. C., Erişir, A., & Sherman, S. M. (2000). Relative distribution of synapses in the A-laminae of the lateral geniculate nucleus of the cat. *Journal of Comparative Neurology*, *416*(4), 509–520. https://doi.org/10.1002/(SICI)1096-9861(20000124)416:4<509::AID-CNE7>3.0.CO;2-H

Wilson, J. R., Friedlander, M. J., & Sherman, S. M. (1984). Fine structural morphology of identified X- and Y-cells in the cat's lateral geniculate nucleus. *Proceedings of the Royal Society of London - Biological Sciences*, *221*(1225), 411–436. https://doi.org/10.1098/rspb.1984.0042

APPENDIX I

Random Sampling of Terminal Volumes in 3D Electron Microscopy Image Stacks Using a Stereological Approach

SIGNIFICANCE STATEMENT

The development of serial section electron microscopy (EM) has provided the tool necessary to study synaptic interactions in a volume of neural tissue. However, studies collecting volumetric data from these image stacks may be limited by large data sets that lack the clarity necessary to ask hypothesis based questions. Therefore, it is necessary to devise a strategy to unbiasedly collect a representative sample of terminal volumes for hypothesis based testing. The present report describes a stereology based technique for collecting random samples of terminal volume information from serial section EM image stacks.

INTRODUCTION

A major aim of neuroscience research is to understand how the brain changes and adapts throughout the lifespan due to internal and external factors. Some of these factors include, embryonic development, aging, addiction, injury, neurodegeneration and environmental toxicity (Fuchs, Czéh, Kole, Michaelis, & Lucassen, 2004; Heuninckx, Wenderoth, & Swinnen, 2008; Kalivas & O'Brien, 2008; Küppers & Beyer, 2001; Petzinger et al., 2013; Stephan, Baldeweg, & Friston, 2006; Thomas, Kalivas, & Shaham, 2008; Vasina et al., 2006; Yao, Petralia, & Mattson, 2016). Many of the functional adaptations made by the brain in response to changing environmental factors are subtle and lead to alterations in the fine structure of the brain. These ultrastructural changes include sprouting or pruning of axonal branches; terminal bouton number and size; the number and shape of dendrites and dendritic spines; the number of synapses; the size and shape of postsynaptic density; and the patterns of myelination (Bosch & Hayashi, 2012; Egawa et al., 2018; Gibson, Geraghty, & Monje, 2018; Long, Wan, Roberts, & Corfas, 2018; Nishiyama & Yasuda, 2015; Russo et al., 2010; Zeng et al., 2018). Furthermore, adaptive

alterations can occur selectively for given inputs or neuron types in any circuitry. Therefore, characterizing the anatomical changes in synaptic circuitries can reveal factors underlying brain adaptation or plasticity across various developmental stages or external insults.

Electron microscopy (EM) has been the best available tool to resolve brain ultrastructure, and effective quantification methods have been developed in order to evaluate changes in the ultrastructure (Bickford et al., 2010; Cucchiaro, Uhlrich, & Sherman, 1991; Erişir, Van Horn, Bickford, & Sherman, 1997; Erişir, Van Horn, & Sherman, 1997; Graziadei, Karlan, Monti Graziadei, & Bernstein, 1980; Raisman, 1969; Schecter et al., 2017; Van Horn, Erişir, & Sherman, 2000; Wilke et al., 2013). Recent advances in techniques to obtain serial electron microscopy images has led to high throughput connectomic approaches that are capable of reconstructing local neuronal circuitries and obtaining detailed maps of neuronal connectivity (Briggman & Bock, 2012; Denk & Horstmann, 2004; Fiala, 2005; Goodman, Benson, Campbell, & Kidd, 2019; Kikuchi et al., 2020; Lakadamyali, Babcock, Bates, Zhuang, & Lichtman, 2012; Morgan & Lichtman, 2013; Peddie & Collinson, 2014). Serial EM material is exceptionally suitable for accurate quantifications of volumetric synapse and spine density and is more reliable for morphometric classification of synaptic inputs. The precision of serial EM offers the potential to replace unbiased estimation approaches used with 2D images which have been the gold standard in revealing synaptic changes in neuroplasticity (Fiala, 2005; Merchán-Pérez, Rodriguez, Alonso-Nanclares, Schertel, & DeFelipe, 2009). The application of these estimation-based approaches to 3D-EM image stack datasets opens new possibilities for hypothesis-based research without having to reconstruct large volumes of brain tissue in multiple ages, experimental conditions or species. One barrier to wider use of serial EM image stacks is the relatively small number of facilities that are able to image the material; thus, high-volume

connectomics analyses are currently limited to a few centers globally. Open source access to stacks made available by imaging centers may allow smaller labs to integrate their own research questions with connectomics technologies.

In this paper, I describe a simple, accurate and replicable method to estimate the number of synaptic terminals that are associated with identifiable input origins using Scanning Blockface Electron Microscopy (SBEM) stacks obtained from the mouse dorsal and ventral lateral geniculate nucleus dLGN and vLGN) and layer 4 of the rat striate cortex (V1/L4). Our objective was to devise a random sampling strategy from a volume of tissue that would allow reliable estimation for the ratios of morphologically identifiable, distinct inputs. Use of this method will allow researchers to quickly obtain a quantification of the synaptic circuitry in a given region of the brain and then to compare this circuitry across any given variable (i.e. age, disease progression, development). In order to obtain a random sample of terminal volumes, I employ systematic sampling with foundations in stereology.

MATERIALS and METHODS

Preparation of Image Stacks:

Tissue Preparation: Mouse and rat tissue used for this study were transcardially perfused with phosphate buffer saline (PBS) followed by a 4% paraformaldehyde and 2% glutaraldehyde solution made in 0.1M cacodylate buffer. Brains were then immediately dissected and cut coronally at 300um sections on a vibratome. The dLGN and vLGN were then dissected from the appropriate section and sent to renovo Neural Inc for staining, embedding, sectioning and imaging.

Image Stacks: A total of 3 image stacks was used: 1 dLGN, 1 vLGN and 1 V1/L4. Two image stacks of mouse LGN were provided by Dr. Michael Fox (Professor, Biological Sciences, College of Science, Virginia Tech) by Renovo, Inc, and were made available to us for this study. The rat striate cortex stack was also produced by Renovo, Inc, for the Erisir lab; this stack will be made available in an online repository. Each electron microscopy image is 5nm/pixel and 41um x 41um. Three image stacks were used in this study: A stack through the mouse vLGN contained 300; a stack from the mouse dLGN contained 200 images; and a third stack from the rat layer 4 of V1 contained 300 images.

Computers, reconstruction software:

All image tracing was done using Reconstruct software (Fiala, 2005). Synapse length and terminal volume were calculated in the Reconstruct software and were recorded in Microsoft Excel. Random number generation for location selection was done in Microsoft Excel.

Selection of stereology parameters:

In this study, I used a stereology grid to count and measure synapses and terminals in the brain regions listed above. In this context, a synapse is all of the synaptic zones between a bouton and a single postsynaptic dendrite. Synapse and terminal volumes have large variability depending on the origin of the axons (Erişir, Van Horn, Bickford, et al., 1997; Erişir, Van Horn, & Sherman, 1998, 1997). This leads to a sampling bias that oversamples larger objects because they are more likely to appear in more sections in the image stack. By using stereology methods to randomly select objects to be counted, I eliminate the sampling bias that can be introduced by the size of an object and ensures that each terminal and synapse have an equal opportunity to be sampled (Gundersen, 1986, 1988; Gundersen et al., 1988; Henny, Brown, Micklem, Magill, & Bolam, 2014).

To eliminate the bias for oversampling large objects, the dimensions of the counting frame should be larger than the size of the largest counting unit, or the *particle*. This principle applies both to the dimensions of the counting frame (that is, the x and y dimensions of the stereology box), and the distance between each stereology grid placed in the 3D stacks (that is, the z dimension of the stereology box). In determining the size of the counting frame, I decided to use the synapse size as opposed to terminal size, because synapse is the 'particle' that is identified or counted in each 2D grid. Thus, the size of the stereology box was 2um x 2um , that is >2x larger than the average synapse diameter measured in the thalamus and the visual cortex. Note that the dLGN in particular may have contained sparse synapses that may be >2x of the average synapse diameter in this particular brain region. In order not to selectively exclude such very large synapses from the sample, synapses that may intersect both the inclusion and the exclusion edges of the counting box are included in the sample. In determining the distance between two subsequent 2D grids, I used the synapse size as the guide and therefore, each grid was placed 2um apart in the z dimension.

The resulting stereology matrix is made of 15x15 individual counting frames and was placed onto 6 total EM images (i.e. *seed image*). This array yielded 225 sampling frames per single *seed image*, and 1,350 total locations within a 12,726 um^3 volume of brain (Figure 1a). Each sampling frame was given a unique identifying number between 1 and 1350. Using a random number generator, we examined 405 frames (30% of total) in the stereology array and made a list of the frames to be examined.

Data Collection:

Neurite Tracing: Each selected frame was examined for synapses completely or partially inside the sampling box. For a partial synapse to be included in the sample, it had to be intersected by the green 'inclusion' line of the stereology box (Figure 1b). If a synapse within the sampling location intersected with a red line, it was not included in the dataset (Figure 1c). After a synapse was traced on the seed image as well as in every adjacent image it appeared, the axon terminal bouton that was associated with that synapse was also traced in the stack until the bulbous structure of the terminal is reduced to a stalk or intrabouton segment. Note that the terminal boutons could extend outside of the sterology box, as long as their synapse appeared in the sampling box of the seed image (Figure 1d). After tracing the synapse and the terminal in the sampling location, we traced the synapse and terminal through adjacent sections until the synapse and terminal were no longer visible in the images. Each sampling location could contain anywhere from zero to four synapses. Each synapse and terminal was given a unique identifying name. This procedure was repeated in all four image stacks used for this study.

Statistical analysis and figures:

All descriptive statistics, non-parametric statistical testing, terminal volume distribution graphs and cumulative probability graphs were completed using Prism software version 8. All images for figures were collected from Reconstruct software and annotated using Photoshop 2020.

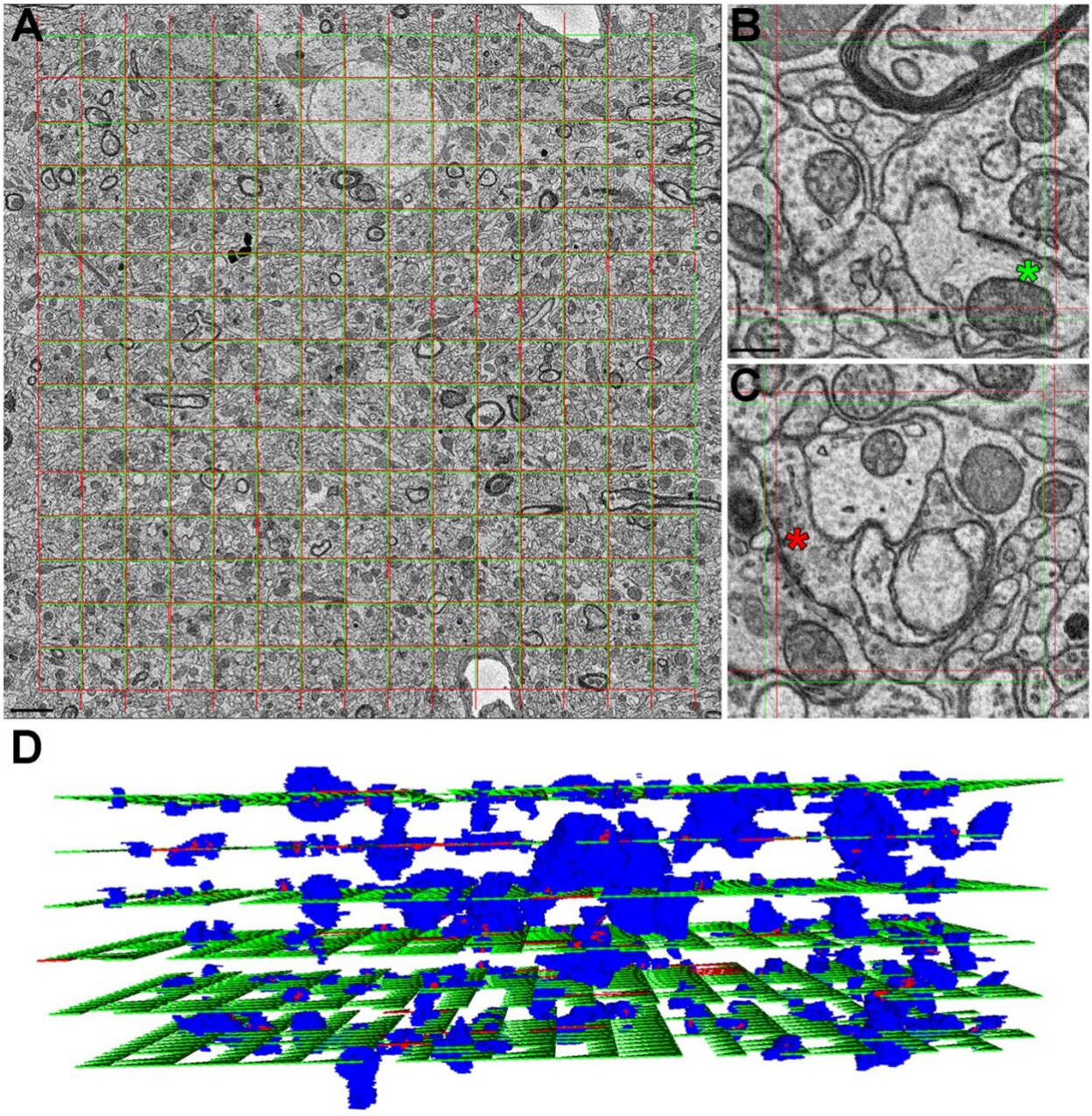

Figure 1: Stereology method used for the collection of random samples of terminal volumes. (A) an example of a seed image with a stereology grid overlaid onto it. Each frame is made from two green inclusion lines and two red exclusion lines. (B) An example of a synapse and terminal that intersects with an inclusion line. This synapse and terminal will be included in the sample because it intersects with the green inclusion line; green asterisk indicates the area postsynaptic

to the cleft. (C) An example of a synapse and terminal that intersects with an exclusion line. This synapse and terminal will not be included in the sample because it intersects with the red exclusion line; red asterisk indicates the area postsynaptic to the cleft. (D) A lateral view of the 3D reconstruction of all stereology grids on seed images. All synapse and terminal reconstructions start on a grid but then are reconstructed to their full volume in using all images in the stack.

RESULTS:

Stereological sampling strategy of like modularities

Stereological approaches to random sampling have the aim to eliminate sampling bias caused by variance in particle size. Successful implementation of stereological approaches allows for all particles to have an equal chance to be sampled regardless of size, and should result in an accurate representation of terminal size distribution in any given brain region. Based on this knowledge, I asked if our sampling strategy accounts for any modularity that might exist in the synaptic circuitry. I answered this question by analyzing a V1-Layer 4 stack twice (referred to henceforth as V1a and V1b) and comparing the terminal volume distribution. Data sets V1a and V1b were collected from the same image stack, but placement of the stereological array varied between the two experiments by changing which EM images served as the seed image and shifting the stereology array in the X and Y position on the seed images. We also generated different lists of frames to sample from for each experiment. By varying the stereology array and frame list in this way, we were able to introduce an element of randomness between the samples while still applying systematic stereological counting rules to each.

Successful validation of this technique should result in no difference in terminal volume distribution between the two V1 samples. The two samples from V1 had both a different starting point for the stereology grid placement as well as different sets of locations within the grid from which I sampled. We traced 212 terminals from V1a. The average terminal volume is 0.28 μm^3 +/- 0.24 μm^3 with a minimum volume of 0.03 μm^3 and a maximum volume of 1.895 μm^3 (Figure 2a,c). Similarly, we traced 235 terminals from V1b with an average terminal volume of 0.32 μm^3 +/- 0.27 μm^3 with a minimum volume of 0.02 μm^3 and a maximum volume of 2.36 μm^3 (Figure 2b,d). A comparison of the cumulative probability of terminal volumes from the two samples

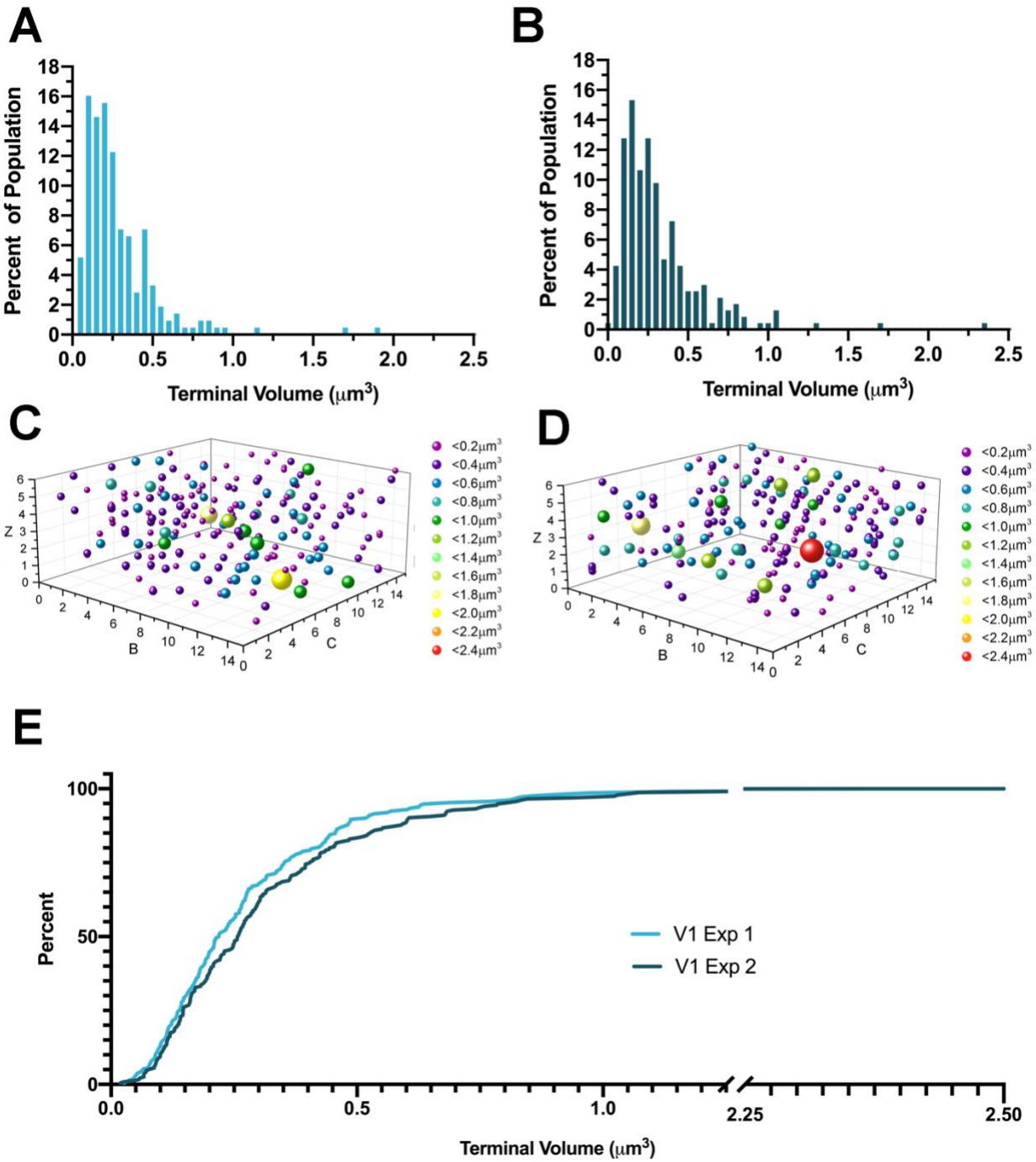

Figure 2: Terminal volume distributions from experiments 1 and 2 of visual cortex. (A,B) Terminal volume distributions from experiment 1 (A) and 2 (B) of the mouse visual cortex.

(C,D) Bubble graph representations of the volume and spatial distribution of terminals in V1 experiment 1(C) and V1 experiment 2 (D). (E) Comparison of the cumulative probability of terminal volumes in both V1 experiments shows there is no difference in the distribution of terminal volumes in these two experiments.

reveals no difference in terminal volume distribution (Figure 2e, Kolmogorov-Smirnov, p=0.24). A direct comparison of terminal volumes from the two samples reveals no statistical difference between the terminal sizes of these two groups (Mann-Whitney U, p= 0.09).

Stereological sampling reveals structural differences

It is known from past EM literature that the terminal size distribution between the dLGN and the vLGN in the mouse differ from each other. The dLGN has a wide distribution of terminal sizes that consists of many small terminals and few, very large terminals whereas the vLGN terminal size distribution is more compact and does not contain the very large terminals seen in the dLGN (Erişir, Van Horn, & Sherman, 1997; Hammer et al., 2014; Van Horn et al., 2000). The difference in terminal distribution between these two regions is a product of their different inputs. In order to determine if our random sampling procedure reveals differences in synaptic circuitry between the dLGN and vLGN, I used our stereology approach to collect terminal volume data and then compared the terminal size distribution. I expect that if our stereology approach gives an accurate representation of terminal volume distribution the data sets collected in dLGN and vLGN will have differences in terminal size distributions and the terminal volume distributions of each will reliably recreate the known terminal distributions of these brain regions.

In the dLGN, 408 terminals had an average volume of 0.783 μm^3 +/- 1.392 μm^3 with a minimum of 0.015μm^3 and a maximum of 14.69μm^3 (Figure 3a,c). 165 terminals were traced from the stack of vLGN images. The average terminal volume in the vLGN was 1.379 μm^3 +/- 1.376 μm^3 with a minimum of 0.02 μm^3 and a maximum of 9.46 μm^3 (Figure 3 b,d). The shape of the terminal volume distributions is in agreement with what has been described in TEM

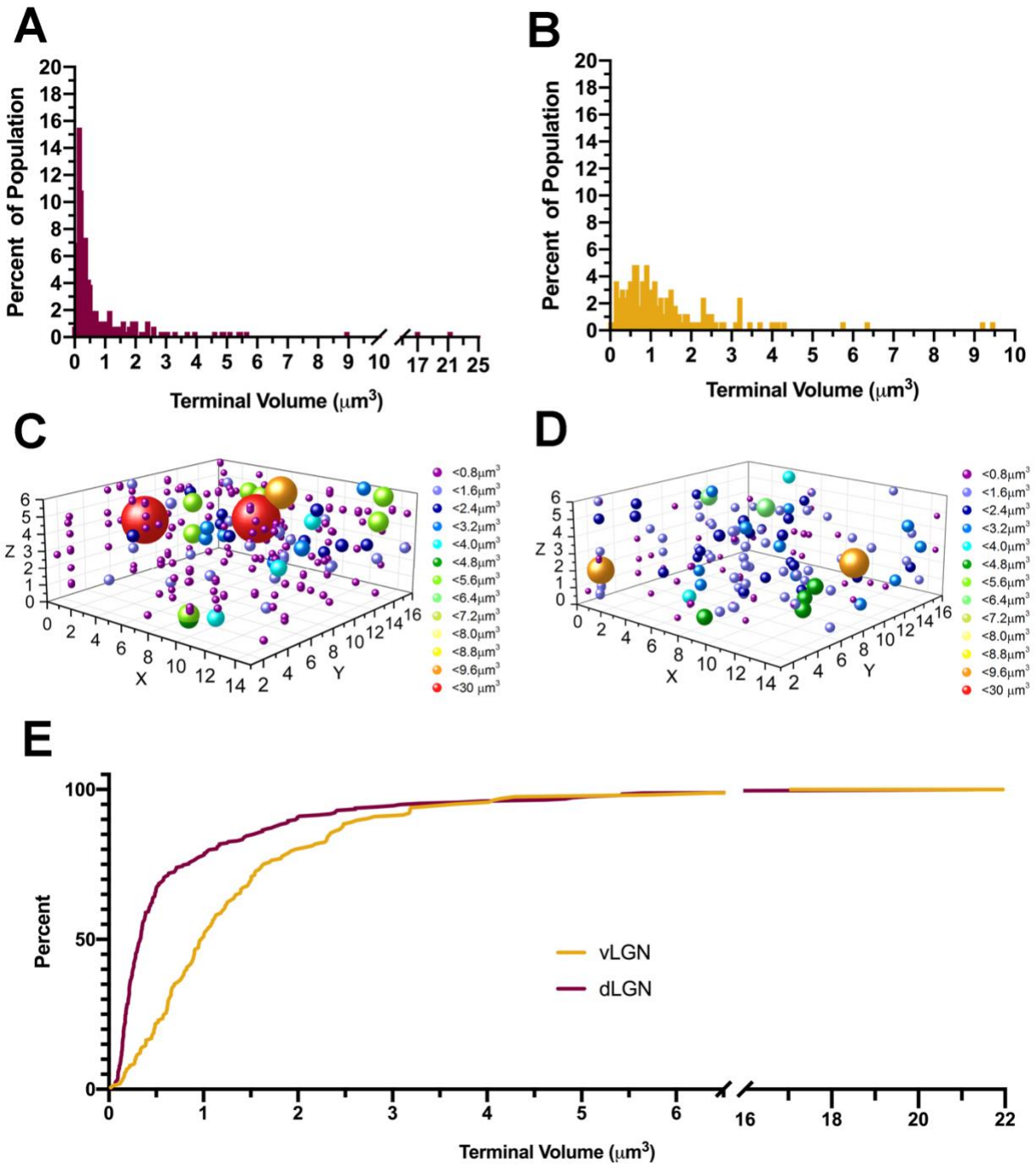

Figure 3: Terminal volume distributions from the mouse dLGN and vLGN. (A) Terminal volume distributions from the mouse dLGN. (B) Terminal volume distribution from the mouse

vLGN. (C,D) Bubble graph representations of the volume and spatial distribution of terminals in the dLGN (C) and vLGN (D). (E) Comparison of the cumulative probability of terminal volumes in dLGN and vLGN shows there is a significant difference in the distribution of terminal volumes in these two brain regions.

literature: the dLGN displays a wide distribution with a heavy left skew and the vLGN displays a more compact distribution with no very large terminals. Comparison of the cumulative probability of terminal size in the dLGN vs the vLGN reveals that the two populations are distinct in their terminal size distribution (Figure 3e, Kolmogorov-Smirnov, $p< 0.0001$). A statistical comparison of these two terminal distributions also reveals that the terminal size distribution between the two brain regions are distinct (Mann-Whitney U, $P < 0.0001$). These results show that our stereological procedure for terminal volume collection gives an accurate representation of the terminal size distribution and can reveal differences in synaptic circuitry between two brain regions with known differences in their synaptic inputs.

DISCUSSION

Sampling strategies devised for 2D TEM images have been carefully constructed to account for varying sampling probability of each synapse or terminal with varying cross-section sizes (Gardi, Nyengaard, & Gundersen, 2006; Gundersen, 1986; Henny et al., 2014). In this study, I take advantage of these sampling strategies and combine them with advances in SBEM imaging techniques in order to collect a random sample of LGN and V1 terminal volumes that represent the distribution of all terminals in a given volume of tissue. While development of automated segmentation approaches will likely enable 3D reconstruction of entire brain circuitries, this simpler estimation tool is sufficient to address hypothesis-based comparisons across multiple experimental conditions, ages or brain regions.

Data collected from the dLGN using this technique was used in chapter 2 of this dissertation. The dLGN receives input from several brain regions, including the retina, the brainstem, the cortex, the TRN, and inhibitory interneurons. Previous studies using TEM and

immunohistochemistry have demonstrated that the inputs from each of these regions make up a certain percent of the total terminals in the dLGN (Erişir, Van Horn, Bickford, et al., 1997; Erişir et al., 1998; Erişir, Van Horn, & Sherman, 1997; Van Horn et al., 2000; Wilson, Friedlander, & Sherman, 1984). Using this knowledge, I was able to determine putative origin of terminals in SBEM stacks by calculating the percent each population contributed to the total number of terminals and comparing these percentages to TEM data. Without an unbiased sample of terminal volumes, I could not reliably use the number of terminals to determine input origin.

One of the main goals in neurosciences has been to devise simple, accurate and replicable methods to estimate the number of synapses or other ultrastructural components of the brain circuitry. Alterations in synapses, spines or vesicles can define changes that occur in development and aging, with experimental conditions, or through the progress of a disease. Recent advances in SBEM imaging have led to the elimination of sampling biases introduced when using 2D TEM data to measure three dimensional objects. Here, I outline the method used in this dissertation to collect a random sample of terminal volumes that represents a similar input heterogeneity as the whole terminal population. I show that using stereological sample collection principles, a representative terminal volume distribution can be collected without the need to reconstruct every neurite in an image stack. This method will be refined and disseminated to allow for the general use of this method to address hypothesis-based comparisons across multiple experimental conditions, ages or brain regions using SBEM stacks.

LITERATURE CITED

Bickford, M. E., Slusarczyk, A. S., Dilger, E. K., Krahe, T. E., Kucuk, C., & Guido, W. (2010). Synaptic development of the mouse dorsal lateral geniculate nucleus. *Journal of Comparative Neurology*, *518*(5), 622–635. https://doi.org/10.1002/cne.22223

Bosch, M., & Hayashi, Y. (2012). Structural plasticity of dendritic spines. *Current Opinion in Neurobiology*, *22*(3), 383–388. https://doi.org/10.1016/j.conb.2011.09.002

Briggman, K. L., & Bock, D. D. (2012). Volume electron microscopy for neuronal circuit reconstruction. *Current Opinion in Neurobiology*, *22*(1), 154–161. https://doi.org/10.1016/j.conb.2011.10.022

Cucchiaro, J. B., Uhlrich, D. J., & Sherman, S. M. (1991). Electron-microscopic analysis of synaptic input from the perigeniculate nucleus to the A-laminae of the lateral geniculate nucleus in cats. *Journal of Comparative Neurology*, *310*(3), 316–336. https://doi.org/10.1002/cne.903100304

Denk, W., & Horstmann, H. (2004). Serial block-face scanning electron microscopy to reconstruct three-dimensional tissue nanostructure. *PLoS Biology*, *2*(11). https://doi.org/10.1371/journal.pbio.0020329

Egawa, J., Zemljic-Harpf, A., Mandyam, C. D., Niesman, I. R., Lysenko, L. V., Kleschevnikov, A. M., … Head, B. P. (2018). Neuron-targeted caveolin-1 promotes ultrastructural and functional hippocampal synaptic plasticity. *Cerebral Cortex*, *28*(9), 3255–3266. https://doi.org/10.1093/cercor/bhx196

Erişir, A., Van Horn, S. C., Bickford, M. E., & Sherman, S. M. (1997). Immunocytochemistry and distribution of parabrachial terminals in the lateral geniculate nucleus of the cat: A comparison with corticogeniculate terminals. *Journal of Comparative Neurology*, *377*(4),

535–549. https://doi.org/10.1002/(SICI)1096-9861(19970127)377:4<535::AID-CNE5>3.3.CO;2-Q

Erişir, A., Van Horn, S. C., & Sherman, S. M. (1997). Relative numbers of cortical and brainstem inputs to the lateral geniculate nucleus. *Proceedings of the National Academy of Sciences of the United States of America*, *94*(4), 1517–1520. https://doi.org/10.1073/pnas.94.4.1517

Erişir, A., Van Horn, S. C., & Sherman, S. M. (1998). Distribution of synapses in the lateral geniculate nucleus of the cat: Differences between laminae A and A1 and between relay cells and interneurons. *Journal of Comparative Neurology*, *390*(2), 247–255. https://doi.org/10.1002/(SICI)1096-9861(19980112)390:2<247::AID-CNE7>3.0.CO;2-1

Fiala, J. C. (2005). Reconstruct: A free editor for serial section microscopy. *Journal of Microscopy*, *218*(1), 52–61. https://doi.org/10.1111/j.1365-2818.2005.01466.x

Fuchs, E., Czéh, B., Kole, M. H. P., Michaelis, T., & Lucassen, P. J. (2004). Alterations of neuroplasticity in depression: The hippocampus and beyond. *European Neuropsychopharmacology*, *14*(SUPPL. 5). https://doi.org/10.1016/j.euroneuro.2004.09.002

Gardi, J. E., Nyengaard, J. R., & Gundersen, H.-J. G. (2006). Using biased image analysis for improving unbiased stereological number estimation - A pilot simulation study of the smooth fractionator. *Journal of Microscopy*, *222*(3), 242–250. https://doi.org/10.1111/j.1365-2818.2006.01552.x

Gibson, E. M., Geraghty, A. C., & Monje, M. (2018). Bad wrap: Myelin and myelin plasticity in health and disease. *Developmental Neurobiology*, *78*(2), 123–135. https://doi.org/10.1002/dneu.22541

Goodman, S. L., Benson, E. K., Campbell, J. M., & Kidd, G. J. (2019). Rapid Automated

Preparation for Serial Block Face Scanning Electron Microscopy. *Microscopy and Microanalysis*, *25*(S2), 1182–1183. https://doi.org/10.1017/s1431927619006640

Graziadei, P. P. C., Karlan, M. S., Monti Graziadei, G. A., & Bernstein, J. J. (1980). Neurogenesis of sensory neurons in the primate olfactory system after section of the fila olfactoria. *Brain Research*, *186*, 289–300.

Gundersen, H.-J. G. (1986). Stereology of arbitrary particles. A review of unbiased number and size estimators and the presentation of some new ones, in memory of William R. Thompson. *Journal of Microscopy*, *143*(1), 3–45.

Gundersen, H.-J. G. (1988). The nucleator. *Journal of Microscopy*, *151*(1), 3–21.

Gundersen, H.-J. G., Bagger, P., Bendtsen, T. F., Evans, S. M., Korbo, L. X. M. N., Marcussen, N., … Sørensen, F. . (1988). The new stereological tools: disector, fractionator, nucleator and point sampled intercepts and their use in pathological research and diagnosis. *Apmis*, *96*(7–12), 857–881.

Hammer, S., Carrillo, G. L., Govindaiah, G., Monavarfeshani, A., Bircher, J. S., Su, J., … Fox, M. A. (2014). Nuclei-specific differences in nerve terminal distribution, morphology, and development in mouse visual thalamus. *Neural Development*, *9*(1), 1–20. https://doi.org/10.1186/1749-8104-9-16

Henny, P., Brown, M. T. C., Micklem, B. R., Magill, P. J., & Bolam, J. P. (2014). Stereological and ultrastructural quantification of the afferent synaptome of individual neurons. *Brain Structure and Function*, *219*(2), 631–640. https://doi.org/10.1007/s00429-013-0523-9

Heuninckx, S., Wenderoth, N., & Swinnen, S. P. (2008). Systems neuroplasticity in the aging brain: Recruiting additional neural resources for successful motor performance in elderly persons. *Journal of Neuroscience*, *28*(1), 91–99. https://doi.org/10.1523/JNEUROSCI.3300-

07.2008

Kalivas, P. W., & O'Brien, C. (2008). Drug addiction as a pathology of staged neuroplasticity. *Neuropsychopharmacology*, *33*(1), 166–180. https://doi.org/10.1038/sj.npp.1301564

Kikuchi, T., Gonzalez-Soriano, J., Kastanauskaite, A., Benavides-Piccione, R., Merchán-Pérez, A., DeFelipe, J., & Blazquez-Llorca, L. (2020). Volume Electron Microscopy Study of the Relationship Between Synapses and Astrocytes in the Developing Rat Somatosensory Cortex. *Cerebral Cortex*, 1–20. https://doi.org/10.1093/cercor/bhz343

Küppers, E., & Beyer, C. (2001). Dopamine regulates brain-derived neurotrophic factor (BDNF) expression in cultured embryonic mouse striatal cells. *NeuroReport*, *12*(6), 1175–1179. https://doi.org/10.1097/00001756-200105080-00025

Lakadamyali, M., Babcock, H., Bates, M., Zhuang, X., & Lichtman, J. W. (2012). 3D multicolor super-resolution imaging offers improved accuracy in neuron tracing. *PLoS ONE*, *7*(1). https://doi.org/10.1371/journal.pone.0030826

Long, P., Wan, G., Roberts, M. T., & Corfas, G. (2018). Myelin development, plasticity, and pathology in the auditory system. *Developmental Neurobiology*, *78*(2), 80–92. https://doi.org/10.1002/dneu.22538

Merchán-Pérez, A., Rodriguez, J. R., Alonso-Nanclares, L., Schertel, A., & DeFelipe, J. (2009). Counting synapses using FIB/SEM microscopy: A true revolution for ultrastructural volume reconstruction. *Frontiers in Neuroanatomy*, *3*(OCT), 1–14. https://doi.org/10.3389/neuro.05.018.2009

Morgan, J. L., & Lichtman, J. W. (2013). Why not connectomics? *Nature Methods*, *10*(6), 494–500. https://doi.org/10.1038/nmeth.2480

Nishiyama, J., & Yasuda, R. (2015). Biochemical Computation for Spine Structural Plasticity.

Neuron, *87*(1), 63–75. https://doi.org/10.1016/j.neuron.2015.05.043

Peddie, C. J., & Collinson, L. M. (2014). Exploring the third dimension: Volume electron microscopy comes of age. *Micron*, *61*, 9–19. https://doi.org/10.1016/j.micron.2014.01.009

Petzinger, G. M., Fisher, B. E., McEwen, S., Beeler, J. A., Walsh, J. P., & Jakowec, M. W. (2013). Exercise-enhanced neuroplasticity targeting motor and cognitive circuitry in Parkinson's disease. *The Lancet Neurology*, *12*(7), 716–726. https://doi.org/10.1016/S1474-4422(13)70123-6

Raisman, G. (1969). Neuronal plasticity in the septal nuclei of the adult rat. *Brain Research*, *14*(1), 25–48. https://doi.org/10.1016/0006-8993(69)90029-8

Russo, S. J., Dietz, D. M., Dumitriu, D., Morrison, J. H., Malenka, R. C., & Nestler, E. J. (2010). The addicted synapse: Mechanisms of synaptic and structural plasticity in nucleus accumbens. *Trends in Neurosciences*, *33*(6), 267–276. https://doi.org/10.1016/j.tins.2010.02.002

Schecter, R. W., Maher, E. E., Welsh, C. A., Stevens, B., Erişir, A., & Bear, M. F. (2017). Experience-dependent synaptic plasticity in V1 occurs without microglial CX3CR1. *Journal of Neuroscience*, *37*(44), 10541–10553. https://doi.org/10.1523/JNEUROSCI.2679-16.2017

Stephan, K. E., Baldeweg, T., & Friston, K. J. (2006). Synaptic Plasticity and Dysconnection in Schizophrenia. *Biological Psychiatry*, *59*(10), 929–939. https://doi.org/10.1016/j.biopsych.2005.10.005

Thomas, M. J., Kalivas, P. W., & Shaham, Y. (2008). Neuroplasticity in the mesolimbic dopamine system and cocaine addiction. *British Journal of Pharmacology*, *154*(2), 327–342. https://doi.org/10.1038/bjp.2008.77

Van Horn, S. C., Erişir, A., & Sherman, S. M. (2000). Relative distribution of synapses in the A-laminae of the lateral geniculate nucleus of the cat. *Journal of Comparative Neurology*, *416*(4), 509–520. https://doi.org/10.1002/(SICI)1096-9861(20000124)416:4<509::AID-CNE7>3.0.CO;2-H

Vasina, V., Barbara, G., Talamonti, L., Stanghellini, V., Corinaldesi, R., Tonini, M., … De Giorgio, R. (2006). Enteric neuroplasticity evoked by inflammation. *Autonomic Neuroscience: Basic and Clinical*, *126–127*, 264–272. https://doi.org/10.1016/j.autneu.2006.02.025

Wilke, S. A., Antonios, J. K., Bushong, E. A., Badkoobehi, A., Malek, E., Hwang, M., … Ghosh, A. (2013). Deconstructing complexity: Serial block-face electron microscopic analysis of the hippocampal mossy fiber synapse. *Journal of Neuroscience*, *33*(2), 507–522. https://doi.org/10.1523/JNEUROSCI.1600-12.2013

Wilson, J. R., Friedlander, M. J., & Sherman, S. M. (1984). Fine structural morphology of identified X- and Y-cells in the cat's lateral geniculate nucleus. *Proceedings of the Royal Society of London - Biological Sciences*, *221*(1225), 411–436. https://doi.org/10.1098/rspb.1984.0042

Yao, P. J., Petralia, R. S., & Mattson, M. P. (2016). Sonic Hedgehog Signaling and Hippocampal Neuroplasticity. *Trends in Neurosciences*, *39*(12), 840–850. https://doi.org/10.1016/j.tins.2016.10.001

Zeng, M., Chen, X., Guan, D., Xu, J., Wu, H., Tong, P., & Zhang, M. (2018). Reconstituted Postsynaptic Density as a Molecular Platform for Understanding Synapse Formation and Plasticity. *Cell*, *174*(5), 1172-1187.e16. https://doi.org/10.1016/j.cell.2018.06.047